IEA
SOLAR R&D

INTERNATIONAL ENERGY AGENCY

solar heating and
cooling programme

task VIII
passive and hybrid
solar low energy buildings

SIMULATION MODEL VALIDATION USING TEST CELL DATA

june 1986

INTERNATIONAL ENERGY AGENCY
solar heating and cooling programme

task VIII
passive and hybrid solar low energy buildings

SIMULATION MODEL VALIDATION USING TEST CELL DATA

Edited by

Ove C. Mørck

June 1986

Report no. 176

THERMAL INSULATION LABORATORY
TECHNICAL UNIVERSITY OF DENMARK

The following persons have contributed specific chapters to this report:

Chapter 3 - Martin Gough, U.K.

Chapter 4 - Ron Judkoff, U.S.A.

Chapter 5 - Sherif Barakat, Canada

Chapter 6 - Charles Filleux, Switzerland

The complete list of Subtask B representatives who have contributed to this work, is given in Appendix A.

Printed at the
Thermal Insulation Laboratory,
Technical University
of Denmark

PREFACE

INTERNATIONAL ENERGY AGENCY - BACKGROUND

The International Energy Agency was formed in November 1974 to establish cooperation among a number of industrialized countries in the vital area of energy policy. It is an autonomous body within the framework of the Organization for Economic Cooperation and Development (OECD). Twenty-one countries are presently members, with the Commission of the European Communities also participating in the work of the IEA under a special arrangement.

One element of the IEA's programme involves cooperation in the research and development of alternative energy resources in order to reduce excessive dependence on oil. A number of new and improved energy technologies which have the potential of making significant contributions to global energy needs were identified for collaborative efforts. The IEA Committee on Energy Research and Development (CRD) comprising representatives from each member country, supported by a small Secretariat staff, is the focus of IEA R&D activities. Four Working Parties (in Conservation, Fossil Fuels, Renewable Energy and Fusion) are charged with identifying new areas for cooperation and advising the CRD on policy matters in their respective technology areas.

SOLAR HEATING AND COOLING AGREEMENT

Solar Heating and Cooling was one of the technologies selected for joint activities. During 1976-77, specific projects were identified in key areas of this field and a formal Implementing Agreement drawn up. The Agreement covers the obligations and rights of the Participants and outlines the scope of each project or "task" in annexes to the document. There are now seventeen signatories to the Agreement:

Australia	Japan
Austria	The Netherlands
Belgium	New Zealand
Canada	Norway
Denmark	Spain
Commission of the European Communities	Sweden
Federal Republic of Germany	Switzerland
Italy	United Kingdom
	United States

The overall programme is managed by an Executive Committee while the management of the individual tasks is the responsibility of Operating Agents. The tasks of the IEA Solar Heating and Cooling Programme, their respective operating Agents, and current status (ongoing or completed) are as follows:

Task I — Investigation of the Performance of Solar Heating and Cooling Systems - Technical University of Denmark (completed).

Task II — Coordination of Research and Development on Solar Heating and Cooling - Solar Research Laboratory - GIRIN, Japan (completed).

Task III — Performance Testing of Solar Collectors - University College, Cardiff, UK (ongoing).

Task IV — Development of an Insolation Handbook and Instrument Package - U.S. Department of Energy (completed).

Task V — Use of Existing Meteorological Information for Solar Energy Application - Swedish Meteorological and Hydrological Institute (completed).

Task VI — Performance of Solar Heating, Cooling and Hot Water Systems Using Evacuated Collectors - U.S. Department of Energy (ongoing).

Task VII	Central Solar Heating Plants with seasonal Storage - Swedish Council for Building Research (ongoing).
Task VIII	Passive and Hybrid Solar Low Energy Buildings - U.S. Department of Energy (ongoing).
Task IX	Solar Radiation and Pyranometry Studies - Canadian Atmospheric Environment Service (ongoing).
Task X	Solar Materials R&D - MITI, Japan (ongoing).
Task XI	Passive and Hybrid Solar Commercial Buildings - Swiss Federal Office of Energy (ongoing).

DESCRIPTION OF TASK VIII

The participants in Task VIII are involved in research to study the design integration issues associated with using passive and hybrid solar and energy conservation techniques in new residential buildings. The overall objective of Task VIII is to accelerate the development and use of passive and hybrid heated and cooled low-energy buildings in the participants' countries. The results will be an improved understanding of the design and performance of buildings using active and passive solar and energy conservation techniques, the interaction of these techniques, and their effective combination in various climatic regions and verification that passive and hybrid solar low energy buildings can substantially reduce the building load and consumption of none-renewable energy over that of conventional buildings while maintaning acceptable levels of year-round comfort. The subtasks of this project are:

0. Technology Baseline Definition
A. Performance Measurement and Analysis
B. Modelling and Simulation
C. Design Methods
D. Building Design, Construction and Evaluation

The participants in this Task are: Austria, Belgium, Canada, Denmark, Federal Republic of Germany, Italy, The Netherlands, New Zealand, Norway, Spain, Sweden, Switzerland, United States and United Kingdom. Michael J. Holtz, Architectural Energy Corporation, serves as Operating Agent (on behalf of the US Department of Energy).

This report documents work carried out under Subtask B of this Task.

CONTENTS

1. EXECUTIVE SUMMARY

1.1 Background

Increasing interest in passive solar design strategies since 1976 has led to a tremendous development in the area of thermal simulation programs for buildings. New subroutines and other fundamental changes were introduced to existing building energy analysis programs, and entirely new programs were developed to simulate these new design strategies. At the outset of Task VIII of the IEA Solar Heating and Cooling Programme, only limited testing of these upgraded and new simulation programs had taken place. As many of these programs are used for the generation of rules of thumb and design guidelines for building designers, it seemed urgent to test the accuracy and applicability of these programs for the analyses for which they had been developed.

In the context of Task VIII, the simulation programs would be used to evaluate design tools, to generate design guidelines and to analyse actual construction projects. Therefore, the validation of these programs was essential to many of the task activities and the overall outcome.

1.2 Objectives

The general objectives of Subtask B (Modelling and Simulation) are: (1) to increase the capability of the participants of the IEA Task VIII to accurately predict and analyse the performance of passive and hybrid solar low energy buildings, (2) to provide a sound basis for the evaluation of design tools and (3) to support the development of innovative designs. The specific objective of the validation activities documented in this report was to test the analysis capabilities of a number of simulation programs selected by the participants against monitored data from several high level instrumented facilities. Performing this activity not only tested the analysis capabilities of the

selected simulation programs, but also led to an increased understanding of the specific problems encountered in certain design strategies, thus serving the overall objective.

1.3 Approach

The participants focussed their collective effort on empirical validation studies and model-to-model comparisons. From the survey of analysis models (1) conducted at the outset of the work, it appeared that the empirical validation experience was extremely limited. It was therefore decided to conduct three empirical studies on the three basic passive solar designs: Direct Gain, Trombe Wall and Attached Sunspace. As the intention was to extrapolate the empirical validation studies in time and space by performing model-to-model comparisons, it was agreed that it would be favourable if the three selected sites were located in quite different climate regions. An international survey of monitored sites revealed very few which met both the location criteria and the requirements for an empirical validation study (2). From these, three were selected, including a direct gain test building in Canada, Fig. 1.1, a Trombe wall test cell in Switzerland, Fig. 1.3, and an attached sunspace in the U.S., Fig. 1.5. The simulation model performance predictions were compared to monitored data for a two-week period. Finally, yearly simulations by the programs using test reference climate data were compared.

1.4 Results

Twelve building energy analysis simulation programs were used to simulate the direct gain test cell; four were used to simulate the Trombe wall test cell, and six for the attached sunspace test cell. Figs. 1.2, 1.4 and 1.6 present examples of comparison plots for the three cases. The results indicate that simple modestly-sized passive solar heating systems can be handled adequately by all the programs evaluated. Such a case was exemplified by the direct gain building in which the

ratio of the solar aperture-to-floor area was about 10%. This system was simple in the sense that such complex heat transfer mechanisms as natural interzone convection, ground conduction and natural infiltration were suppressed.

The Trombe wall and sunspace cases both represented larger and more complex passive solar heating systems. In the Trombe wall case, the solar aperture-to-floor area ratio was approximately 1. Ground and infiltration heat transfer were minimal, and natural convection through the Trombe wall vents was a major mode of heat transfer. For this case, the disagreement between predicted and measured zone temperature was, in general, much larger than for the direct gain case. Disagreement among the various codes used in the study was also generally greater for the Trombe wall than for the direct gain case.

The sunspace case was also quite complex. The solar aperture-to-floor area ratio was about 30% for the entire building, and 70% for the sunspace zone. Interzone natural convection through an open doorway was an important mode of heat transfer. Infiltration was suppressed in the back room, but was present in the sunspace. Ground heat transfer was relatively small. Here again, temperature and energy predictions showed markedly greater disagreement with the measured values than in the direct gain case. The range of disagreement among code predictions themselves was also much larger than in the direct gain case.

1.5 Conclusions

In general it appears that prediction inaccuracy increases as 1) the solar forcing functions become stronger, and 2) the solid conduction heat transfer mode becomes dominated by other, more complex heat transfer mechanisms. A third reason for increased inaccuracy is lack of an algorithm or subroutine in a code to adequately model some aspect of the building, its equipment, or controls. These sources of inaccuray can work independently or together.

The results from this report and other validation efforts support the following general conclusions:

- Diffusion of heat in solid media is adequately modelled by the current generation of building energy analysis simulations (assuming one dimensional heat transfer).
- The major sources of error and disagreement between codes used to model passive and hybrid low energy buildings are due to the algorithms which handle:
  - calculation of interior and exterior radiative and convective surface coefficients
  - calculation of exterior and interior incident solar radiation
  - interzone natural convection heat transfer and stratification
  - ground heat transfer
  - latent loads

Further research is needed to develop algorithms which model these mechanisms with sufficient accuracy for reliable use in strongly passive and hybrid low energy buildings.

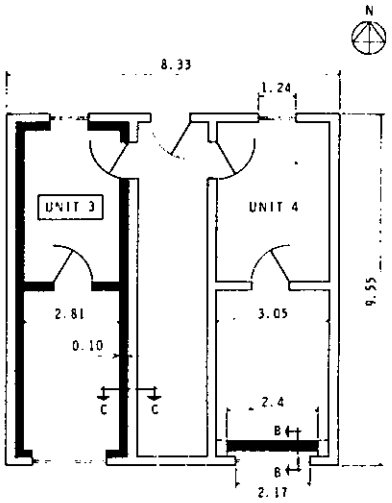

Fig. 1.1 Canadian direct gain test cell floor plan.

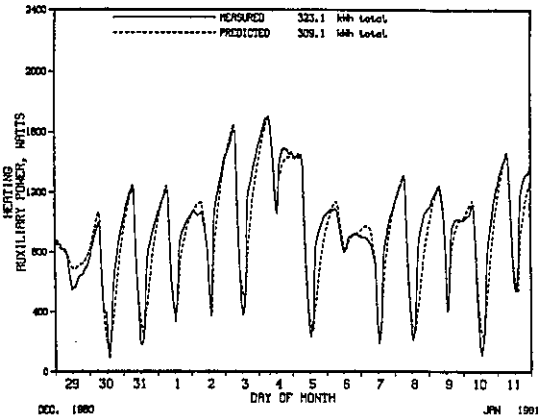

Fig. 1.2 Direct gain test cell comparison plot.
Model: ENCORE-CANADA.

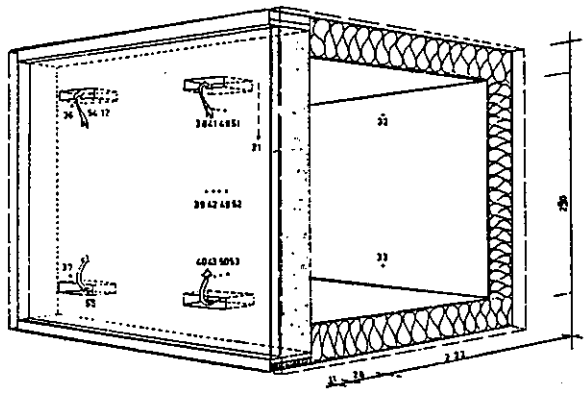

Fig. 1.3 Perspective of Swiss Trombe wall test cell.

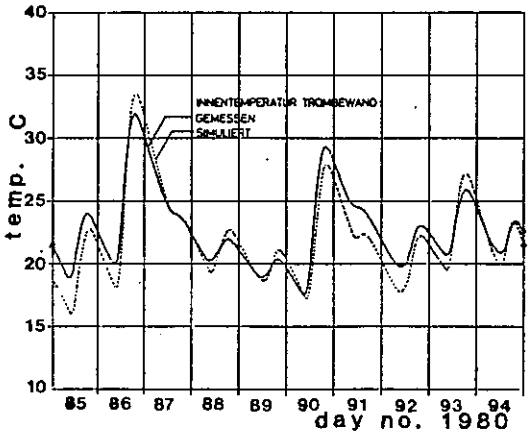

Fig. 1.4 Trombe wall test cell comparison plot.
Model: SERIRES.

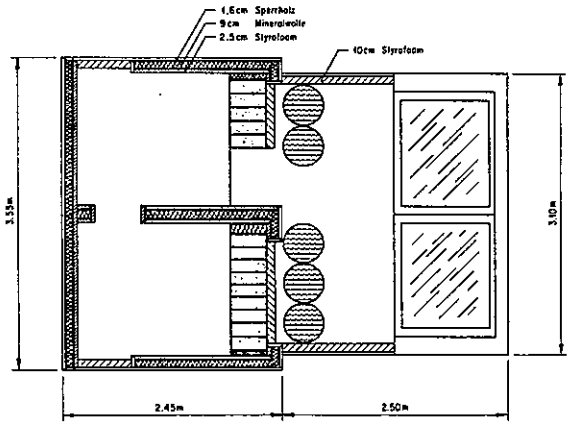

Fig. 1.5 U.S. Los Alamos National Laboratory attached sunspace test cell floor plan.

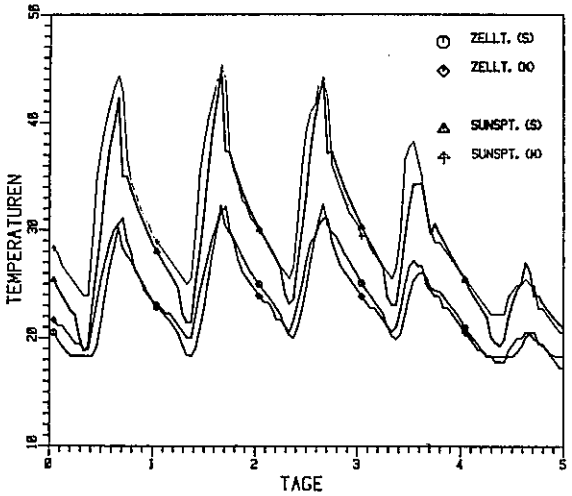

Fig. 1.6 Attached sunspace test cell comparison plot.
Model: DEROB.

REFERENCES

1. Jørgensen, O. (1983). Analysis Model Survey. IEA Solar Heating and Cooling Programme, Task VIII. Thermal Insulation Laboratory, Technical University of Denmark. Report No. 143.

2. Mørck, O. and M. Holtz. (1986). Performance Data Sources, IEA Passive and Hybrid Solar Low Energy Buildings, Task VIII. Thermal Insulation Laboratory, Technical University of Denmark. Report No. 175.

2. INTRODUCTION

2.1 Objectives and Main activities of Subtask B

The objectives of Subtask B (Modelling and Simulation) of Task VIII are: (1) to increase the capability of the participants of Task VIII to accurately predict and analyse the performance of passive and hybrid solar low energy buildings, (2) to provide a sound basis for the evaluation of design tools and (3) to support the development of innovative designs. Four main activities were defined at the outset of the work to fulfil these objectives. The four activities are:

1. Survey of existing simulation models.
2. Validation of a selected number of models.
3. Parameter sensitivity study for design guidelines development.
4. Analysis of Subtask D designs.

This report documents the second of these activities.

2.2 Survey of Existing Simulation Models

At the outset of the work in 1983, very little was known about the analysis capabilities, user interface, and other features of the models developed in the different countries. The objectives for the survey were threefold, namely:

1. Assess the state-of-the-art.
2. Create an overview of available models.
3. Provide sufficient information about each model to enable a potential user to evaluate it for a given purpose.

The survey was completed in 1983 and published in an IEA report entitled "Analysis Model Survey" (1). The conclusions of this survey of 31 models were the following:

1. Hybrid systems can be simulated by very few programs.
2. Even when written in FORTRAN, most programs are machine/operating system-dependent and therefore not readily portable to another machine/operating system.
3. Most of the programs have been developed for research purposes. In general, they do not represent energy analysis tools useful to building designers.
4. Validation experience with these models is extremely limited.

Thus, the recommendations derived from this survey are that future models developments should aim at user-friendly, computer-independent, design-oriented programs, capable of handling a wide variety of passive and hybrid systems.

2.3 Test Cell Validation

The approach used in this validation study was adopted from a methodology developed at the Solar Energy Research Institute (SERI) in 1982 (2). This method involves the combined use of comparative, analytical and empirical techniques for testing building energy analysis simulation programs. The method also specifies criteria for selecting data sites useful for empirical validation studies.

As a first step, the subtask participants decided to focus their collective efforts on the comparative and empirical aspects of the methodology. This was done because most participants stated that the codes developed in their respective countries had already been subjected to analytical tests.

An international survey of monitored sites revealed few which met the requirements for empirical validation as specified in the IEA adopted methodology (3). From these, three were selected: (1) a direct gain test building in Ottawa, Canada, (2) a Trombe wall test cell in Lausanne, Switzerland, and (3) an attached sunspace test cell in Los Alamos, New Mexico.

The work was divided into two parts. Part I involved modelling the three monitored facilities based on two-week periods of actual measured weather data; input data were provided in site handbooks for each facility. Calculated results were then compared to the actual measured hourly zone air temperature, loads and peak loads. Part II of the work involved using the input files developed in Part I to run the codes for an entire year based on standard annual hourly weather data from Copenhagen and Denver. The annual heating and cooling loads calculated by the codes were then compared.

The simulations were performed by:

CODE	SIMULATOR	AFFILIATION
ENCORE-CANADA	Barakat, S.	National Research Council, CANADA
BA4	Mørck, O.	Thermal Insulation Laboratory
PASOLE	- " -	Technical University of Denmark
SOLMAT	- " -	DENMARK
SMP	Butera, F.	Istituto di Fisica Tecnica, ITALY
ENCORE	Larsen, B.T.	Norwegian Building Research Institute, NORWAY
BFEP	Augenbroe, G.L.M.	BGP, Delft University of Technology, THE NETHERLANDS
KLI/PAS	Hensen, J.L.M	FAGO/TPD, University of Technology, Eindhoven, THE NETHERLANDS
ESP	Allen, E.	Building Research Establishment, U.K.
	Bloomfield, D.	- " -
	Gough, M.	- " -
BLAST-3.0	Judkoff, R.	Solar Energy Research Institute, USA
DOE-2.1A-C	- " -	- " -
SERIRES-1.0	- " -	- " -
SERIRES-1.0	Filleux, C.	Basler & Hofmann, SWITZERLAND
DEROB	Gütermann, A.	Eidgenössische Materialprüfungs- und Versuchsanstalt, EMPA, SWITZERLAND

REFERENCES

1. Jørgensen, O. (1983). Analysis Model Survey. IEA Solar Heating and Cooling Programme, Task VIII. Thermal Insulation Laboratory, Technical University of Denmark. Report No. 143.

2. A Methodology for Validating Building Energy Analysis Simulations. SERI/TR-254-1508, 8/83. Judkoff, Wortman, O'Doherty, Burch.

3. Mørck, O. and M. Holtz. (1986). Performance Data Sources. IEA Passive and Hybrid Solar Low Energy Buildings, Task VIII. Thermal Insulation Laboratory, Technical University of Denmark. Report No. 175.

3. MODELLING TECHNIQUES

3.1 Introduction

This chapter presents a review of modelling techniques in current use in building energy simulations, and is divided into 3 main sections. Section 3.2 identifies and establishes mathematical descriptions for the most important mechanisms of heat transfer operating in a building. This is followed (Section 3.3) by a review of algorithms for modelling the dynamic flow of heat in walls, and the chapter is concluded in Section 3.4 with a discussion of procedures for integrating the various sub-models into a complete building simulation program.

3.2 Models of Thermal Processes

The thermal behaviour of a building is governed by a complex interaction of conductive, radiative and convective elements of heat flow. These elements are in balance at any solid surface, where heat conducted into the surface is in instantaneous equilibrium with heat exchanged by radiation and convection with its surroundings. The heat balance in a room is in addition influenced by exchange of air with spaces at different temperatures, for example through the action of draughts, or by the operation of an air-based heating or cooling system. Conduction, radiation, convection and air exchange phenomena are discussed separately in the following sections, the purpose of which is to introduce the procedures used to model these processes in building simulations.

3.2.1 Conduction

Heat flow in a solid is governed by the two equations:

$$\underline{q} = - \lambda \Delta T \qquad (1)$$

$$\nabla q = - \rho c \frac{\partial T}{\partial t} \qquad (2)$$

where

$T = T(\underline{r},t)$ is the temperature (^{o}C)
$q = \underline{q}(\underline{r},t)$ is the heat flux (Wm^{-2}),
$\lambda = \lambda(\underline{r})$ is the thermal conductivity ($Wm^{-1}\ K^{-1}$) and
$\rho = \rho(\underline{r})$ is the density ($kg\ m^{-3}$)
$c = c(\underline{r})$ is the specific heat capacity ($J \cdot kg^{-1} \cdot K^{-1}$)
at the point

$$\underline{r} = (x, y, z), \tag{3}$$

Over the range of temperature found in buildings, the wall properties λ and c may be assumed to be independent of temperature. The heat conduction equations are thus <u>linear.</u> In building simulations, it is commonly assumed that the equations are, in addition, <u>invariant:</u> λ, ρ and c do not vary with time. (This assumption may not be strictly valid for building elements in which the moisture content varies). Equation 1 states that the flow of heat is proportional to the temperature gradient at every point and directed towards regions of lower temperature. Equation 2 is a compact expression of the continuity of heat flow. (It is assumed that the solid contains no internal sources of heat). Combining these equations by eliminating q we obtain

$$\nabla \cdot (\lambda \nabla T) = \rho c \frac{\partial T}{\partial t} \tag{4}$$

the differential equation governing the evolution of the temperature distribution in the solid.

In regions where the thermal properties λ and ρc do not vary with position, Equation 4 can be expressed more simply as

$$\nabla^2 = \frac{\rho c}{\lambda} \quad \frac{\partial T}{\partial t} \tag{5}$$

Equation 5 is the heat diffusion equation. The quantity $\lambda/(\rho c)$

is termed the diffusion constant, or diffusivity, of the medium,

$$\alpha = \frac{\lambda}{(\rho c)} \tag{6}$$

For a solid in which the thermal properties vary only in the direction perpendicular to a particular plane (for example a layered wall) it can usually be assumed that heat flow parallel to that plane is negligible. Equations 1, 2, 4 and 5 then simplify to the following one-dimensional forms,

$$q = - \lambda \frac{\partial T}{\partial x} \tag{7}$$

$$\frac{\partial q}{\partial x} = - \rho c \frac{\partial T}{\partial t} \tag{8}$$

$$\frac{\partial}{\partial x} \frac{(\lambda \partial T)}{\partial x} = \rho c \frac{\partial T}{\partial t} \tag{9}$$

$$\frac{\partial^2 T}{\partial x^2} = \frac{\rho c}{\lambda} \cdot \frac{\partial T}{\partial t} \tag{10}$$

where now

$T = T(x,t)$ is the temperature,
$q = q(x,t)$ is the heat flux in the positive x direction,
$\lambda = \lambda(x)$ is the thermal conductivity,
$\rho = \rho(x)$ is the density, and
$c = c(x)$ is the specific heat capacity,
a distance x from the reference plane.

Equations 7, 8 and 9 are valid at all points in the solid. Equation 10, in which c and λ are constant, is valid in any homogeneous portion. The problem of determining the temperature and heat flux everywhere inside a wall, given data relating to its thermal environment, reduces to the mathematical

problem of solving equation 9 for a variety of different types of boundary condition. The most frequently used boundary condition specifies the temperatures at the internal and external surfaces of the wall; other types of boundary condition involving surface fluxes are on occasion appropriate.

3.2.2 Radiation

Radiation plays a significant role in the thermal activity in and around a building, continuously transferring heat between room surfaces and providing an important channel of thermal communication between the building and its environment.

The equations describing longwave radiation exchanges between surfaces are

$$d\phi_r = \varepsilon\sigma T^4 \cos\theta \, d\Omega dA \tag{11}$$

$$\phi_a = \varepsilon\phi_i \tag{12}$$

where $d\phi_r$ is the energy flux (Watts) radiated by a surface element of emissivity ε and area dA at a temperature T into an element of solid angle $d\Omega$ lying in a direction which makes an angle θ with the surface normal and ϕ_a is the energy absorbed by the same surface when it is subjected to an incident longwave flux ϕ_i $\sigma = 5.67 \times 10^{-8}$ Wm^{-2} K^{-4} is Stefans' constant. It is usual in building models to assume that the surfaces are diffuse radiators, which is to say $\varepsilon \neq \varepsilon(\theta)$. This allows radiation exchanges between surfaces in certain commonly occurring relationships to be calculated from standard shape factors obtained by integrating Equation 11. The shape factor F_{12} for a given configuration is defined by

$$\phi_{12} = F_{12} A_1 \sigma T_1^4, \tag{13}$$

where ϕ_{12} is the total flux radiated by surface 1 (temperature T_1) which is intercepted by surface 2. Tables of shape factor

formulae are given in many texts (for example (8)). The inverse shape factor F_{21} is related for F_{12} by

$$F_{12} A_1 = F_{21} A_2. \qquad (14)$$

Shape factors can be used directly to calculate heat transfer between black surfaces ($\varepsilon = 1$) at given temperatures. However, if the emissivities are less than unity, the existence of multiple reflections rapidly complicates the heat transfer expression as the number of surfaces involved increases. The general problem of N radiating surfaces is solved using the illumination tensor (9), a matrix of coefficients each of which gives the incident intensity at a specified surface resulting from a unit source of radiation at another surface, taking all inter-reflections into account.

The degree of sophistication in inter-wall radiation modelling varies greatly between existing models. Whereas some recently developed large-scale programs (5, 6) apply the full illumination tensor treatment, others (4) base their calculations on unmodified shape factors. A third approach involves the concept of 'mean radiant temperature' (MRT). Carroll (10) has recently reviewed methods of this type and compares their accuracy and efficiency with that of algorithms using a simple shape factor approach. MRT methods use a simplified model of radiation processes in which a given surface is imagined to exchange radiation with a fictitious surface or node whose properties are such as to constitute an approximation to the radiation environment in the room. The 'MRT/balance' of Walton (11), and Carroll's 'MRT network' method (12) are two implementations of this concept. These methods improve on the accuracy obtained using the simpler approaches to detailed inter-wall radiation modelling, which, as Carroll and Walton have pointed out, can give rise to net radiation imbalances violating energy conservation. MRT methods also allow large swings in the solution of room heat balance equations (Section 3.4). The MRT

concept and the allied concepts of environmental temperature and radiation surface resistances have been in existence for several years, and are exploited in the BRE/CIBS admittance procedure (13, 14).

Methods for radiation analysis very frequently use a linearisation assumption. Consider the formula for radiation heat transfer between two parallel surfaces at temperatures T_1 and T_2 (eg a wall cavity):

$$q_{12} = \frac{\sigma(T_1^4 - T_2^4)}{\varepsilon_1^{-1} + \varepsilon_2^{-1} - 1} \qquad (15)$$

The non-linearity of this expression arising out of the fourth powers of temperature makes it impractical for use in fast simulation algorithms, and it is therefore replaced by the following linear expression:

$$q_{12} \simeq \frac{4\bar{T}^3\sigma\ (T_1 - T_2)}{\varepsilon_1^{-1} + \varepsilon_2^{-1} - 1} \qquad (16)$$

which is a good approximation provided that $T_1 - T_2$ is not too large. Here $\bar{T}$, a constant, is an estimate of the average of T_1 and T_2.

For modelling thermal radiation from heat sources such as hot water radiators and lights, a common approach is to divide the output of these devices into 'radiant' and 'convective' portions, the radiant portion being distributed among the room surfaces in proportion to their areas, and convective portion delivered to the air point.

Radiation incident on the external surface of a building has both shortwave and longwave components. The shortwave radiation, solar in origin, is generally calculated for simulation purposes as the sum of directional (circumsolar) and isotropic

components, quantities which may be calculated from data available on weather tapes. The directional component is resolved in the wall normal direction using a knowledge of sun position, and the absorbed flux is calculated as

$$\phi_a = \alpha \phi_i \qquad (17)$$

where ϕ_i is the total incident flux and α is the solar absorptivity of the surface. In complex models, the shadowing effect of nearby buildings and trees is taken into account in calculating shortwave fluxes. The quantity ϕ_i calculated as described above and modified by an absorption factor, is also used for the calculation of solar gains through window glass.

A variety of techniques have been used to model the longwave radiation exchange between a building and its surroundings. Approaches to this problem have been reviewed by Cole (15, 16). Until quite recently the assumption was commonly made that the net longwave exchange at external surfaces was negligible by comparison with absorption of solar radiation. Experimental studies, however, prove the importance of the effect. The net longwave imbalance can be large on clear, dry nights when the sky emissivity is low. Practical methods for estimating sky and ground radiation rely on formulae derived from correlations of incident flux with meteorological variables. These formulae provide expressions for the effective emissivity of a clear sky in terms of the local water vapour pressure (and in certain cases the air temperature). A correction factor is applied to allow for overcast or cloudy conditions. Kondrat'yev (17) presents results from a number of experimental studies which, while supplementing the relations given by Cole, serve to highlight the variable nature of atmospheric radiation and the difficulty of estimating fluxes accurately. In the case of vertical or inclined surfaces it is necessary to take account of ground radiation. This consists of a component characteristic of the ground temperature plus reflected sky radiation, and can

be calculated from a knowledge (or estimates) of ground temperature, ground emissivity and the downward flux from the sky.

Mathematical modelling of the effects of external radiation exchanges on heat conduction through the envelope is simplified by the use of the concepts of sol-air temperature and convection-radiation surface resistances. Sol-air temperature, a concept developed by Mackey and Wright (18), simplifies the treatment of thermal exchanges at the external surface of a building by combining air temperature and the effects of radiation exchange phenomena in a single quantity.

Several other methods have been suggested for a simplified approach to deal with these phenomena (3). The concept of radiation air temperature has been proposed by Haferland and Heindl (1, 2). The radiation temperature is defined as the equilibrium temperature of a surface element adding temperature corrections due to the absorption of global radiation and to the long wave radiation exchange to the ambient air temperature.

3.2.3 Convection

Convection forms a second component in the boundary condition equation applying at a wall surface. Convection is a complicated process and its complexity is reflected in often intractable mathematical relations which describe it. Models of convection processes suitable for incorporation in building simulations can, however, be developed by simplifying where necessary and making heavy use of linearisation.

Convection problems divide into those involving free convection - a buoyancy induced effect which occurs in the relatively still conditions inside a building - and those involving forced convection, in which a fluid is actively propelled past an object. Convection at the external surfaces of buildings is generally assumed to belong to the second category, although

exceptions to this regime occur at very low wind speeds.

Heat transfer relations for convection processes, giving the heat flow rate between a body of fluid and a solid surface at a different temperature (or between two solid surfaces with fluid between) are expressed in terms of the Nusselt, Grashof, Prandtl and Reynolds numbers (Nu, Gr, Pr and Re), dimensionless groups of physical constants defined as follows:

$$Nu = hL/\lambda \tag{18}$$

$$Gr = \frac{g\Delta T\, L^3 \rho^2}{T\mu^2} \tag{19}$$

$$Pr = \mu c_p/\lambda \tag{20}$$

$$Re = vL\rho/\mu \tag{21}$$

where

- h ($Wm^{-2}K^{-1}$) is the heat transfer coefficient
- L (m) is a characteristic length,
- g (ms^{-2}) is the acceleration due to gravity,
- ΔT (K) is the temperature difference between the fluid and the surface,
- T (K) is the average of the fluid and surface temperatures,
- ρ (kg m^{-3}) is the density,
- μ (Ns m^{-2}) the dynamic viscosity,
- λ ($Wm^{-1}K^{-1}$) is the thermal conductivity.

Natural convection heat flow through doorways has a special interest in passive solar application. The German participant of the Task has prepared a documentation of known algorithems to mathematically account for this phenomenum (38).

TABLE 3.1 FREE CONVECTION FORMULAE

Geometry	Formula	Applicable Range	Reference
Vertical plate (L = height)	$\overline{Nu} = 0.59\ (GrPR)^{1/4}$	$10^4<GrPR<10^9$	[83]
	$\overline{Nu} = 0.129\ (GrPR)^{1/3}$	$10^9<GrPR<10^{12}$	[83]
Horizontal plate (L = mean of dimensions)			
(a) Upper surface of warm plate or lower surface of cool plate	$\overline{Nu} = 0.54\ (GrPr)^{1/4}$	$10^5<GrPR<2x10^7$	[83]
	$\overline{Nu} = 0.14\ (GrPr)^{1/3}$	$2x20^7<GrPr<3x10^{10}$	[83]
(b) Upper surface of cool plate or lower surface of warm plate	$\overline{Nu} = 0.44\ (GrPr)^{1/5}$	$10^5<GrPR<2x10^7$	[83]
Vertical enclosed space (L=height, d=width, L/d>3)	$\overline{Nu}=0.18\ Gr^{1/4}(L/d)^{-1/9}$	$2x10^4<Gr<2x10^5$	[82]
	$\overline{Nu}=0.065\ Gr^{1/3}(L/d)^{-1/9}$	$2x10^5<Gr<10^7$	[82]
Horizontal enclosed space (L = height) (a) Lower surface warmer	$\overline{Nu} = 0.195\ Gr^{1/4}$	$10^4<Gr<4x10^5$	[82]
	$\overline{Nu} = 0.068\ Gr^{1/3}$	$Gr>4x10^5$	[82]
(b) Upper surface warmer	$\overline{Nu} = 1$		[82]

λ ($Wm^{-1}K^{-1}$) the thermal conductivity, and
c_p ($J\ kg^{-1}\kappa^{-1}$) the constant-pressure heat capacity of the fluid, and
v ($m\ s^{-1}$) is the flow velocity (in forced convection problems).

Free convection formulae for some simple geometries are given in Table 3.1. These relations are mainly empirically determined. In real buildings, the idealized conditions represented in Table 3.1 are seldom met, but these relations often represent the best estimate that can be achieved without a great deal of very detailed analysis.

The fact that the exponents of Gr in the formulae appearing in Table 1 are not unity indicates that free convection is a non-linear process. Linearisation of free convection formulae is

almost universally applied in building simulations. The principle is the same as that applied in the radiation case, though the more pronounced non-linearity in the case of convection means that the errors introduced by the linearisation are somewhat greater. After linearisation, the convection relation is characterised by a single coefficient, h_c:

$$q = h_c \Delta T \tag{22}$$

In Table 3.1 it will be noted that, as a consequence of the nature of buoyancy, different relations apply for convection from horizontal surfaces depending on whether the surface is warmer or cooler than the fluid in contact with it, and whether the upper or lower surface is referred to. This asymmetry is often modelled by the use of different values of h_c depending on the sign of the temperature gradient.

Convective heat transfer at the external surface of a building, primarily a forced convection effect, presents modelling problems on account of its strong dependence on windspeed. The shape of the building, orientation with respect to wind direction and surface roughness also affect the heat transfer characteristics. Cole and Sturrock (19) have reviewed the state of knowledge on the external convection coefficient. They demonstrate that agreement between published prediction methods is in general rather poor. These methods fall into three classes: theoretical calculations, wind-tunnel tests and field measurements.

Results derived from theory take the form of functional relations between Nu, Re and Pr. They tend to apply to rather simple geometries and not to take account of surface roughness (a parameter which wind-tunnel experiments have shown can be responsible for a doubling of the heat transfer coefficient). Theoretical relationships do nevertheless provide useful insights into scaling laws which can be applied to wind tunnel

results to extend their applicability. Cole and Sturrock observe that in the past wind-tunnel measurements have frequently been applied to buildings - and the methodology incorporated into design guides - without allowance being made for scaling. The consequence of overestimation of the convection coefficient can be significant, particularly for large buildings. Field measurements of the external convection coefficient at the surfaces of real buildings have been made in recent years by Ito et al (20) and by Sturrock (21). The results of these two investigations are, however, in poor agreement. Sturrock finds the following relationship between convection coefficient h_c and windspeed v (both in SI units).

$$h_c = 11.4 + 5.7\ v \tag{23}$$

for windward facing surfaces, and

$$h_c = 5.7\ v \tag{24}$$

for leeward facing surfaces. Ito's results suggest much smaller values for h_c for both windward and leeward facing surfaces, amounting to only 50% and 30%, respectively, of Sturrock's values at a windspeed of 10 m/s. The majority of wind-tunnel measurements and theoretical calculation for h_c lie in the range between these two sets of results.

The external convection coefficient generally has a fairly small effect on the overall admittance of walls and roofs (19). The position this coefficient occupies in the sol-air temperature expression shows, however, that it is important as a determinant of the proportion of solar radiation which is absorbed by opaque surfaces. Thus the present level of uncertainty surrounding this coefficient cannot be regarded as completely satisfactory.

3.2.4 Air Exchange: Infiltration and Ventilation

The exchange of air between the interior and exterior of a building can represent an important mechanism of heat loss. However, a comprehensive review of the subject is not attempted here. Instead, we shall simply identify the mechanisms by which air exchange occurs, and indicate how they can be taken into account in a simple way in thermal models of a building. The discussion is confined to natural ventilation: mechanical ventilation poses few problems for thermal analysis as the air exchange rate is in this case known in advance.

In the process of natural ventilation, air enters and leaves a building through openings in the envelope, driven by pressure differences between the interior and exterior. Pressure differences can be either wind-generated or the result of buoyancy forces (stack effect). If the infiltration is $\dot{V}$ cubic metres of air per second, the associated heat loss is

$$\phi = \rho c_p \dot{V} (T_A - T_o) \qquad (25)$$

Watts, where ρ and c_p are, respectively, the density and specific heat of the air, and $T_A - T_o$ is the temperature difference between the interior and exterior air masses. In the calculation of infiltration heat loss, attention centres on the accurate estimation of $\dot{V}$.

In simple models a constant rate of infiltration is assumed, expressed as AC being the number of air changes per hour. AC is often set for example to a value of one air-change per hour - a rate typical of those measured in experiments carried out in houses (22). For more accurate simulations, attempts can be made to estimate $\dot{V}$ on an hour-to-hour basis using a knowledge of the size and distribution of the the draught openings. A methodology for this is given in the ASHRAE Handbook of Fundamentals (23). In the recommended procedure, infiltration rates are obtained in a two-stage process involving the calculation

of pressure differences (both wind- and buoyancy-generated) as an intermediate step.

Infiltration/pressure difference characteristics are described in the Handbook for openings of various kinds.

Infiltration models can be developed to high levels of sophistication, for example by detailed modelling of air exchange between individual rooms (24). All models are however subject to the limitation that knowledge relating to the permeability of the envelope is inevitably incomplete. The most reliable estimates of infiltration rates are obtained from in situ measurements using tracer-gas techniques. In many modelling situations, however, this is not an option open to the analyst.

3.3 Methods for Modelling Conduction Heat Flow in Walls

Methods for analysing the thermal behaviour of walls can be divided into three main classes, namely harmonic methods, finite difference methods and response factor methods. The aims of each of these types of method are essentially the same: to determine the thermal state of a wall, given information relating to temperature or heat flux conditions at its surfaces. Their most common application is in the calculation of surface fluxes, usually from given surface temperature data. They are also applied to the determination of temperature (and less frequently flux) distributions inside the wall. An account is given below of the principles underlying each of the three approaches, and their particular strengths and limitations are stated.

The methods described in this section can be applied to all solid building components (walls, ceilings, roofs) with the exception of ground floors. Ground floors form a special category requiring a fundamentally different approach. An introduction to this large subject is provided by refs (33-35).

3.3.1 Harmonic Methods

The basis of harmonic methods for wall heat transfer calculations is the assumption that conditions at the wall surface follow a repeating pattern, calculations being performed in these methods for an endless succession of identical days. This assumption of exact periodicity simplifies the thermal analysis considerably; for each Fourier component of the input signals the response of the wall is determined using transfer functions derived using the matrix technique, and these responses recombined to generate the overall response. The simplicity of this approach, and the fact that it can be extended to the analysis of complete buildings using techniques borrowed from electrical network theory, are factors which have contributed to its widespread adoption (25, 26, 27). Its strength is its ability to provide estimates of indoor temperature swings and time-dependent heating loads for design purposes - information which an elementary analysis based on steady state response cannot provide. Its principal limitation is its assumption of periodicity, which restricts its use to approximate 'design-day' calculations: the detailed simulation of heating system controls is outside the scope of the method. A further restriction is its unsuitability for modelling non-linear heat transfer processes occurring at the surfaces of walls.

3.3.2 Finite Difference Methods

Finite difference methods operate on the principle of approximating the thermal state of a wall by a finite set of numbers representing the temperature at internal points. The differential equation describing the conduction characteristics of the wall is replaced by a set of difference equations involving the nodal temperatures, and these difference equations are solved to determine the temperature distribution at successive time intervals. Finite difference methods have the merit of conceptual and computational simplicity, and are particularly well suited to modelling non-linear and multi-dimensional systems. For problems in linear, one-dimensional heat flow - their most

common application in building simulations - they tend to be somewhat less efficient, at given levels of accuracy, than response factor based methods.

3.3.3 Response Factor Methods

Methods based on response factors constitute a powerful class of calculation procedures in which output quantities are computed directly from the sample records representing the history of inputs at the walls surfaces. These methods are based on the superposition principle, responses to general input signals being constructed from the precalculated response to a simple pulse function. In mathematical terms, if a certain output attains a value p^k at a time $t = k\Delta$ (where k is an integer and Δ is a fixed interval) after the application of a pulse of unit height at one of the inputs T, then the response generated by an input consisting of a succession of such pulses of heights $---T^{-1}$, T^0, T^1, ... T^j,... will be

$$p^j = \sum_{k=0}^{\infty} p^k T^{j-k} \qquad (26)$$

at time $t = j$. This equation represents the response factor method in its simplest form. The response factors are the coefficients p^k. Refinements of the basic method have been developed which make use of previously calculated output values in addition to the input samples. This modification improves computational efficiency.

The full expression for an output quantity involves two response factor sums of the form 27, one for each of the surface inputs.

The use of simple response factor expressions (equation 26) tends to be computationally inefficient owing to the large number of terms that must be included in the sum to achieve acceptable accuracy in calculated outputs. Dramatic improvements in efficiency can be achieved by incorporating terms pro-

portional to values of the output variables obtained in previous calculation steps. The formalisms of z-transforms and z-transfer functions (29) provide an elegant means of determining the values of the coefficients used in this type of calculation procedure. An alternative approach to the calculation of the coefficients, based on 'conduction transfer functions' of specified order, achieves a similar result by different means (30).

The attractions of response factor methods lie in their efficiency, their accuracy and their generality. These methods allow complete freedom in the specification of the input variables (unlike harmonic methods) and show advantages both in speed and accuracy over finite difference methods. Their one limitation is their implicit reliance on the linearity and invariability of the systems they model. Only if the system has these properties can the superposition principle be applied with validity. This is not a serious limitation in practice since in virtually all building simulations linearity and invariability in conduction processes are assumed. However, this is problematic for modelling situations where such non-linear or non-constant mechanisms as convection, radiation, and moisture migration are important. An example would be wall cavities in which radiation barriers are used.

Use of the response factor principle is not restricted to wall analysis. Mitalas and Stephenson (28) have described methods for determining the response of a room to various thermal excitations such as external temperature and heat input from lights. Quantities of interest such as the room heating load and wall surface temperature are expressed in terms of these inputs as response factor sums. The terms 'room thermal response factor' and 'weighting factors' are used for the response factor coefficients in such cases. DOE-2 (10) is an example of an advanced computer program using this principle. DOE-2 (10) is an example of a computer program using this principle. How-

ever, this approach does require that loads be calculated based on a constant interior temperature. In the DOE program actual loads and zone temperatures are then re-calculated based on a perturbation routine in the "systems" portion of the program. With this approach it is not possible for the user to do a simple energy balance check on the code results for the case where internal temperatures are varying. Also, the user must choose the interior zone temperature at which the response factors will be calculated. This can cause problems where zone temperatures vary widely such as in atriums or sunspaces. A more advanced response factor approach is used in BLAST-3.0 where both internal and external temperatures may vary as loads are calculated.

3.3.4 Finite Elements Methods

Contrary to the finite-difference-method the finite-element-method is based on a discretisation in space and in time performed separately.

The finite element method deals with the space discretisation in the following way.

The space is represented by a network of nodes. Between the nodes the thermal relation is created by selecting suitable interpolation functions. It is also possible to incorporate the boundary conditions in the spatial system together with additional heat flow between nodes, for example radiation. Thus, a set of ordinary time-dependent differential equations is derived. This set always has the same structure and can therefore be resolved by the computer in a uniform way with a suitable time discretisation.

This approach allows a high level of flexibility in the determination of the spatial network and makes it easy to model 3 dimensional phenomena.

3.4 Whole-Building Models

The preceding sections of this chapter have been concerned with the physical principles of heat transfer in buildings and the computational procedures used to obtain solutions to wall conduction problems. In this section we shall look briefly at ways in which whole-building models can be constructed from the various elements we have identified above.

The procedure used to model a complete building is largely dictated by the type of algorithm used in the calculation of wall heat flows. If the wall solution is based on a harmonic analysis, parameters describing the thermal response of the building as a whole can be derived by algebraic solution of a network of admittances, each admittance in the network representing either a solid building component or else a purely resistive convection or radiation linkage. Periodically varying heat sources form inputs to the network at appropriate points and other nodes represent temperature inputs. The BRE admittance procedure (13, 14) is an example of such a method. In methods of this kind it is usual to simplify the description of radiation and convection exchanges by the use of fictitious temperatures, combined surface coefficients and MRT concepts (31, 32).

In the case of finite difference methods, it is again possible to extend the principle applied to the wall solution to an analysis of the complete building. Equations describing convective and radiative exchange at wall surfaces couple together the sets of difference equations describing the temperature evolution in each separate wall, and the complete set of equations, which incorporate the influence of heat inputs and specified temperatures, is solved simultaneously at every time-step. Clarke (7) describes a solution algorithm for such a set of equations.

With response factor methods it is usual to adopt a modular approach to the whole-building solution, in which outputs from

independent wall models are combined in obtaining solutions to room heat balance equations, and any residual inaccuracies are resolved by iteration.

REFERENCES

1. Haferland F. & W. Heindl. Einfluss des Schichtaufbaues von Aussenwänden auf den Temperaturverlauf bei periodischen Aufheizung- und Abkühlungsvorgängen infolge Sonneneinstrahlung. WT 21 (1969), H.11, H.12, WT 22 WT 22 (1970), H.2.

2. Haferland F., W. Heindl & H. Fuchs. Rechnerische Untersuchung zur Ermittlung der Grössenordnung bestimmter Einflüss von Bauweise und Konstruktion sowie sonstiger Parameter auf die Temperaturstabilität in Räumen. Berichte aus der Bauforschung, Heft 99, Berlin 1975. Verlag Wilton Ernst und Sohn.

3. Koch H. & U. Pechinger. Möglichkeiten zur Berücksichtigung von Sonnen- und Wärmestrahlungseinflüssen auf Gebäudeoberflächen. Gesundheitsingenieur 98 (1977), H.10.

4. NBSLD the Computer Program for Heating and Cooling Loads in Buildings. T. Kusuda, US Department of Commerce, National Bureau of Standards. April 1981.

5. Introduction to the Computer Program TAS. Jones Cassidy Mellor Ltd. Cranfield Institute of Technology, Cranfield, Bedford, MK43 OL (1981).

6. DEROB III. The DEROB System Vol 1, 'Users' Manual for the DEROB System, by F. Arumi-Noe, M. Wysocki. Numerical Simulation Laboratory, University of Texas, Austin, June 1979.

7. J.A. Clarke. Environmental Systems Performance (SP). Ph.D. Thesis, Univ. of Strathclyde, Glasgow, June 1977.

8. H.C. Hottel, A.F. Sarofim. Radiative Transfer, McGraw-Hill 1967.

9. F. Arumi-Noe. Personal communications to D. Bloomfield, Building Research Station, Carston, Watford.

10. J.A. Caroll. A Comparison of Radiant Interchange Algorithms. Energy Centre, University of California, San Diego.

11. G.N. Walton. A New Algorithm for Radiant Interchange in Room Loads Calculations. ASHRAE Trans. No 2590.

12. J.A. Carroll. An MRT Method of Computing Radiant Energy Exchange in Rooms. Proceedings of the 2nd Systems Simulation and Economic Analysis Conference, San Diego 1980, 343-348.

13. N.O. Milbank, J. Harrington-Lynn. Thermal Response and the Admittance Procedure. Building Research Station CP16/74.

14. Chartered Institution of Building Services (CIBS) Guide, 1979.

15. R.J. Cole. The Longwave Radiation Incident on the External Surfaces of Buildings. Building Services Engineer, December 1976, Vol 44.

16. R.J. Cole. Review Paper. The Longwave Radiative Environment around Building. Building and Environment, Vol 11, 3-13.

17. K.Y. Konfrat'yev. Radiative Heat Exchange in the Atmosphere. Pergamon Press, Oxford 1965.

18. C.O. Mackey, L.T. Wright. Summer Comfort Factor as Influenced by the Thermal Properties of Building Materials, A.S.H.V.E. Trans. Vol 49, 1943, p 148. (See also ref (47).

19. R.J. Cole, N.S. Sturrock. Review Paper. The Convective Heat Exchange at the External Surface of Buildings. Building and Environment, Vol 12, 207-214.

20. N. Ito, K. Kimura & J.Ok. A. Field Experiment Study on the Convective Heat Transfer Coefficient on Exterior Surface of a Building. ASHRAE Trans. 1972 Vol 78(1), 184-191.

21. N.S. Sturrock. Localised Boundary Layer Heat Transfer from External Building Surfaces. Ph.D. Thesis, University of Liverpool, 1971.

22. P.R. Warren & B.C. Webb. Ventilation Measurements in Housing. CIBS Conference 'Natural Ventilation by Design'. December 1980.

23. ASHRAE Handbook and Product Directory. 1977 Fundamentals. ASHRAE, New York 1980.

24. F.W. Sinden. Multi-Chamber Theory of Air Infiltration. Building and Environment, Vol 13, 21-18, Pergamon Press, 1978.

25. F.M. Camia. Calcul d'une Modulation Thermique Entretenue dans les Murs Composites: Fonctions S. Revue General de Thermique, Vol 15(171) March 1976, 203-214.

26. B. Boettcher. Verhalten Mehrschichtiger Baukonstruktionen bei Periodischer Oberflaeschernerwaermung. Materialpruefung Vol 19(4), 4 April 1977, 143-148.

27. K.R. Rao, P. Chandra. A computer program for the calculation of individual room air temperature of multiroomed buildings. First Symposium on the use of computers for environmental engineering related to buildings. US National Bureau of Standards, Building Science Series No. 39, Washington.

28. G.P. Mitalas, D.G. Stephenson. Room Thermal Response Factors. ASHRAE Trans. 1967, Vol 73, I.III.2 1-10.

29. D.G. Stephenson, G.P. Mitalas. Calculation of Heat Conduction Transfer Functions for Multi-Layer Slabs. ASHRAE Trans. 1971, Vol 77, II, 117-126.

30. B.A. Peavy. A Note on Response Factors and Conduction Transfer Functions. ASHRAE Trans. Vol 84, 1978.

31. E. Danter. Heat Exchanges in a Room and the Definitions of Room Temperature. Building Services Engineer. Vol 41, 231-243 (1974).

32. M.G. Davies. On the Basis of Environmental Temperature Procedures. Building and Environment, Vol 13(1). Pergamon Press 1978.

33. A.H. Lachenbruch. 3-dimensional Heat Conduction in Permafrost beneath Heated Buildings. Geological Survey Bulletin (USA) 1052B 1957, IV, 51-69.

34. B. Adamson, G. Domner, M. Ronning. Soil Temperatures under Houses without Basement. Statens Institut for Byggnadsforskning, Hanlinger Nr 46, Stockholm, 1964.

35. R.W.R. Muncey, J.W. Spencer. Heat Flow into the Ground under a House. ICHMT International Seminar on Heat Transfer in Buildings, Dubrovnik, Yugoslavia, 649-660.

36. M. Jakob. Heat Transfer Vol 1. John Wiley and Sons, Inc. New York 1949.

37. A.J. Chapmen. Heat Transfer 3rd Ed. Macmillan, New York 1974.

38. R. Stricker. Free Convection Model Comparison. IEA Task VIII, Working Document. Universitaet Essen. Fachgebiet Bauphysik. Oct. 1984.

4. VALIDATION METHODOLOGY

4.1 The Need for Validation

Using computer programs for building energy analysis is not new. Since the late 1960s, the number of computer programs in both the public and private sectors has proliferated. Fig. 4.1 shows this development in the United States. Similar developments have also occurred in Canada and Europe as shown in Table 4.1. With almost 20 years of development behind some of these programs, it is tempting to believe that they are sufficiently accurate. However, studies have shown large disagreements between codes for very simple test cases (4,8).

Until the oil embargo of 1973, these programs were used for sizing heating, ventilating, and air conditioning (HVAC) equipment. Little emphasis was placed on the ability to predict envelope loads accurately in other than conventional building types. Therefore, the authors of these programs made simplifying assumptions and chose solution approaches that, although quite reasonable for computational efficiency, were not adequate for innovative energy efficient building designs.

In 1973, it became evident that designers had to rethink energy use in buildings. At first, the trend was toward utilization of active solar systems that presented little difficulty for existing building energy analysis simulation (BEAS), since the solar components could be added much as another HVAC system. The original TRNSYS program was exclusively an active solar system simulation and was incorporated into such simulations as DOE and BLAST without necessitating major reworking of these programs (2,3).

By 1976-1977, more attention was being devoted to passive and innovative design strategies involving architectural modification of the building design to reduce load and to utilize environmental sources and sinks of energy. However, the exist-

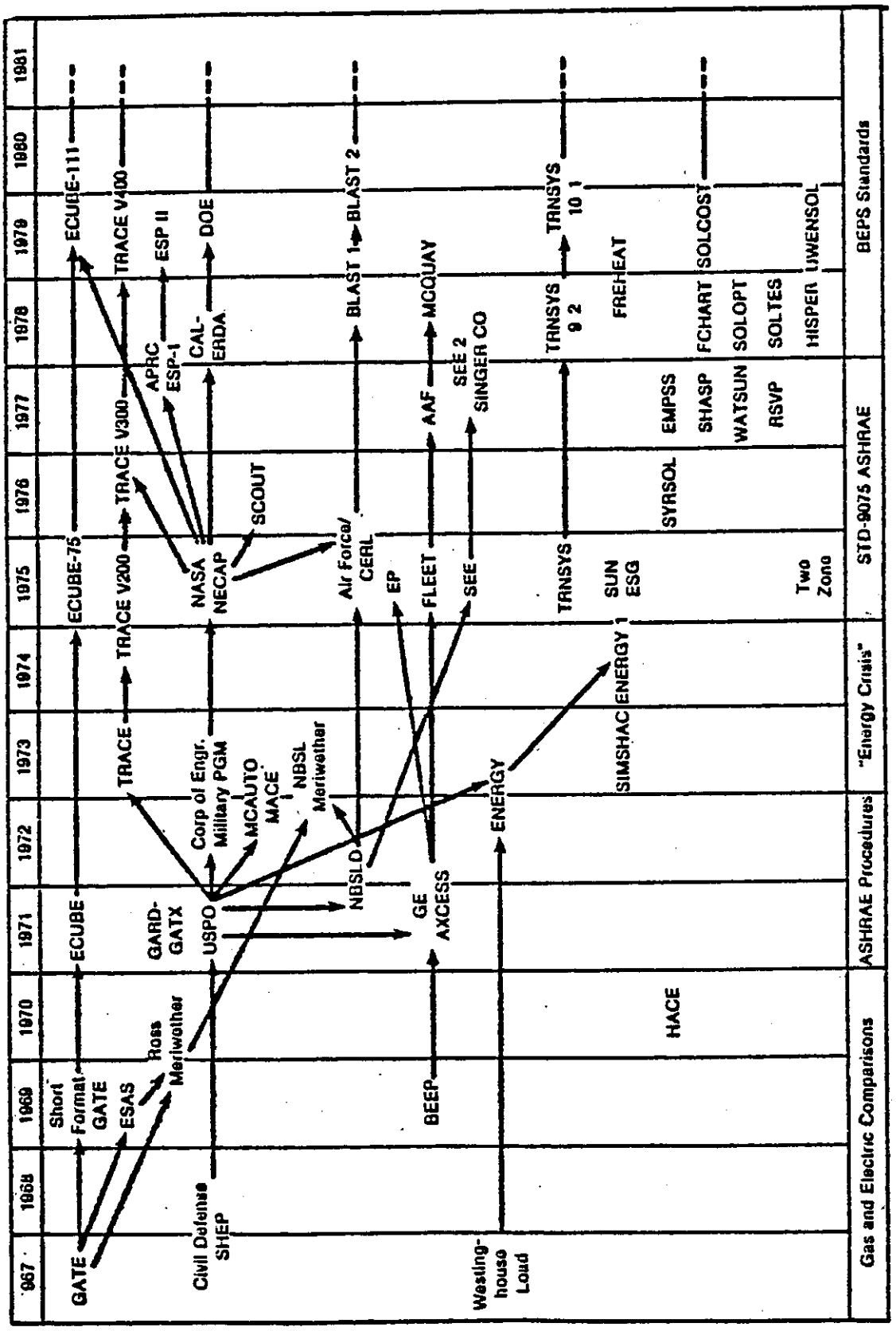

Fig. 4.1. History of computerized energy analysis up to 1979 in the U.S.

TABLE 4.1 RECENT DEVELOPMENTS IN BUILDING ENERGY ANALYSIS SIMULATION PROGRAMS IN EUROPE AND NORTH AMERICA

Country	Simulation Program
Belgium	LBP1, SOLPA
Canada	Passive House Design, Encore, Passive SIMMET
Denmark	BA4
W. Germany	HAUSER, ROUVEL
Italy	MORE, SMP
Norway	BYVOK, Encore
Netherlands	KLI, BFEP
Switzerland	PASSIM, MODPAS, IGLOU, BAUDYN STEMOD/DYWAN, MUR DIODE, SOLAR TRAP HELIOS I
USA	BLAST-3.0, DEROB-IV, DOE-2.1C EMPS-2.0, SERIRES-1.0, TRNSYS-11.1
UK	ESP, HTB2

ing BEAS were no longer appropriate under these new conditions. Adding new subroutines to existing programs did not ensure accurate energy analysis. Instead, fundamental changes to the analysis approach were often necessary to handle these innovative design strategies.

The attempt on the part of code developers to accurately analyse passive design options has fostered an entirely new generation of building energy analysis simulations. Considerable controversy remains about what techniques are most appropriate. Calculating the impact of a wide variety of innovations on total building load involves considerable study of building physics and the development of new algorithms. The question of validation is important because

there has not yet been time for extensive testing and application of this new generation of BEAS. Nevertheless, many simplified design tools, energy audit procedures, and rules of thumb have been generated from these simulations (9). These tools have a significant impact on the design of new buildings and the retrofit of existing buildings. Major inaccuracies in these tools could have a negative impact on public acceptance of energy-efficient buildings.

4.2 Validation Methodology

The validation methodology adopted from the Solar Energy Research Institute (1) employs three different techniques: 1. Code-to-code comparisons, 2. analytical tests, and 3. empirical tests. This section describes the philosophy behind the methodology and explains the relationship between the three techniques.

4.2.1 Validation levels

Many levels of validation exist depending on the degree of control exercised over the possible sources of error in a simulation. There are seven principal sources of error:

1. Differences between the actual weather surrounding the building and the statistical weather input used with BEAS;
2. Differences between the actual effect of occupant behaviour and those effects assumed by the user;
3. User error in deriving building input files;
4. Differences between the actual thermal and physical properties of the building and those input by the user (generally from engineering handbook values);
5. Differences between the actual thermal transfer mechanisms operative in and between individual components, and the algorithmic representation of those mechanisms in BEAS;
6. Errors in solution technique;
7. Coding errors.

At the most simplistic level, the actual long-term energy usage of a building is compared to that calculated by the computer program with no attempt to eliminate sources of discrepancy. This level is similar to actual use of BEAS and, therefore, is favoured by many representatives of the building industry. However, it is difficult to interpret the results of this kind of validation exercise because all possible error sources are operating simultaneously. Even if good agreement is obtained between measured and calculated performance, the possibility of compensating errors prevents drawing conclusions about the accuracy of the method. More informative levels of validation are achieved by controlling or eliminating various combinations of error types. At the most detailed level, all known sources of error are controlled to identify and quantify unknown error sources.

Error sources 1 through 4 are external since they are independent of the internal workings of the method of calculation. Error sources 5 through 7 are internal and are directly linked to the internal workings of a prediction technique. To identify internal errors, external error sources must be carefully controlled.

External errors

Although external errors may be a large source of discrepancy, they do not necessarily negate the usefulness of BEAS as a design or analysis tool. Weather data used by BEAS may differ somewhat from the particular microclimate surrounding a building, adversely affecting the prediction of building energy consumption. However, comparisons of the relative difference in energy consumption between design alternatives remain useful despite our imperfect characterization of climatic factors. In empirical validation studies, this uncertainty can be removed by using weather data recorded at the building.

Occupant behaviour can introduce large discrepancies between actual and predicted building performance. However, if

internal errors are eliminated, the simulations allow us to quantify the effects of various occupant behaviour patterns. This information could lead to guidelines to better inform and motivate occupants to operate their buildings optimally, or components that control the building automatically. The effect of occupants in smaller buildings can be eliminated from validation studies by using unoccupied buildings. This is not economically feasible in large commercial buildings. However, in such buildings the great number of occupants may cancel the random effect of any single occupant.

User input errors can overpower all other effects in a simulation. As the user becomes more experienced at preparing input files, these errors become less common. Nevertheless, an excellent area for investigation is the effect of different user interfaces on speed, ease, and accuracy of input. In validation studies, these effects can be minimized by having several experienced users independently prepare input files from the same information. The files are then compared until unanimous agreement is reached.

Imperfect representation of the building's thermal properties usually has less effect on simulation accuracy than errors 1, 2, and 3. Ordinarily the practising architect or engineer should find handbook values adequate for comparing the relative performance of design alternatives. In validation studies, however, use of accurate thermal properties becomes important. Both destructive and non-destructive testing procedures may be used to determine the actual thermal properties of the building. This is especially important when the validation study is attempting to isolate internal errors.

Internal errors

We have seen in the previous section that successively more sophisticated levels of validation may be achieved by eliminating external error sources. Once all external sources are controlled, it is then possible to investigate internal error sources. Here again, the process of successive elimination may be applied.

Internal errors are more readily understood if we break the simulation process into two parts, modelling and numerical solution (see Fig 4.2). Modelling implies a simplification of the real physical processes at play in real buildings. These simplifications are made by code authors through the use of assumptions that allow the problem to be solved more easily within practical constraints. These constraints may be related to such things as the core capacity and run-time of computer hardware or the availability of generally accepted mathematical expressions for certain physical processes. Two examples of such simplifying assumptions are 1) the one-dimensionality of wall conductance, 2) the representation of interior infrared exchange as a constant increase to surface-to-zone convective film coefficients. These assumptions will influence the accuracy of a simulation depending on the building being analysed. A small test cell with a relatively large ratio of "corner condition" would be more affected by the one-dimensional wall conduction than would a large building. A room with large temperature differences on different interior wall surfaces would be more affected by the lack of an infra-red radiation network than a room with small temperature differences. Especially the phenomena, that during a temperature night set back the heat flow from internal adiabatic elements will change gradually, demonstrates that the use of constant film coefficients cannot work sufficiently (11).

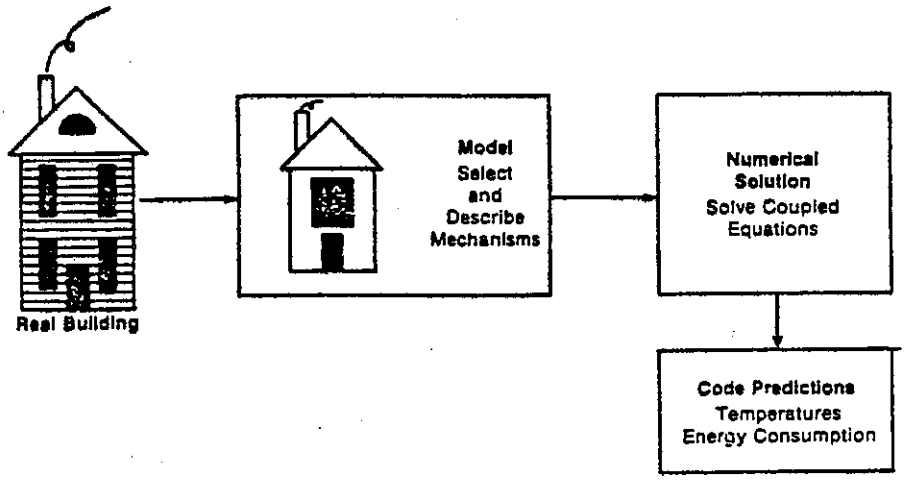

Fig. 4.2 Simulation Process.

The second step of the simulation process is the numerical solution of the model. A model may lend itself to more than one numerical solution approach. For example, either transfer functions or finite differencing may be used to solve for one-dimensional wall conduction. The code author selects the numerical solution based on both objective and subjective criteria. Differences between measured and calculated results can be due to either the model used or the numerical solution technique applied for both.

Error source 5 refers to the modelling of individual and coupled heat transfer mechanisms, and error source 6 refers to the numerical solution of these mechanisms. Error source 7 is self-explanatory.

At the most simplistic level, internal validation in the past has involved comparing measured long and short-term building performance data to simulated data. The long-term performance data generally show total energy usage for a period several times longer than the time constant of the building. This is to allow initialization effects to stabilize. Short-term performance data usually show average hourly temperature and hourly integrated energy fluxes. These data depend somewhat on the code solution technique and output capabilities. In either case, system level data is inconclusive because at this level of validation, many algorithms in each program are exercised simultaneously. As with external errors, if the calculated and measured performances disagree significantly, we cannot determine the internal source of disagreement. If close agreement is obtained, we cannot ascertain whether this is due to compensating internal errors. We must therefore find ways to control, measure, or eliminate simultaneous internal errors, through detailed instrumentation of the building and by selecting relatively simple buildings.

A building energy analysis simulation code contains literally hundreds of variables, parameters and algorithms. Ideally, validating an entire program would involve testing each algorithm in isolation and combination at some reasonable maximum and minimum value for each parameter. This would be

impossibly expensive and time consuming. Even instrumenting a single building to the level necessary for one empirical validation test is a lengthy and expensive process. Therefore, validation test cases should be selected with great care, and the validation tests should be sequenced to obtain the most information from the least expenditure of time and resources.

One way to do this is to look at the structure of the simulations themselves. Most of them are divided into distinct blocks for modelling loads, systems, and plant. The loads portion determine the envelope load on the building. The systems portion deals with controls and distribution systems. The plant portion models the primary boilers, furnaces, or chillers that power the system. The loads portion of a simulation has the most general effect on all other portions of the program, especially in passive buildings. If a particular algorithm for a piece of equipment is faulty, this will not affect the final results unless that piece of equipment is used in the simulation. However, if a basic heat transfer algorithm is faulty in the loads block, all results obtained with the program must be suspect regardless of the accuracy of the rest of the program. For this reason, the approach has been to focus first on the ability of BEAS to correctly calculate envelope loads.

Extrapolations

Because of the great number of parameters in any BEAS, five extrapolations are frequently made in validation studies as shown in Table 4.2 and described in the following sections.

a. Extrapolation No. 1

Since testing under every weather condition is impossible, a few representative climates must be selected to stress different heat transfer mechanisms. Testing in one climate can easily conceal large errors in a code, so two or more very different climates should be used. This kind of concealed error was revealed in a SERI comparative study

where a simple direct-gain building was modelled (4). Using Madison, Wis., TMY (typical meteorological year) weather data, it was found that BEAS agreed within ± 0.5%. When Albuquerque, N.Mex. TMY weather data was used, the codes disagreed by as much as 50%. In IEA Task VIII, Denver and Copenhagen climate data were used.

TABLE 4.2 EXTRAPOLATIONS MADE IN VALIDATION STUDIES

	Obtainable Data Points	Extrapolations
1.	A few climates	Many climates
2.	Short-term (monthly) total energy usage	Long-term (yearly) total energy usage
3.	Short-term (hourly) temperatures or fluxes	Long-term (yearly) total energy usage and temperature extremes
4.	A few buildings representing a few sets of variable mixes	Many buildings representing many sets of variable mixes
5.	Small-scale, simple test cells and buildings	Large-scale complex buildings

b. Extrapolation No. 2

Long-term (yearly) empirical tests are generally impractical, so most parameters must be tested in the short term. Based on the short-term accuracy of the program, (usually a week to a month), the extrapolation must be made to the yearly accuracy of the program. Unfortunately, short-term tests tend not to reveal small additive errors, and only certain heat transfer mechanisms may be stressed by the particular short-term weather sequence at the time of the test. In IEA Task VIII, Denver and Copenhagen typical annual hourly weather data were used in addition to the weather measured at the test building sites to control this effect.

c. Extrapolation No. 3

It is difficult to tell what effect short-term temperature discrepancies will have on the accuracy of long-term energy usage prediction. The relationship between hourly temperature measurements and yearly energy prediction in part depends on other parameters in the simulation such as the thermostat control strategy used. For example, if the upper or lower limit of a dead band frequently falls between the extremes of predicted and actual temperature as in Fig. 4.3a, nontrivial, total energy usage differences could occur even though predicted hourly temperatures were quite close. However, if predicted and actual temperatures are frequently within the dead band when they disagree, then the effect on total energy usage would be small even though the temperature differences were relatively large as in Fig. 4.3b. In addition, even if the temperature is accurately predicted, the algorithms that calculate energy loads based on temperature could be faulty.

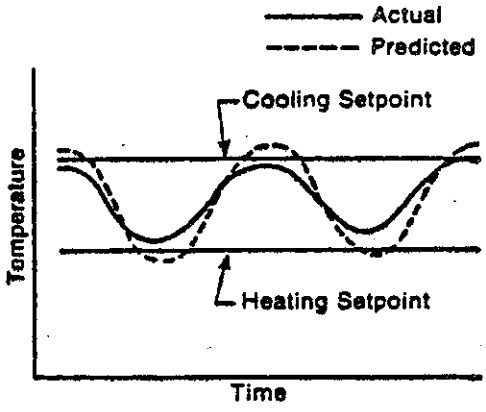

Fig. 4.3a Deadband limits between measured and calculated temperatures.

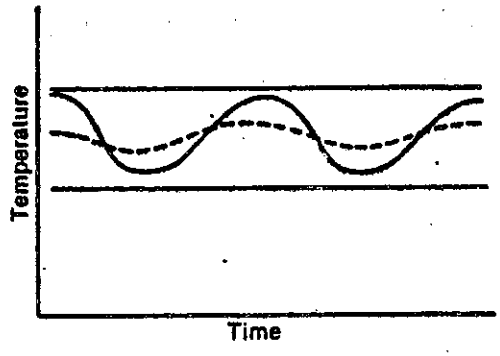

Fig. 4.3b Deadband limits outside measured and calculated temperatures.

d. Extrapolation No. 4

Extrapolation No. 4 is unavoidable since it is impossible to test the simulation against every conceivable building

that the simulation should properly handle. This would eliminate the need for the simulation itself, since we would already have data on every building that we could simulate. Therefore, we must select configurations that stress those heat-transfer mechanisms representative of the kinds of buildings with which we are most concerned. In Task VIII, a two-zone direct gain configuration, an attached sunspace, and a trombe-wall configuration were selected.

e. Extrapolation No. 5

It would be prohibitively expensive to achieve the same level of instrumentation and control in a large commercial building as in a small residence. Therefore, it is necessary to extrapolate from the ability of the simulations to accurately calculate small building envelope loads to their ability to handle large building envelope loads. This is an acceptable extrapolation since small buildings are dominated more by skin loads than larger buildings. However, in large buildings the accuracy of BEAS in modelling the systems and plant response needs to be checked in addition to the response to skin loads.

4.2.2 Methodological approach

Each comparison between measured and calculated performance represents a single data point in an immense N-dimensional parameter space. Budget and time constrain the problem to establishing very few data points within this space. Yet, we must somehow be assured that the results at these points are not coincidental and are representative of the validity of the simulation elsewhere in the parameter space. The validation approach is an attempt to minimize the uncertainty of the extrapolations we must make in any validation study by using three related techniques:

- Comparative studies
- Analytical verification
- Empirical validation.

These three approaches are shown schematically in Fig. 4.4. Each approach focuses on different aspects of the validation problem. By integrating these approaches in the overall process, the advantages of each are enhanced and the disadvantages minimized.

Comparative studies

A comparative study involves a direct comparison of the results obtained from two* or more BEAS using equivalent input. The comparative study is a useful technique because it does not require data from a real building. Buildings can be created and placed in a real or imagined environment such that various heat transfer mechanisms are stressed as desired. The investigator has complete control over the accuracy of the input, and all external errors are easily eliminated. Comparisons may be sequenced to test the sensitivity of the simulations to various input modifications. Comparative studies quickly show if further, more detailed investigation is merited. A large number of different test cases can easily be run in a relatively short time. Proper sequencing of test cases indicates those portions of the simulation that should be investigated in detail. Test cases may be simpler than any real building, or as complex and realistic as needed. Internal discrepancies may be investigated by defining test cases that successively eliminate or add various transfer mechanisms.

The great disadvantage of the comparative technique is the absence of a truth model. For this reason the comparative study is best done using BEAS with very different modelling and solution approaches. If several simulations based on similar modelling approaches agree, it is still quite possible that they are all incorrect. If several simulations based on

---

* A code may be run against itself to quantify the effect of using one subroutine versus another. This is similar to a parametric study where one parameter is varied in the building to quantify the sensitivity to that parameter.

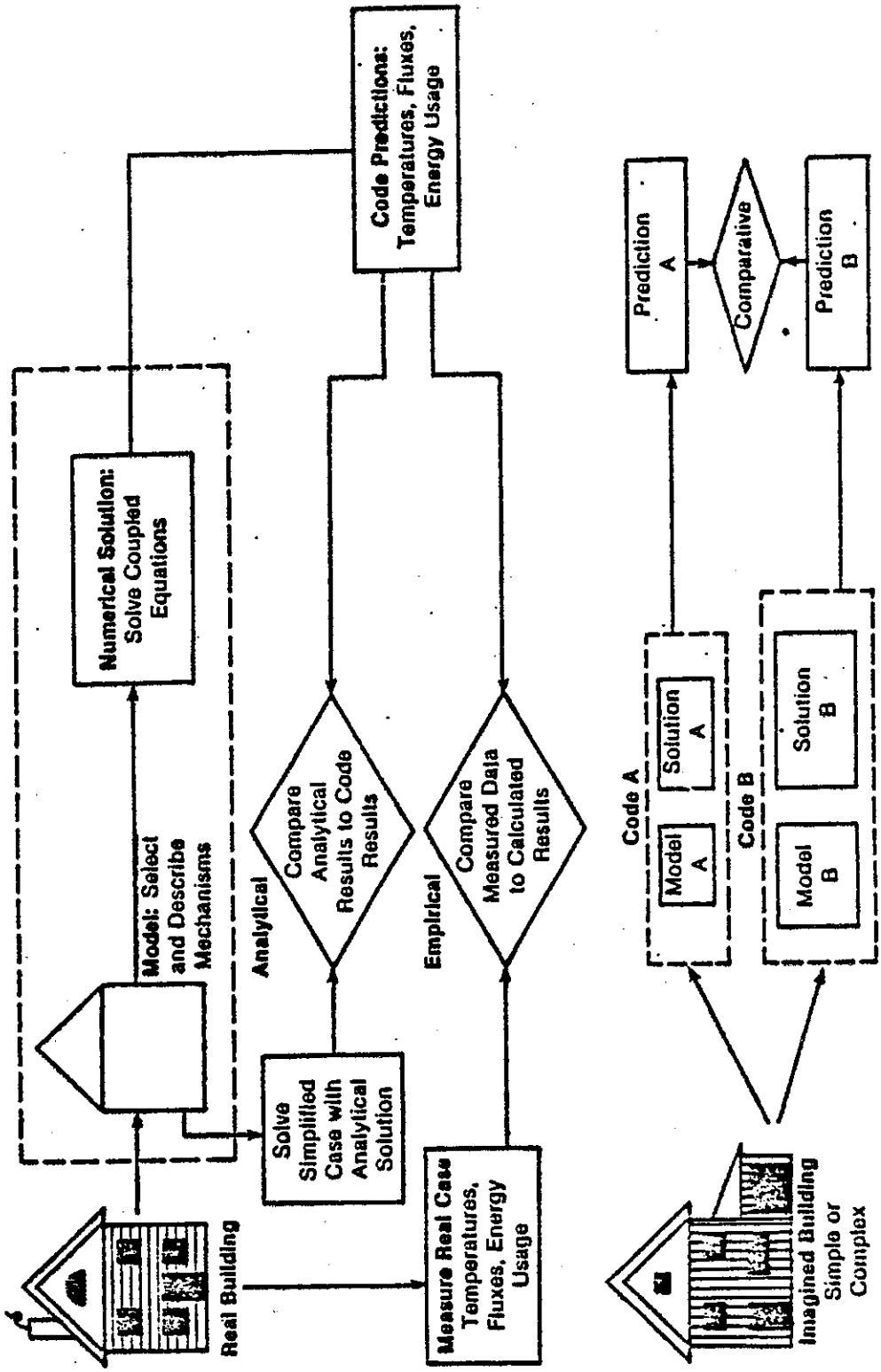

Fig. 4.4. Analytical, empirical and comparative techniques.

completely different modelling approaches agree on a number of different test cases, it is likely that the physical systems are being well characterized.

Because of the lack of a truth model, the comparative technique is most powerful when used with the analytical and empirical technique. The comparative technique may be used before empirical validation studies are done to identify the need for empirical validation and to define the level of empirical validation needed. For example, if most BEAS agree on analyses of conventional buildings but disagree on passive buildings, we design our empirical validation study to test passive building types. If the simulation always agree in the loads portion of the program but diverge when systems and plant are included, we then know how to design our empirical validation study to include these factors.

The comparative technique is also useful after an empirical validation study has been completed since it allows us to extrapolate the results of the empirical validation test cases to other cases. For example, assume that we record data on a building in Ottawa, Canada, and that after some corrections to the BEAS we are able to obtain close agreement for both long and short-term data with several of the simulations. We can quickly test the generality of these results by simulating the test building in several different climates. If close agreement between codes is still obtained, we can then vary the building to establish the range of building types within which the programs are validated. Any case in which the results diverge is useful for defining an empirical validation study if the cause of the divergence cannot be found through less expensive means.

Analytical verification

A typical building energy analysis simulation program contains hundreds of variables and parameters. The number of possible cases that can be simulated by varying each of these parameters

in combination is astronomical and can never be fully tested. However, universal to the accurate calculation of any case are the fundamental heat-transfer mechanisms of conduction, radiation and convection. It is possible to define simple test cases that can be solved analytically and that can also be simulated using BEAS. These cases can be defined to test those fundamental heat-transfer mechanisms that, in isolation or limited combination, have the greatest impact on building thermal performance (5). These analytical test cases are much simpler than real buildings in that the boundary conditions are strictly controlled so they can be solved analytically. The power of this technique is that major errors in the thermal solution algorithms of a simulation may readily be identified and isolated.

The analytical solution is the truth model, and all the uncertainty of simultaneous error sources is eliminated. The disadvantage of this technique is the limited number of configurations and combined mechanisms for which analytical solutions may be derived. Additionally, analytical verification can only test the correctness of the numerical solution (internal error source 6). It cannot test the correctness of the model itself. Even though a simulation may pass all analytical tests, it may not be correct when used on real buildings. However, the power of analytical verification is increased when used with the comparative study technique. By starting with the very simple analytical test case, baseline agreement may be established between different BEAS and the analytical solution. The test cases may then be modified one parameter at a time toward the more complex case of a real building. The point at which BEAS diverge indicates an area for investigation with empirical techniques. Additionally, the disagreement is easily quantified so that the value of a sophisticated and time consuming algorithm may be assessed against that of a simplified approach.

Empirical validation

In empirical validation a real building or test cell is instrumented and the calculated results from BEAS are compared to the measured results obtained from the instrumentation. A disadvantage of this technique is the uncertainty associated with measurement error. The comparison variables are uncertain because of direct measurement error. Measurement error also causes a degree of input uncertainty that when propagated through the simulation leads to some output uncertainty. The total uncertainty consists of both these uncertainties. For purposes of validation, deviations between measured and calculated values significantly beyond these uncertainty bands are attributed to either a modelling or numerical solution problem (error sources 5 and 6 or 7) given that all inputs have been measured.

For the more highly controlled levels of validation, an extremely detailed level of data acquisition is required. This level of data acquisition has been termed a Class A system by investigators in the field (1,10). This system requires many sensors for relatively simple buildings, and the building must be unoccupied to control external error source 2. There are very few Class A sites. The purpose is to attempt to measure all key input and output quantities. In IEA Task VIII, three sites were selected which appeared to meet "CLASS A" criteria.

The empirical, analytical and comparative techniques combined

Empirical validation is so time consuming and expensive that the empirical test cases must be chosen with great care. The analytical and comparative techniques provide information that help define and prioritize the empirical test cases. Once empirical data are collected, the comparative technique allows us to extrapolate to cases for which we have no empirical data.

Table 4.3 shows the advantages and disadvantages of each technique. When used separately, they fail to provide enough information for an overall validation. However, when used together, they form a powerful validation methodology.

TABLE 4.3 VALIDATION TECHNIQUES

Technique	Advantages	Disadvantages
Comparative Relative test of model and solution process	No input uncertainty Any level of complexity Inexpensive Quick: Many comparisons possible	No truth standard
Analytical Test of numerical solution	No input uncertainty Exact truth standard given the simplicity of the model Inexpensive	No test of model Limited to cases for which analytical solutions can be derived
Empirical Test of model and solution process	Approximate truth standard within accuracy of data acquisition system Any level of complexity	Measurement involves some degree of input uncertainty Detailed measurements of high quality are expensive and time consuming A limited number of data sites are economically practical

The flow diagram in Fig. 4.5 shows how these techniques are used together. The first step is to run the codes against available analytical test cases (6). This checks the numerical solution of the major heat transfer models in the code. If a discrepancy occurs, the source of the difference must be identified and corrected before any further testing is done. The next step is to run the codes against available Class A empirical validation data and to correct obvious discrepancies. Comparative studies or successive parametric runs can be used at this point if necessary to assist in identifying the source of a discrepancy. The next step is to define comparative test

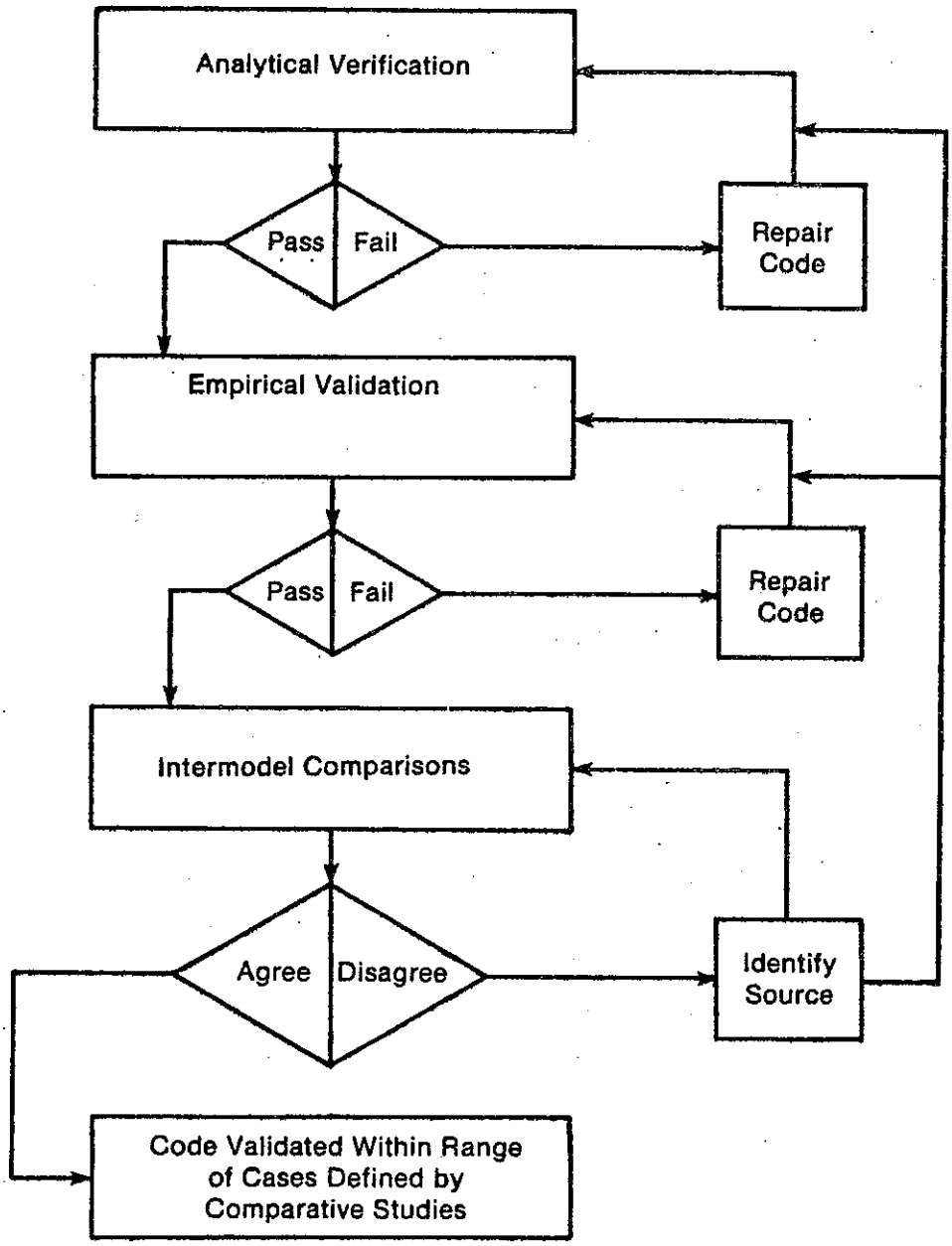

Fig. 4.5 Flowchart of validation methodology.

cases which help us to extrapolate beyond the empirical test cases. These comparative cases can serve to define a range of building and climate types for which the codes may be used with confidence.

The comparative studies also help in the definition of new empirical or analytical studies when unacceptable divergence between codes is observed. Once a code has been run through this process it can be reasonably used in the testing of simplified design tools as long as the test cases are within the range of validated cases.

The approach used in the validation study documented in this report was to focus on the comparative and empirical aspects of the methodology. This was decided because most of the participants stated that the codes developed in their respective countries had already been subjected to analytical tests. Besides the work documented in this context, the Subtask B participants have undertaken two other comparative studies using a subset of the simulation programs. A design tool evaluation exercise was undertaken and documented under Subtask C of this task, and within Subtask B a working group is currently working on model-to-model comparative studies on a so-called shoebox, a simple building structure for which very detailed model input specifications have been worked out. The outcome of these activities will be documented in 1987.

REFERENCES

1. A Methodology for Validating Building Energy Analysis Simulations. SERI/TR-254-1508, 8/83. Judkoff, Wortman, O'Doherty, Burch.

2. DOE-2 Reference Manual. Edited by York, LBL-7689-M Ver. 2.1, 5/80.

3. BLAST Users Manual. Hittle, Herron, Walton, Lawrie, Cameron. University of Illinois, Urbana-Champaign. Blast Support Office, 6/79.

4. "A Comparative Study of Four Building Energy Simulations: Phase II, DOE-2.1, BLAST-3.0, SUNCAT-2.4, and DEROB-4". Judkoff et al. SERI/TP-721-1326, 8/81.

5. "The Implementation of an Analytical Verification Technique on Three Building Energy Analysis Codes: SUNCAT-2.4, DOE-2.1, and DEROB III. SERI/TP-721-1008. Wortman et al., 1/81.

6. Installation Manual: SERI Class B Passive Solar Data Acquisition System. Frey, McKinstry, 3/81.

7. "Passive Solar Homes: A National Study". SERI Technical Information Branch, 1984.

8. "Comparison of Load Determination Methodologies for Building Energy Analysis Problems". IEA Confidential Memo, IEA Energy Conservation, Buildings and Community Systems, Annex 1, Jan. 1981.

9. Design Tool Survey. IEA Task VIII, SUBTASK "C". P.R. Rittelman, S.F. Ahmed, Burt, Hill, Kosar, Rittelman Assoc. Butler PA, USA, 1/85. DRAFT.

10. "Program Area Plan: Performance Evaluation of Passive/Hybrid Solar Buildings". Solar Energy Research Institute Report, SERI/PR-721-788, October 1980. Holtz, M.J., Hamilton, B.

11. Erhorn, H., Stricker, R., Szerman, M. Sunspace Calculation Comparison SUNCODE-DEROB. Working document IEA Task VIII, Fraunhofer Institut für Bauphysik, Stuttgart, May 1986.

5. DIRECT GAIN MODEL VALIDATION

5.1 Introduction

This chapter presents the validation efforts by the participating countries for the direct gain system case. This effort involved seven countries using twelve simulation models. These are all listed in Table 5.1.

TABLE 5.1 LIST OF SIMULATION PROGRAMS

Country	Simulation Program
Canada	ENCORE-CANADA
Denmark	BA4, PASOLE, SOLMAT
Italy	SMP
Norway	ENCORE
The Netherlands	BFEP, KLI/PAS
United Kingdom	ESP
USA	BLAST-3.0, DOE-2.1A, SERIRES-1.0

The building used for the validation is one of the test units monitored at the National Research Council of Canada as part of the Passive Solar Test Facility.

In this chapter the test building is described along with all the supplied physical and monitored data. Input data files are compared to the supplied data and the simulation results of each model are presented. Finally, the results of a yearly simulation of the same test unit using Copenhagen weather data are presented and compared.

5.2 Description of the Test Unit

All simulation runs were performed for unit 3 of the test facility (1). The unit, the floor plan of which is shown in Fig. 5.1, consists of a south and north room with

a connecting door. The north room opens onto a corridor through an insulated steel door (thermal resistance of 1,25 $m^2 \cdot$ K/W) fitted with magnetic edge seals. Each south room has a south-facing window of 2.6 m^2 net glass area; each north room has a 1 m^2 window facing north. All the windows are of the casement type containing sealed double-glazing with an air-space thickness of 6.35 mm (thermal resistance of 0.35 $m^2 \cdot$ K/W). The interior surfaces of all the walls and ceilings (other than mass walls) are finished with an off-white paint and the floors are carpeted.

The building itself (containing Units 3 and 4) is a one-storey insulated wood-frame superstructure over a basement. The exterior walls and the roof of the above-grade construction have thermal resistance values of 2.1 and 3.5 $m^2 \cdot {}^{o}C/W$, respectively. Since the basements are being used for the study of basement heat loss, the floors of the solar units were insulated to a resistance value of 7 $m^2 \cdot$ K/W. The measured air exchange rate was close to zero for all rooms and units.

All interior walls of the units are lined with a 100 mm course of solid cement bricks, as shown in Fig. 5.2, except for the wall between the south and north rooms which is made of a single course of the same brick.

Data was supplied for the unit operating in two modes. In the first mode, the unit is monitored as two separate rooms; in the second mode the connecting door is opened and air is circulated between the two rooms using a small fan (2.8 m^3/min) located above the door. The unit was modelled only in Mode 2.

Each of the rooms in the test facility is heated individually with an electric baseboard heater driven by a precision controller to avoid the temperature variations caused by conventional room thermostats. In addition, the south room of the two-zone unit is equipped with an exhaust fan which cools the room with outdoor air whenever the room temperature reaches a preset maximum. The exhaust fan is controlled by the space-heater controller.

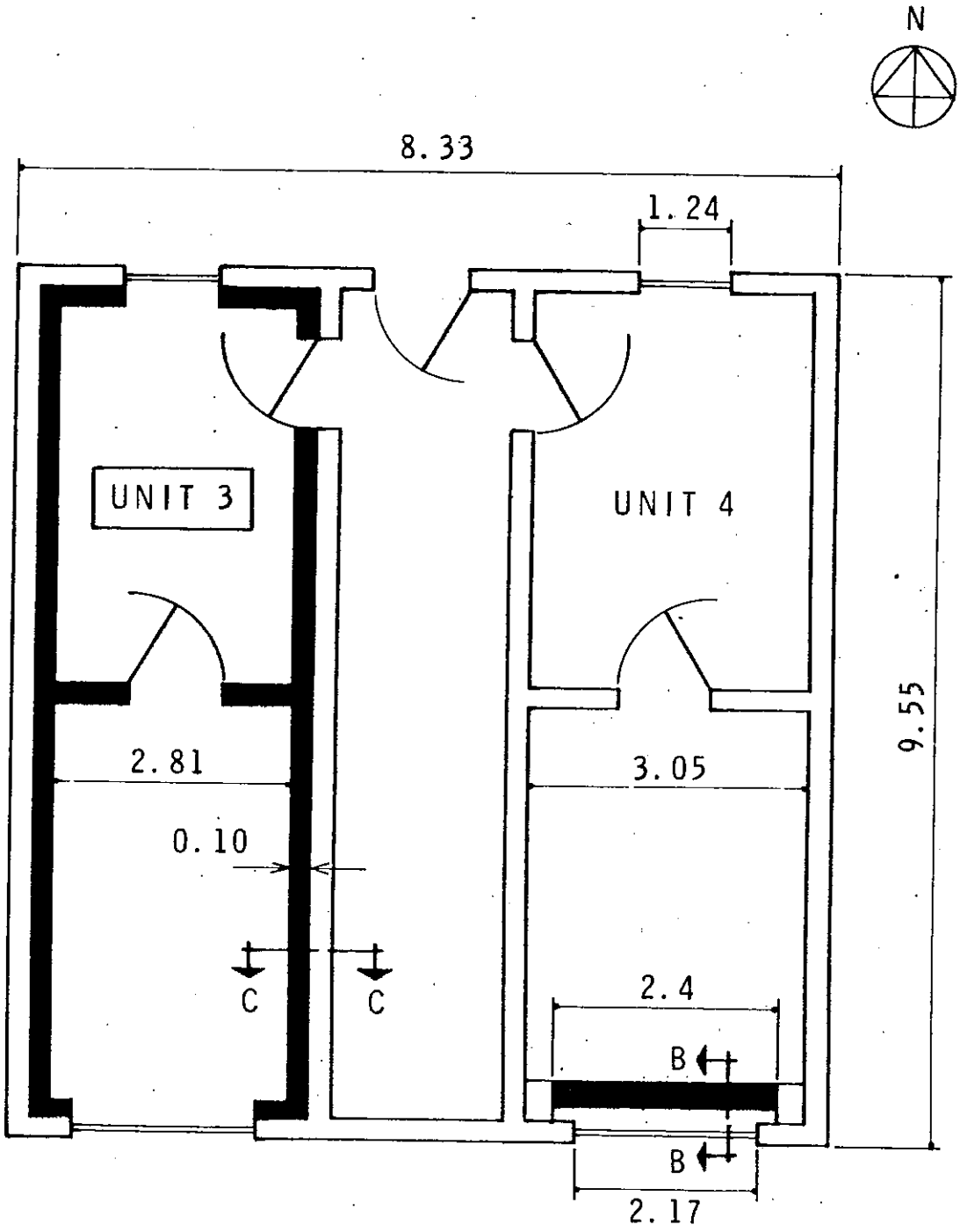

Fig. 5.1 Plan of test unit (unit 3).

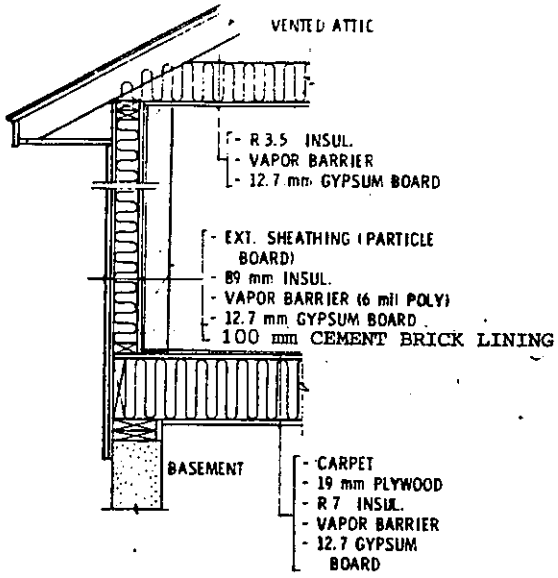

(a) Exterior wall construction, unit 3.

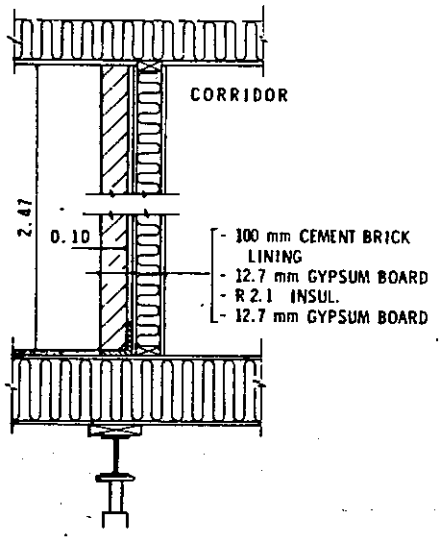

(b) Corridor wall construction, unit 3.

Fig. 5.2 Construction details of test facility (thermal resistance values - $m^2 \cdot K/W$).

A summary of the characteristics of the Unit given as input data is given in Tables 5.2, 5.3 and 5.4.

TABLE 5.2 CHARACTERISTICS OF TEST UNIT

Room length, m	4.38
Room width, m	2.81
Room height, m	2.4
Floor area per room, m^2	12.3
Overall wall* thermal resistance, $m^2 \cdot K/W$	2.1
Overall ceiling thermal resistance, $m^2 \cdot K/W$	3.5
Overall floor thermal resistance, $m^2 \cdot K/W$	7.0
Gross south window area, m^2	3.4
Net south window glass area, m^2	2.6
Gross north window area, m^2	1.4
Net north window glass area, m^2	1.0
Window glazing thermal resistance, $m^2 \cdot K/W$	0.35
Window frame thermal resistance, $m^2 \cdot K/W$	0.37
Partition door area, m^2	1.65
Partition thermal resistance, $m^2 \cdot K/W$	0.44
Corridor door area, m^2	1.9
Corridor door thermal resistance, $m^2 \cdot K/W$	1.25
Circulation fan power, Watts	21
Heating set point, ^oC	20
Heating Controller deadband, ^oC	o.1
Ventilation set point, ^oC	27
Basement temperature, ^oC	21
Corridor set point temperature, ^oC	20
Thermal storage mass, kg	13,565
Heat capacity, MJ/K	11.55
Infiltration rate, ach	~ 0.0

* All walls are of wood frame construction, 38 x 89 mm studs at 0.6 m centres

TABLE 5.3 DETAILS OF BUILDING ELEMENTS

ELEMENT TYPE	CONSTRUCTION	THERMAL RESISTANCE ($m^2 \cdot K/W$)
Wall, heavy (Unit 3)	Cement bricks, Gypsum board, Insulation, Particle board	2.04
Internal Partition, heavy	10 cm Brick	0.06
Window, double glazed	Glass, Air space, Glass	0.2
Metal insulated door		1.03
Wood partition door		0.2
Ceiling	Gypsum board, Insulation	3.33
Floor	Carpet and underlay, Wood Insulation, Gypsum board	7.34
Outdoor air film		0.03
Outdoor air film, Ceiling/Attic		0.09
Indoor air film, Walls		0.12
Indoor air film, Ceiling		0.11
Indoor air film, Floor		0.09

TABLE 5.4 PROPERTIES OF ROOM THERMAL MASS

PROPERTY	GYPSUM BOARD	CEMENT BRICKS	CARPET AND UNDERPAD
Density kg/m^3	800	2114	650
Specific heat J/(kgK)	837	837	1380
Thermal Conductivity W/mK	0.16	1.5	0.06
Solar absorptance (measured)	0.26	0.66	0.92
Normal emittance (measured)	0.88	0.91	0.84

Weather Data

The weather data supplied were actual measurements at the test site in Ottawa, Canada. It includes hourly values (averages or totals integrated over the hour) for 14 days (December 29, 1980 to January 11, 1981).

The following hourly weather parameters were supplied:

Average outdoor air temperature, ^{o}C

Total global horizontal radiation, W/m^2

Total vertical south radiation, W/m^2

Total vertical north radiation, W/m^2

Direct normal solar radiation, W/m^2

Average wind speed, km/h

Wind direction, deg.

Plots of the weather values supplied on the tape are given in Figs. 5.3 and 5.4.

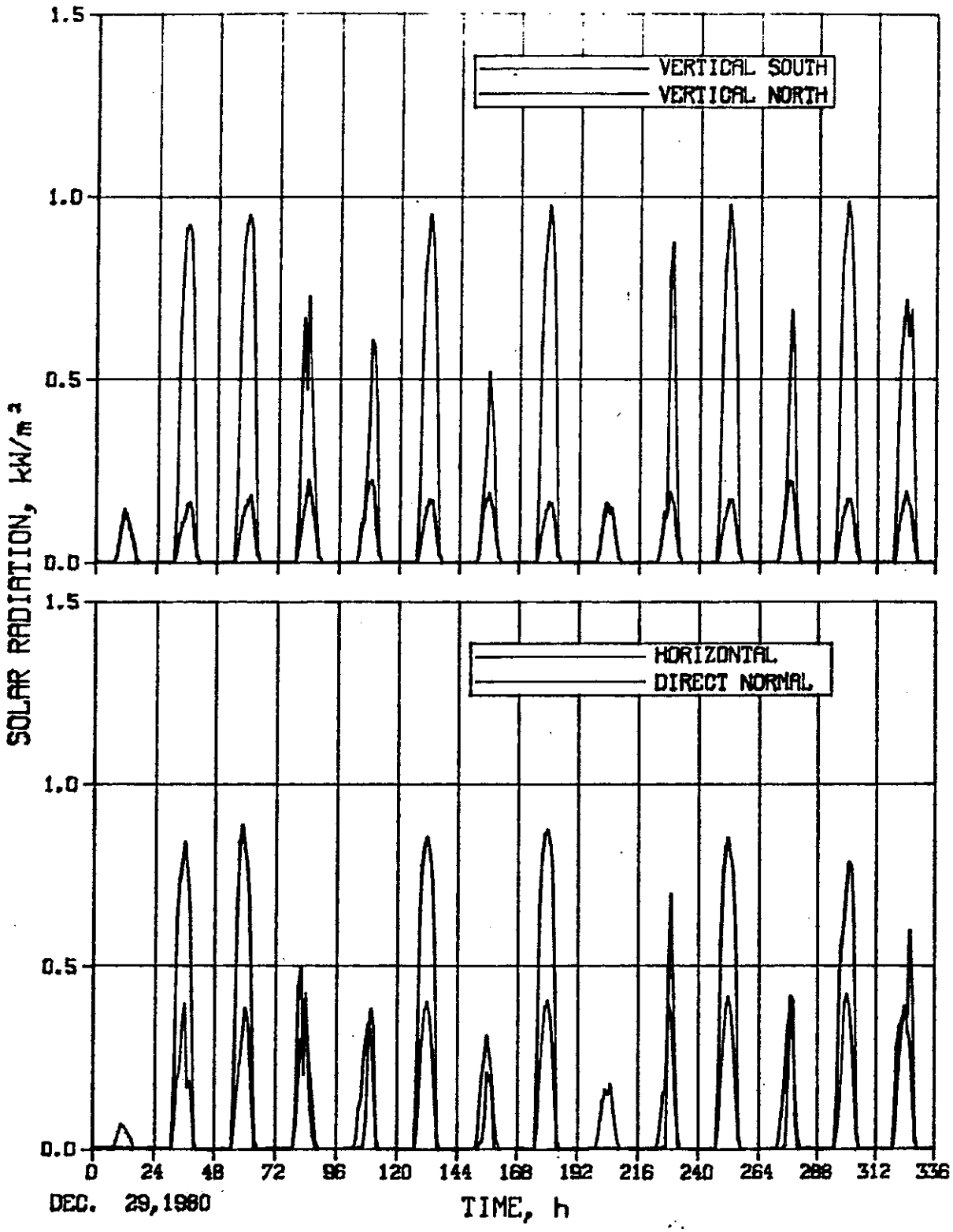

Fig. 5.3 Solar radiation data.

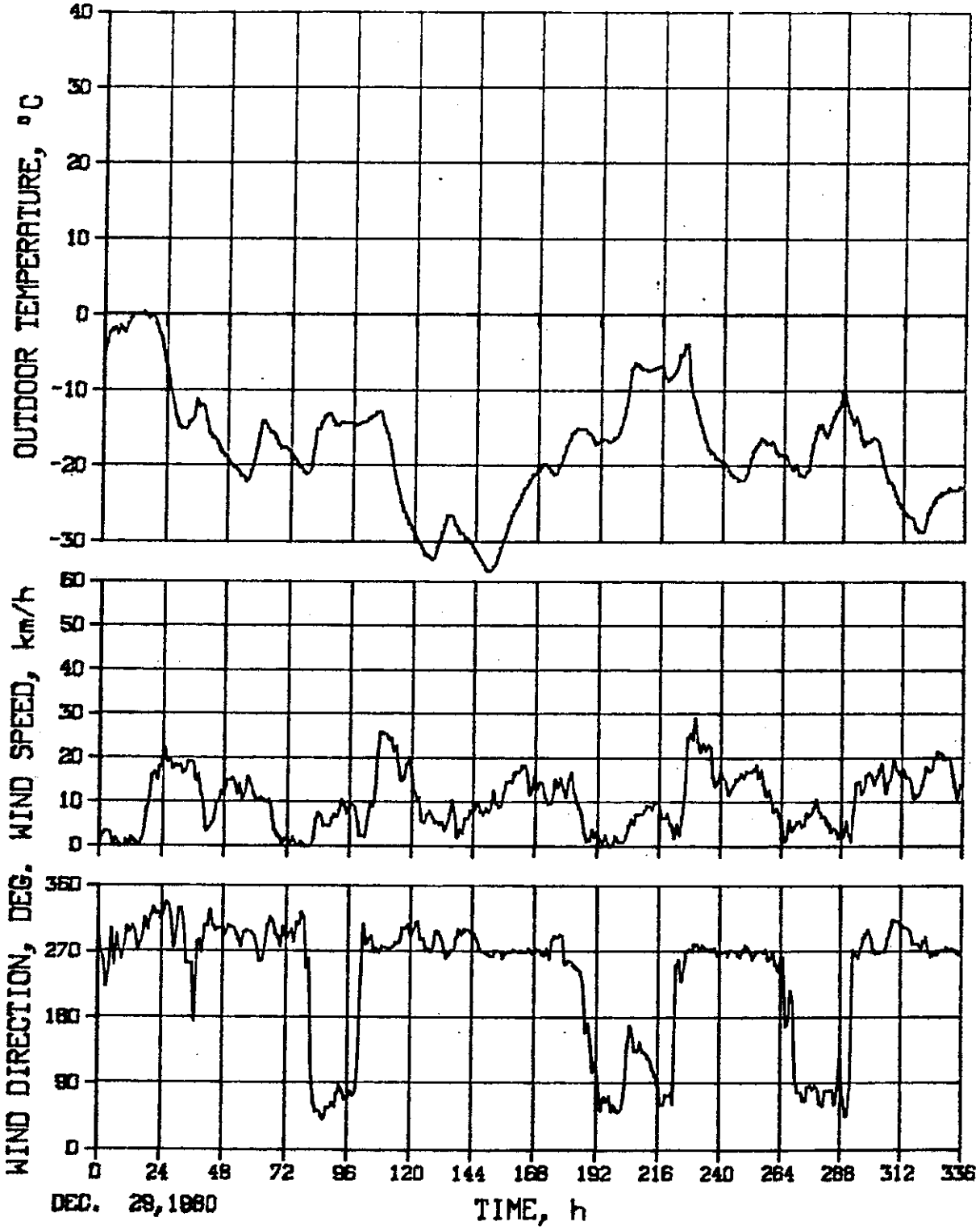

Fig. 5.4 Outdoor temperature and wind data.

Monitored Unit Data

On the same tape along with weather data, the following hourly monitored data were supplied for comparison with the corresponding calculated values:

Average south room air temperature, ^{o}C

Average north room air temperature, ^{o}C

Average corridor air temperature, ^{o}C

Average attic air temperature, ^{o}C

Total heating power for the unit, Watts

South room cooling (vented) energy, Watts

5.3 Summary of Simulations and Results

Before presenting the simulation results, an attempt is made here to list the input parameters and assumptions of each model as supplied by the participants. These assumptions were necessary in order to adapt the simulation model to the specific problems and input data. The results of the simulation are then presented for each model separately. Values of the total energy consumption for the two-week period are given in Table 5.5 for all models.

TABLE 5.5 COMPARISON OF MEASURED AND PREDICTED HEATING ENERGY FOR TWO-WEEK PERIOD

COUNTRY/MODEL(S)	TOTAL AUXILIARY HEATING ENERGY (kWh)	DIFFERENCE FROM MEASURE %
Measured	323	-
Canada - ENCORE-CANADA	309.1	4.3
Denmark - BA4	312	3.4
- PASOLE	300	7.1
- SOLMAT	323	0.0
Italy - SMP	312	3.4
The Netherlands - BFEP	307	5.0
- KLI/PAS	297	8.0
Norway - ENCORE	NOT REPORTED	
United Kingdom - ESP	349	-8.0
USA - BLAST	301.7	6.7
- DOE-2	285	11.8
- SERIRES	322.8	0.0

1. Country: CANADA

Simulation Model: ENCORE-CANADA

ENCORE-CANADA is a program designed to calculate the hourly energy consumption in residential buildings (2). The program uses the response factor method to calculate building loads. It has the capability of modelling multi-room buildings if individually heated. It does not take into account natural convection between rooms.

Modelling assumptions

- the test unit is modelled as separate rooms with a connecting door having a transmission coefficient of 34 W/m^2K corresponding to the air circulation between the rooms;
- the corridor is modelled as a separate space controlled to $20^{\circ}C$;
- the attic is modelled as a separate space with 0.5 ach;

- the floor is assumed to be adiabatic (no heat loss/ gain to the basement);
- the unit is simulated as a heavy structure (0.42 MJ/ m^2K);
- the program uses direct normal and diffuse components of solar radiation to calculate the solar radiation on all other surfaces;
- windows shading coefficient is assumed as 0.88.

Modelling results

The calculated hourly values of room temperature and average power consumption are given in Figs. 5.5, 5.6 and 5.7. The agreement with measured data is very good. There is a tendency to underpredict the peak room air temperature by about 1.0^{o}C which could be due to the inaccuracy of the representation of convective heat flow mechanism between the south and north room. The total energy consumption is calculated to be 309.1 kWh compared to a measured value of 323.1 kWh (a difference of 4.3%).

2. Country: DENMARK

a. Simulation Model: BA4

Program BA4 (3) calculates for a room half-hour values of room temperature utilizing a simplified method. Further it can calculate heating and cooling loads taking into account solar radiation, fixed and movable sun shading devices, varying ventilation and infiltration, electric lighting and other heat sources in the room.

Modelling assumptions

- unit is modelled as a single zone;
- temperature of the attic is assumed to be equal to ambient;
- the corridor and basement are assumed to be as one source at a constant temperature.

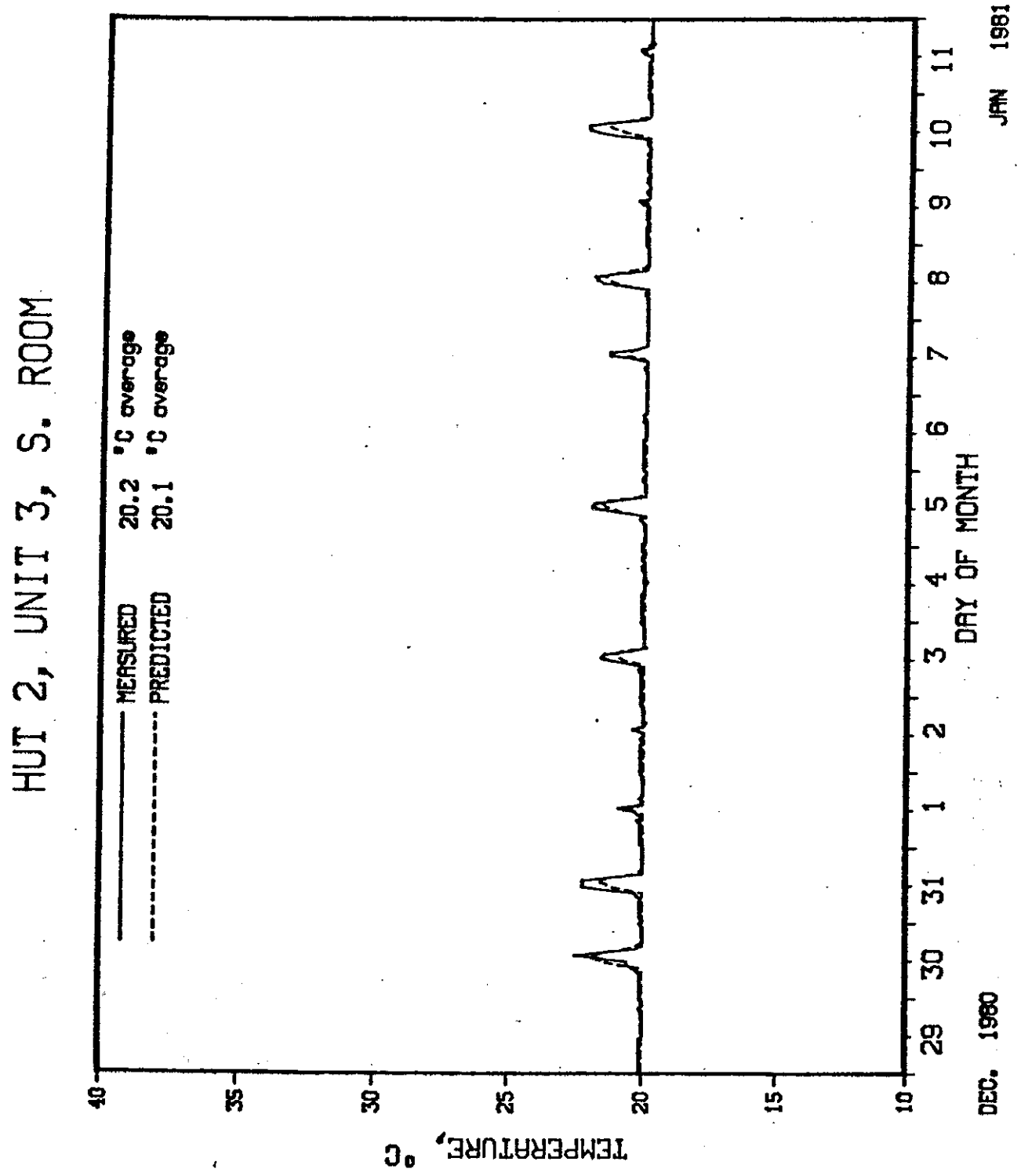

Fig. 5.5 ENCORE-CANADA results, south room temperature.

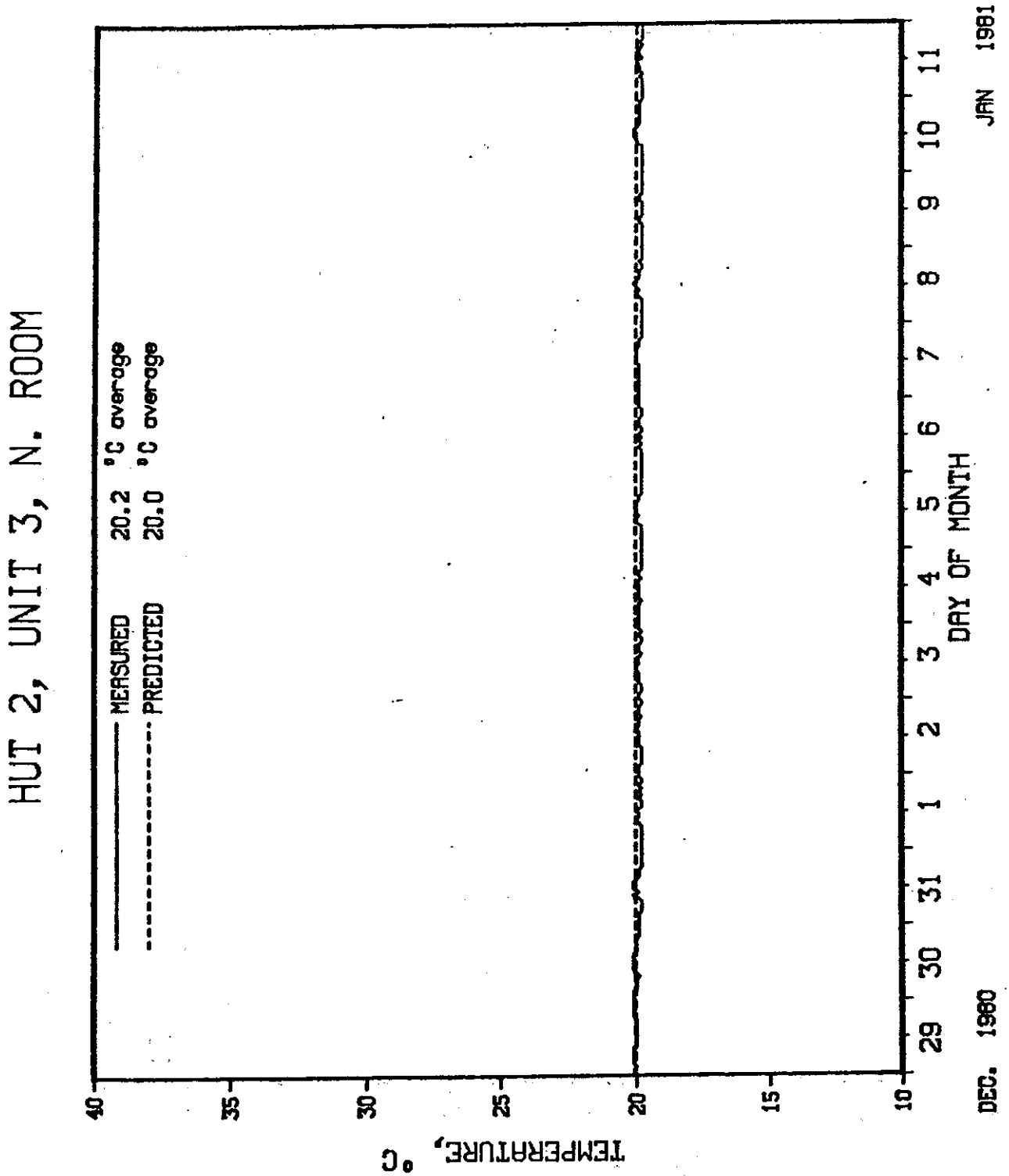

Fig. 5.6 ENCORE-CANADA results, north room temperature.

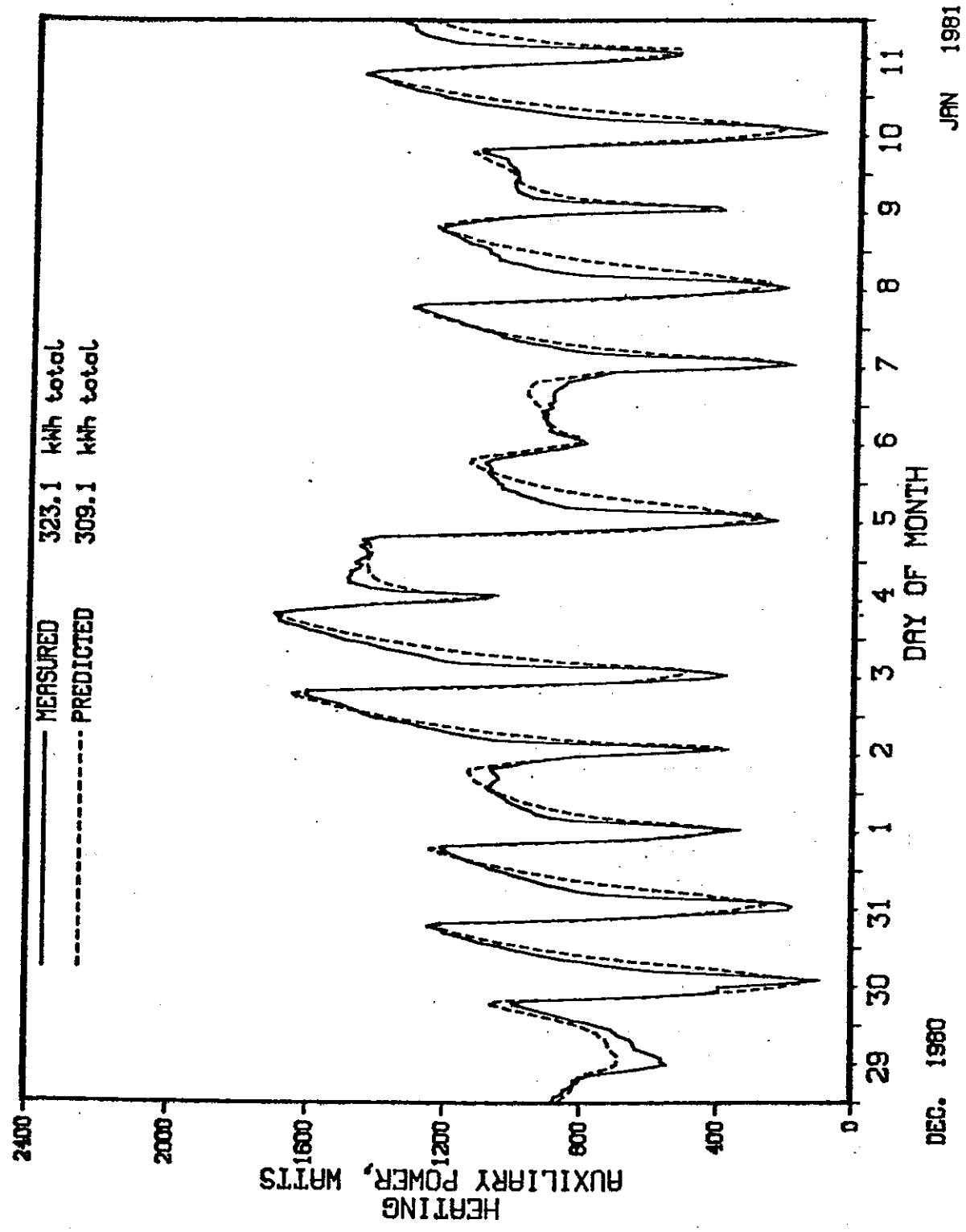

Fig. 5.7 ENCORE-CANADA results, total heating energy.

Results:

The BA4 predicted average unit temperature and energy consumption are 20.2°C and 312 kWh, respectively.

Those gross results for the two week period BA4 predictions are in good agreement with the measured data. The temperatures compared are the predicted and actual mean temperatures of the two rooms. However, the computer plots of temperature and auxiliary power shown in Figs. 5.8 and 5.9 show that the program does not predict the detailed dynamic behaviour of the test rooms very well. Peak temperatures are somewhat higher and heating power occasionally drops to zero almost every day. It seems likely that the one-zone simplification of the program is the major reason for these differences.

Another reason could be that in the BA4 program all heat accumulation of the entire building is assumed to take place in one theoretical layer. This means that the estimation of the heat transfer coefficient from the inside surfaces to this common accumulating layer is very critical. In this case it is probably too low.

b. Simulation Model: PASOLE

PASOLE is a building energy analysis program using the thermal network method (4), and it is a research tool allowing the advanced user great flexibility in modelling.

Modelling assumptions

The unit was simulated using a built-in, two-zone model, designated "a room with an attached sunspace". The thermal behaviour of the test unit resembled that of a room with an attached sunspace. The north room being "the room" with very stable temperature and heat load, and the south room being "the sunspace" acting dynamically on the solar input. Other input parameters were calculated based on the same values as used for the BA4 simulation.

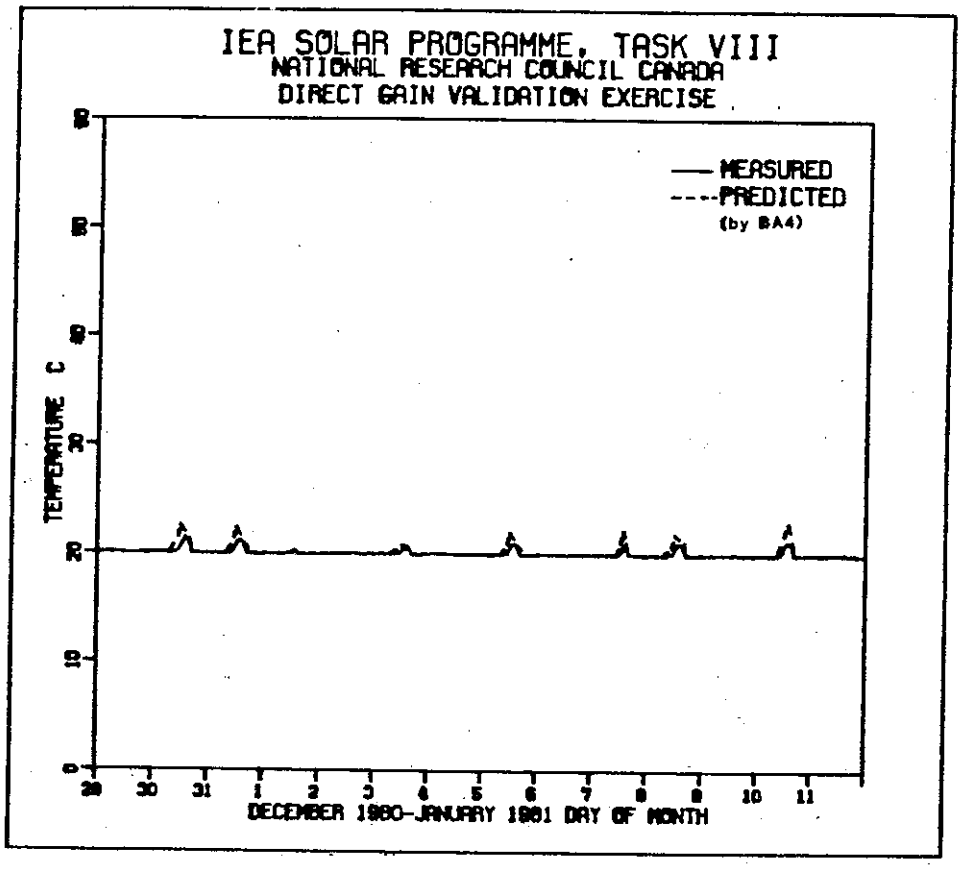

Fig. 5.8 BA4 results, mean temperature of the two rooms measured and predicted.

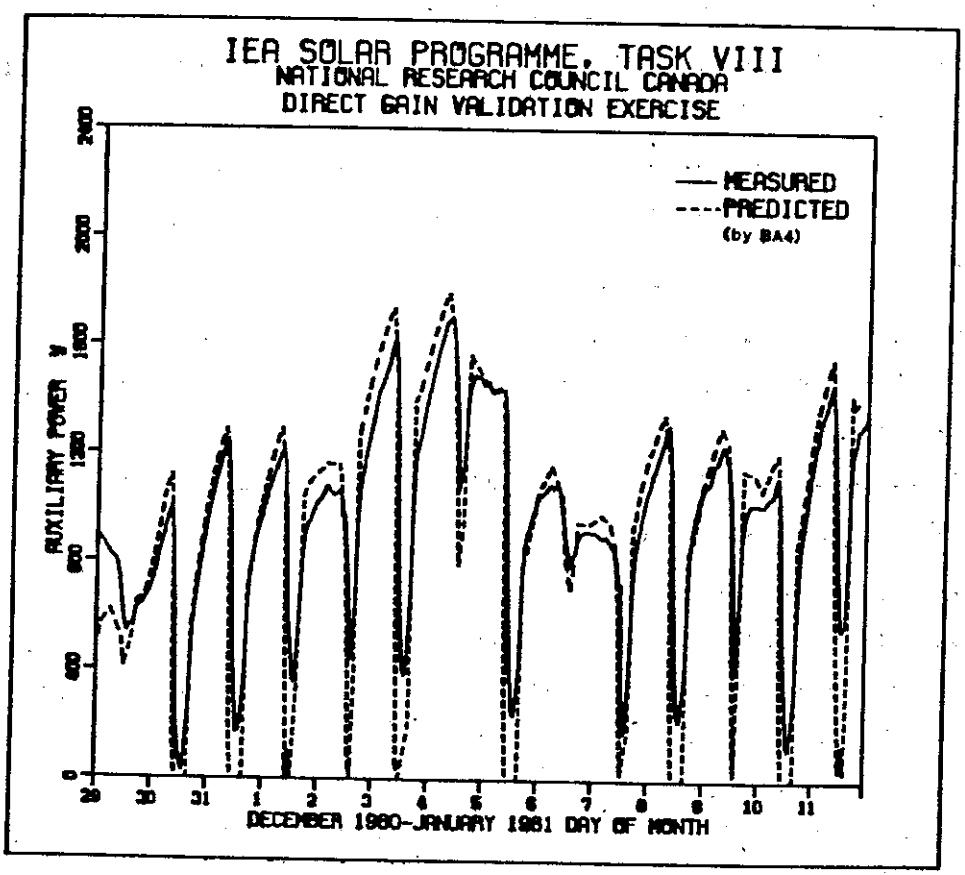

Fig. 5.9 BA4 results, auxiliary power requirement for the test building measured and predicted.

Results

According to the participant, considerable effort was put into the modelling of the system using PASOLE, and too much time was spent on making it run properly using SI units. For some reason, the attempt to adjust the solar processor of PASOLE to work on the given vertical south insolation values did not succeed. When the work had to be stopped, the predicted solar radiation on the south facade was still somewhat lower than the actual value. This is the reason for a large overestimation of the auxiliary energy (397 kWh). When the predictions for the period were corrected for that by a hand calculation, a reasonable agreement to the measured results (300 kWh) was obtained. The two plots in Figs. 5.10 and 5.11 show that the dynamic performance of the test buildings is reasonably tracked by PASOLE. The higher peak temperature predicted by PASOLE is difficult to understand as the solar input was lower. It may be an air node/mass nodes distribution problem.

c. Simulation Model: SOLMAT

SOLMAT (14) is a general thermal network model developed for a personal computer. The numerical integration of the set of equations is performed on implicit integration method by utilizing a set of inverted matrices.

Modelling assumptions

Assuming isotropicly distributed diffuse solar radiation from the sky and reflected from the ground, the direct solar radiation at the south facade was obtained by subtracting the measured global north radiation from the measured global south radiation.

A 13 capacity node network configuration was set up to model the test building. The massive concrete partition wall between the south and north zone, directly irradiated by solar radiation, was assumed to be the most dynamically active part of the construction and was consequently modelled by 3 nodes. All the other walls were modelled with 2 capacity nodes. The side and end walls towards

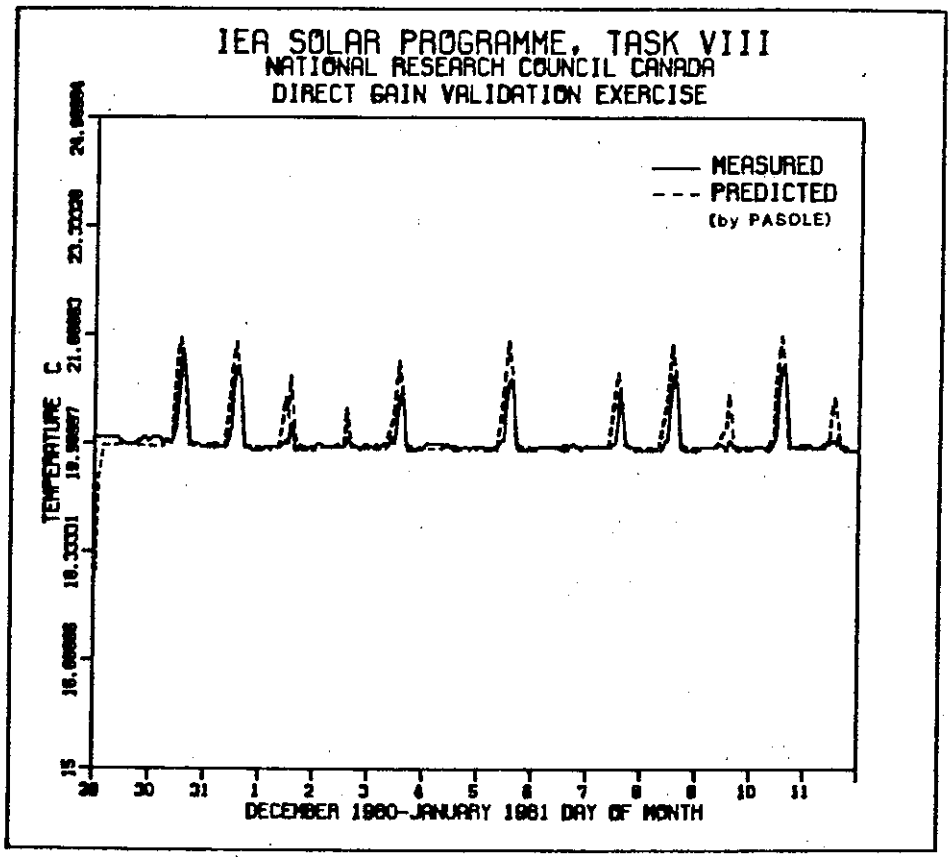

Fig. 5.10 PASOLE results, mean temperature of the two rooms measured and predicted.

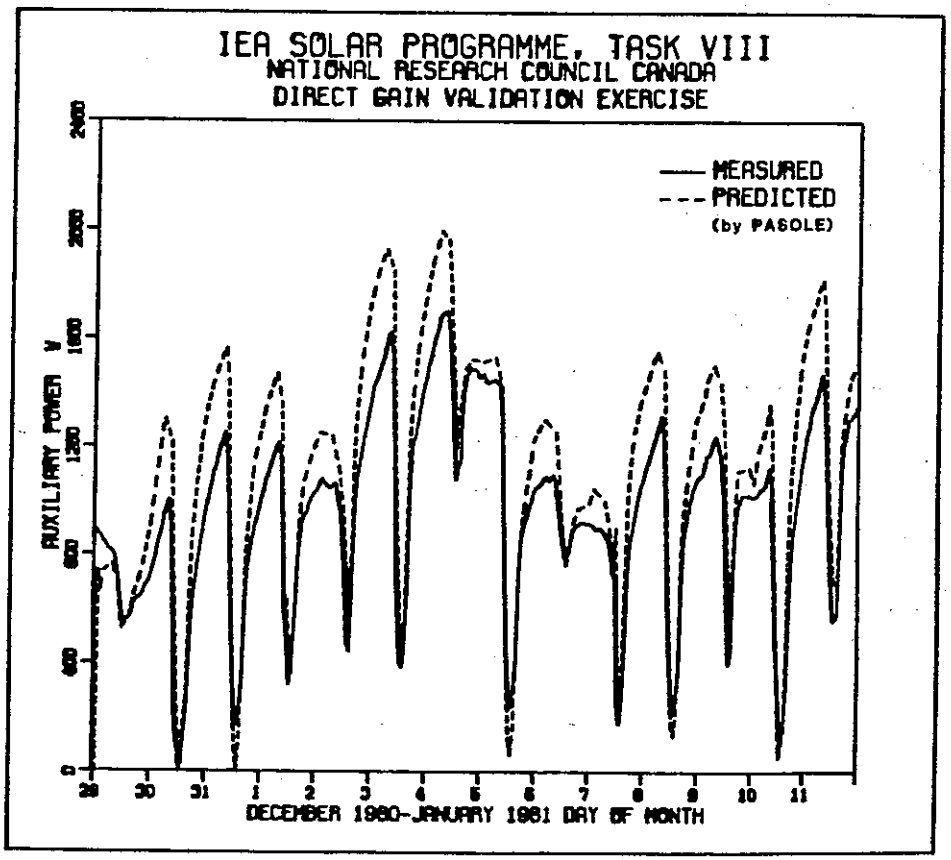

Fig. 5.11 PASOLE results, auxiliary power requitement for the test building measured and predicted.

the ambient were lumped into one wall for each zone. Finally, one node was used for each zone, covering the zone air capacity and the capacity of the surfaces of floor and ceiling.

Inter-nodal, overall heat transfer coefficients were calculated based on the λ-value and the thickness of the materials and a lumped radiation and convective film coefficient of 9 W/m^2K. For the inter-zone heat exchange, the fan coupling was modelled as a corresponding overall heat transfer coefficient.

Results

Figs. 5.12 and 5.13 present results obtained. It is seen that the model tracks the dynamic performance of the test building very well. Also for the total auxiliary heating requirement for the period, very close agreement was obtained.

The sensitivity to the distribution of incoming solar radiation was investigated by the modeller. This appeared to be very crucial for the prediction of the south zone air temperature.

Alternative modelling strategies were investigated as well and are documented in ref. 14.

3. Country: ITALY

Simulation Model: SMP

The SMP model is a finite difference model that simulates the thermal behaviour of one or two rooms thermally connected (5).

Simulation assumptions

- Exterior opaque surfaces absorptivity = 0.4.
- 99% of the incoming solar radiation is assumed to heat the floor (1% goes directly to the air).
- Assumed that the given R-values do not include the wood studs; the studs are, therefore, added as

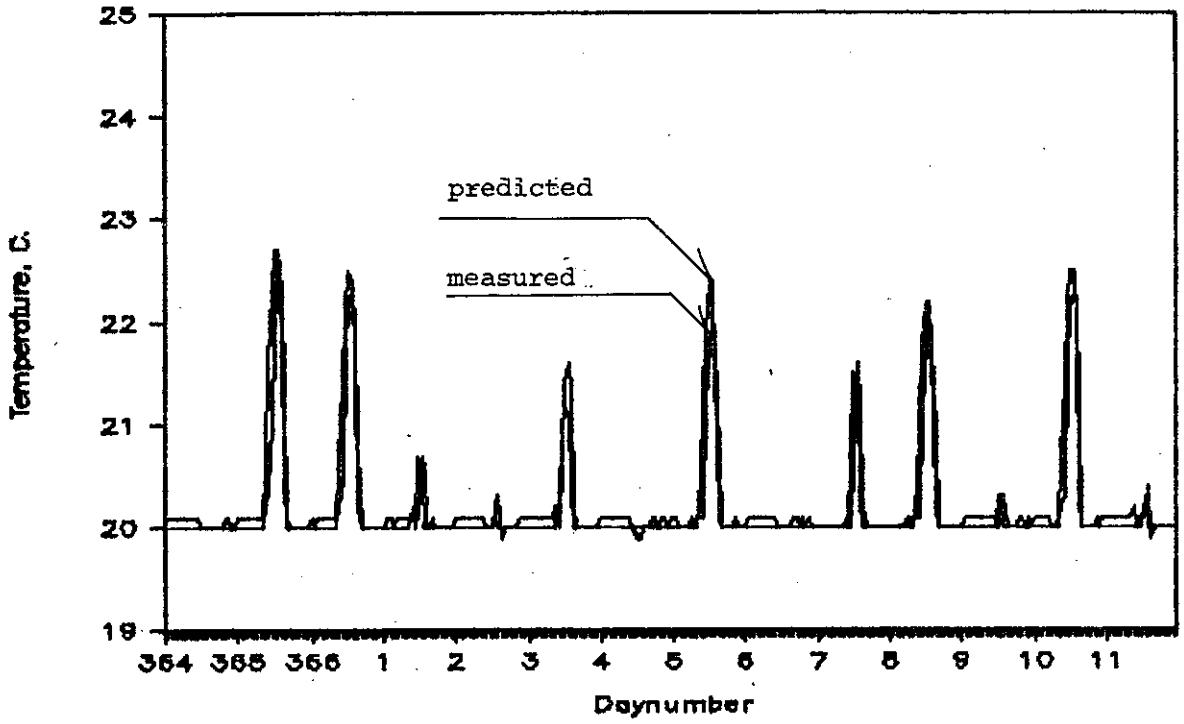

Fig. 5.12 SOLMAT direct gain validation results. Measured and predicted temperatures of south room, zone air fraction of solar gain = 0.3.

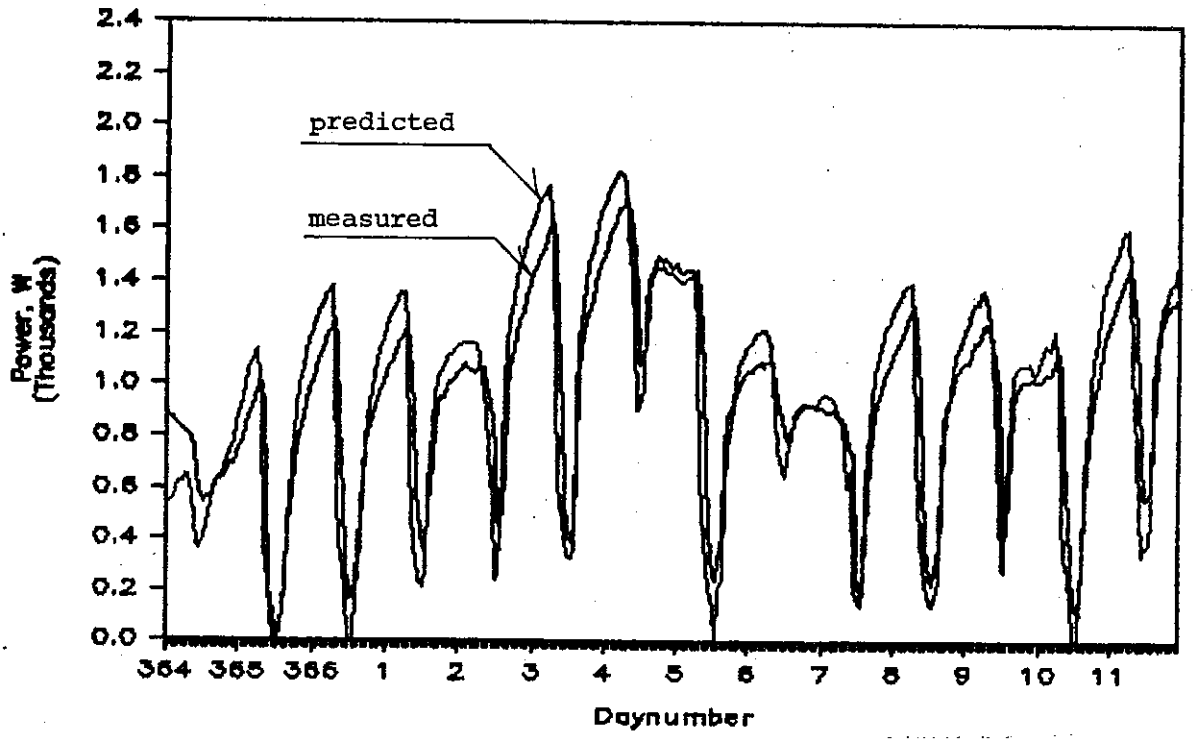

Fig. 5.13 SOLMAT direct gain validation results. Measured and predicted auxiliary power, zone air fraction of solar gain = 0.3.

thermal bridges. (In fact, the given R-values did take account of the studs).

. The floor (wood and carpet) are combined into an "equivalent floor" of R = 0.25 m^2K/W, 0.029 m thickness and 0.145 x 10^{-6} m^2/sec thermal diffusivity which permitted the use of relatively large time steps in the simulations.

Simulation results

Plots of calculated and measured energy consumption and room temperature are given in Figs. 5.14 and 5.15. The SMP predictions agreed well with measured values. A consistantly higher energy consumption at noon could be due to underestimation of solar gain as a result of a difference between the assumptions of the glazing properties and the actual properties (glass properties were not specified in the supplied input file). There also appears to be a problem with the ability of the program to control the room temperature at the fixed set point. Fig. 5.14 shows that room temperature drifted by about 0.5°C during night. This may partially explain the underprediction of the peak power requirement during these periods (for example on January 2 and 3).

4. Country: NETHERLANDS

a. Simulation Model: BFEP

BFEP is a finite element base computer program intended for the calculation of temperatures in buildings (6). The major distinction between BFEP and other programs is that the user has to perform his own modelling tasks prior to any BFEP calculation. This user-modelling facility, however, offers maximal flexibility and use.

Modelling assumptions

A great deal of detail (in some instances, greater than that given by the supplied data) is required for BFEP. Some of these are:

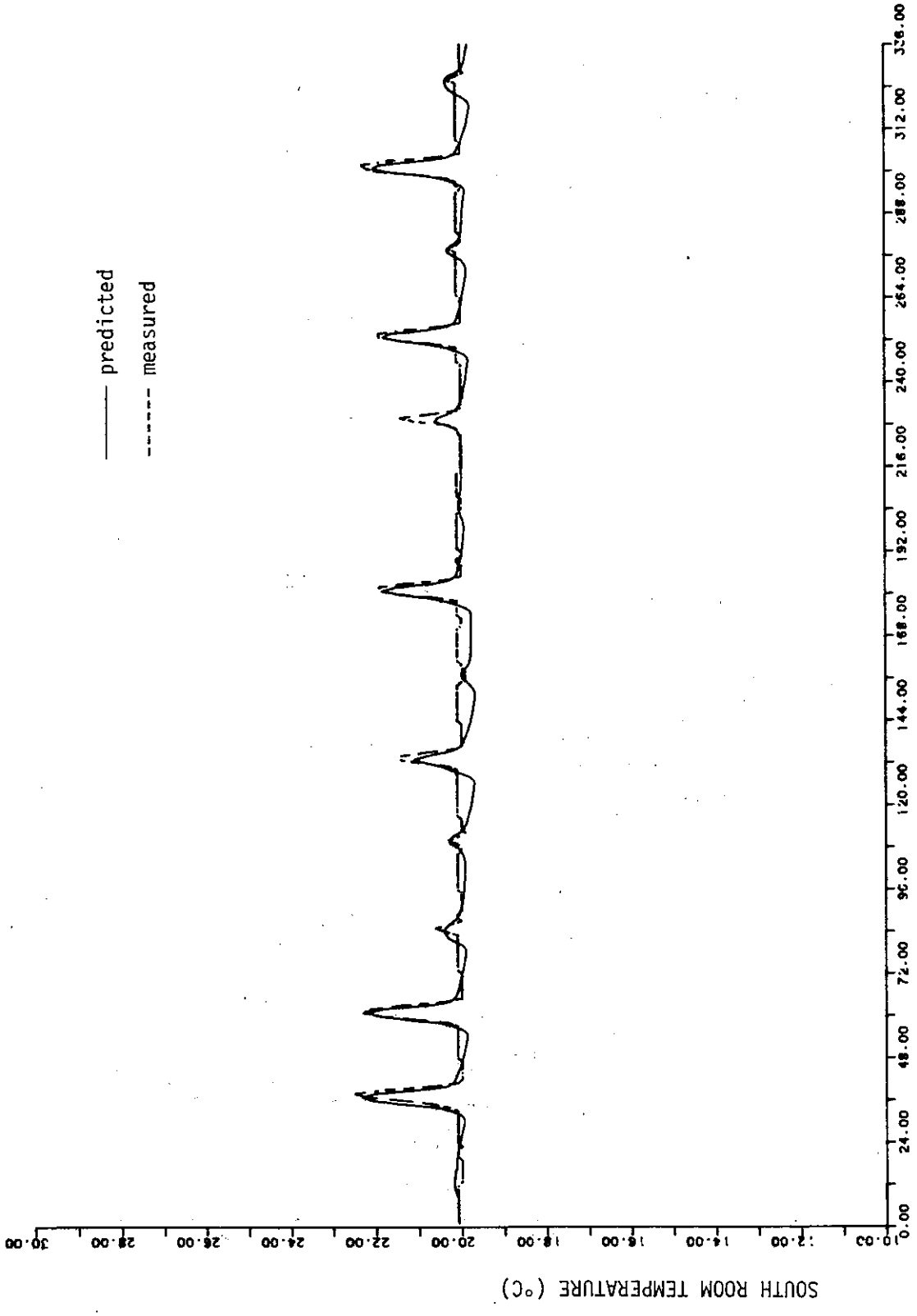

Fig. 5.14 SMP results. South room temperature.

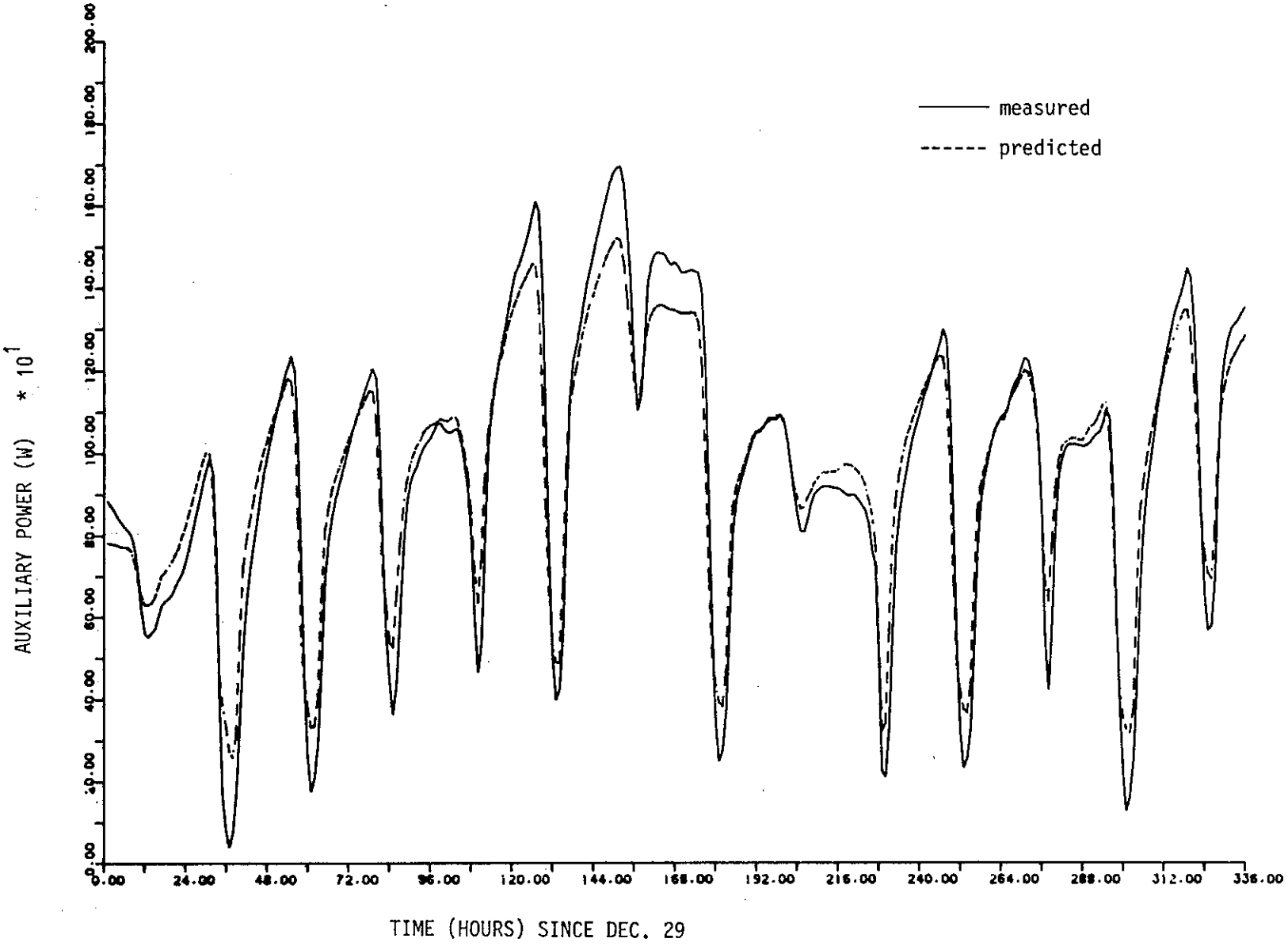

Fig. 5.15 SMP results. Total heating power.

- All walls, ceiling, floor, doors and windows are described in separate layers.
- The indoor air film heat transfer coefficient is taken to be constant but somewhat increased to account for air movement induced by the fan operation.
- View factors are used to calculate radiative exchange between walls.
- Radiation as well as convection exchange through open door is accounted for.
- Absorptance of opaque walls to solar radiation taken as 0.5.
- For direct solar radiation inside room, the fractions falling on each wall are computed and absorbed according to absorptance factor for the specific wall.
- Half of the diffuse radiation is assumed to strike the floor while the other half is distributed on other wall areas.

Results

Comparison of measured and calculated values is given in Figs. 5.16 and 5.17 for south room temperature and total unit power consumption, respectively. Generally, the BFEP results are in very good agreement with measured data. Total energy consumption is only 4.4 percent different, some of it due to the uncertainties in the input data supplied for the building. The slight lag seen in Fig. 5.17 of calculated data (with respect to measured data) could be due to the difference in integration periods. While measured data were value integrated over the hour and reported at the beginning of the hour (i.e. hours 0-23 given for a day), most programs assume that input values are instantaneous on the hour value.

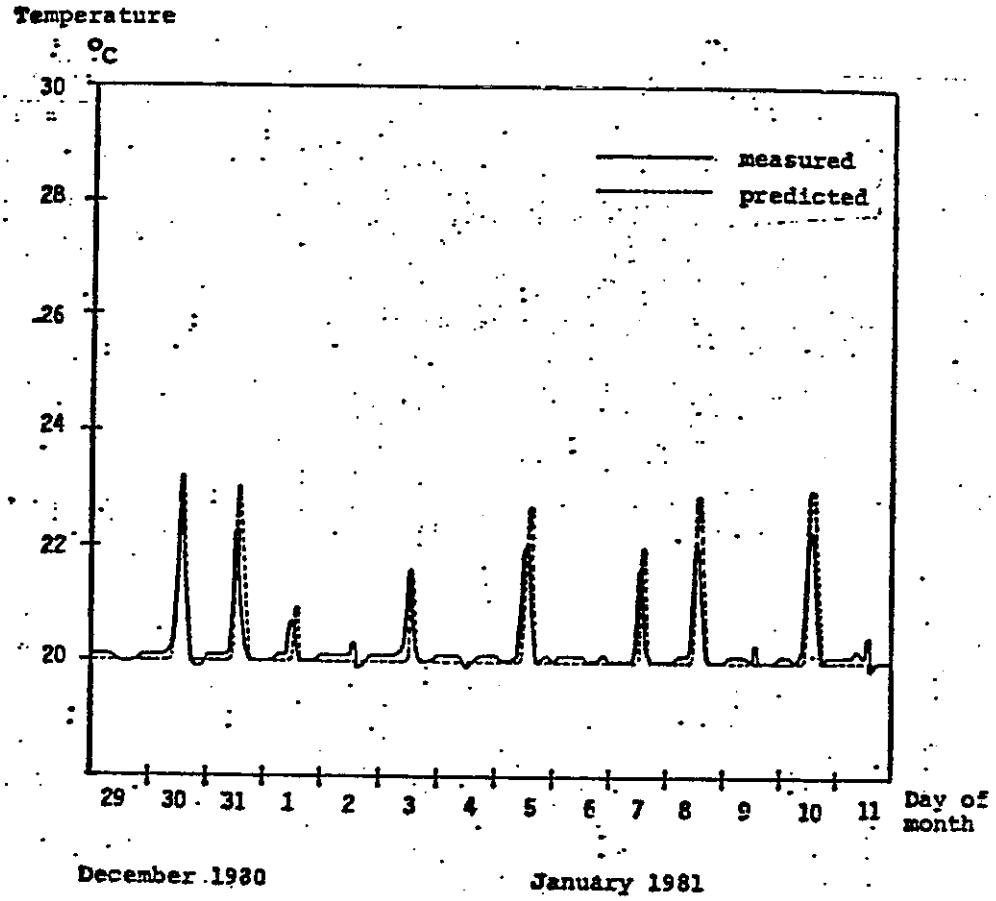

Fig. 5.16 BFEP results. South room temperature.

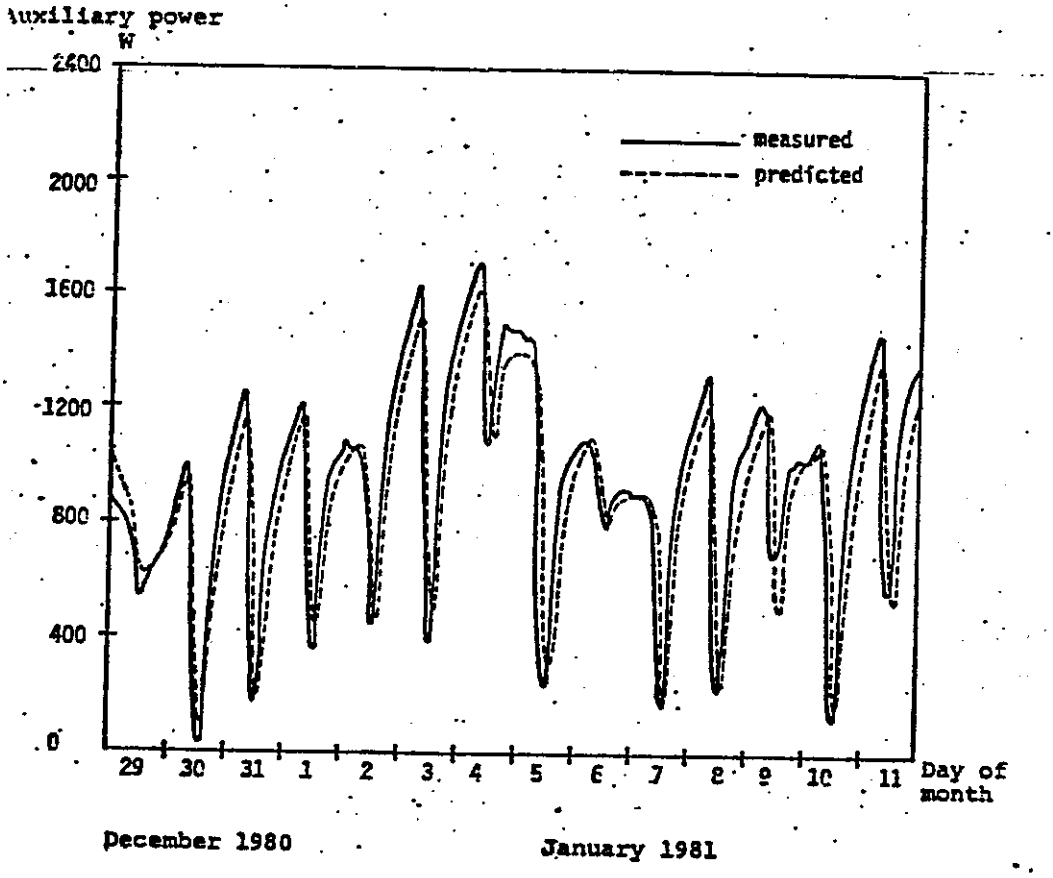

Fig. 5.17 BFEP results. Total heating power.

b. Simulation Model: KLI/PAS

KLI is a multizone building energy analysis program utilizing the thermal network (7).

Simulation assumptions

- Doors are accounted for by decreasing the thickness of the wall (total mass remains the same).
- The attic, basement and corridor are modelled as separate (rectangular) spaces with their air temperatures taken from the monitored data.
- Each wall layer is divided into 4 sublayers giving 5 nodes per layer.
- Wall studs are accounted for by calculating an area-weighted average of the thermal conductivity.
- 90% of the incoming direct solar radiation is absorbed by the floor, the remainder and the diffuse radiation are equally distributed on all internal surfaces of a room.
- Auxiliary heating is 50% convective and 50% radiative.
- External surfaces have short wave absorption of 0.4 and emissivity of 0.9 (sky temperature = air temperature).

Results

South room air temperature and total unit power consumption are given in Figs. 5.18 and 5.19. The program predicted south room temperature to within $1^{o}C$, however always on the low side. It also consistently underpredicted the peak power consumption and overpredicted the minima. The shape of the power consumption plots suggests an overestimation of the amount of thermal mass in the building.

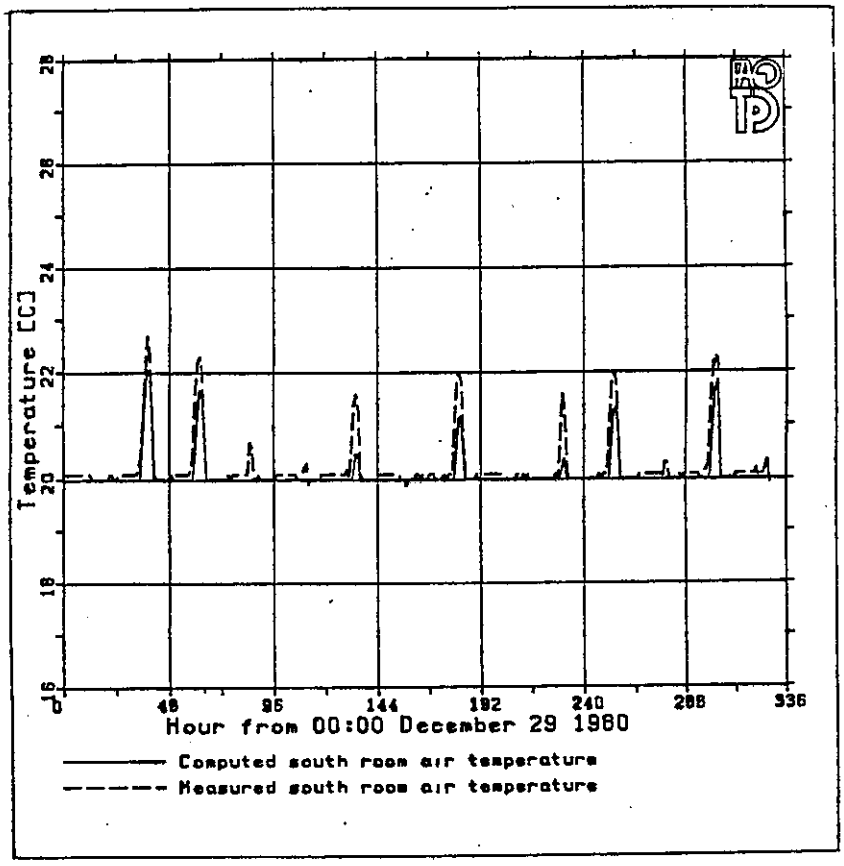

Fig. 5.18 KLI/PAS results. South room temperature.

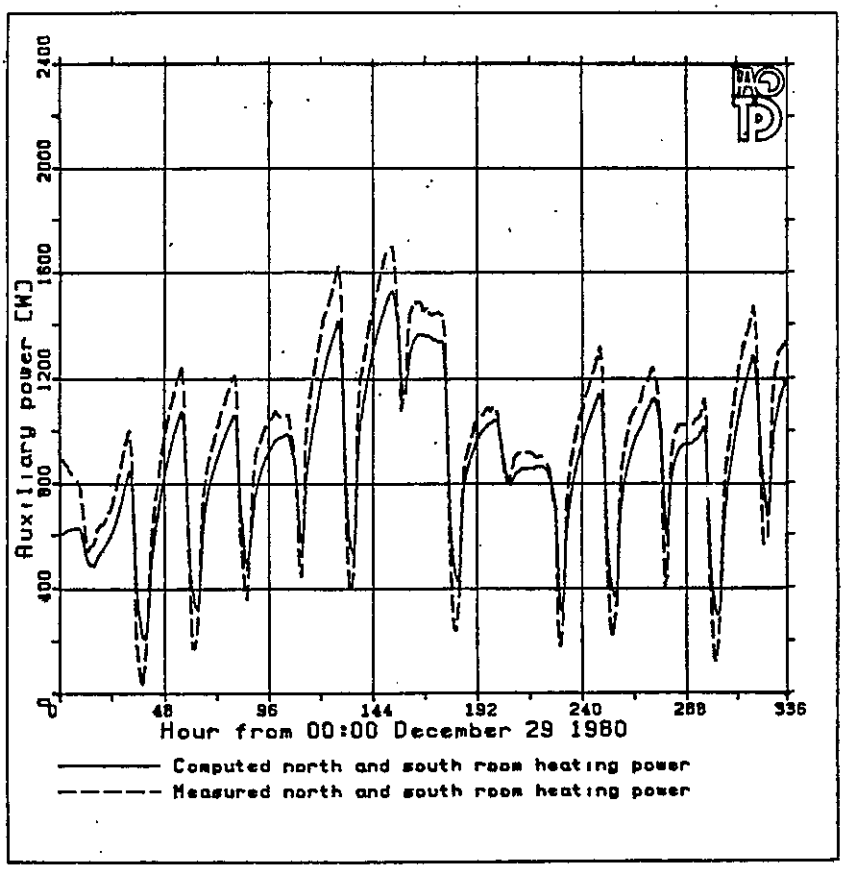

Fig. 5.19 KLI/PAS results. Total heating power.

5. Country: NORWAY

Simulation Model: ENCORE

ENCORE is a program for calculating energy consumption of residential buildings (8). Calculations are done hour by hour according to the "transfer function method" of ASHRAE.

Simulation assumptions

- To account for air circulation, the door between the two rooms is given a high U-value (100 W/m^2K).
- The ENCORE model uses cloud cover factor in the calculation of solar radiation. The meteorological data had to be processed to meet this requirement. Cloud cover factor is calculated as the ratio between measured global solar radiation and calculated global radiation under cloudless sky.
- Measured vertical south and north radiation were used directly.
- The unit is simulated as heavy construction, with an assumed mass of 615 kg/m^2 floor area (actual mass is 550 kg/m^2).
- The unit was simulated both as a single room, and as two rooms. In the results these are labelled as Modes 3 and 2, respectively.

Results

Results are presented for 4 days only in Figs. 5.20 and 5.21 for Mode 2 and Figs. 5.22 and 5.23 for Mode 3.

Mode 2

Fig. 5.20 shows that in this case there is good agreement between calculated and measured room temperatures. Fig. 5.21 shows that there is considerable difference in combined room heating power at noon. That is when the combined heating power is very small, otherwise (e.g. hour 84) the agreement is much better.

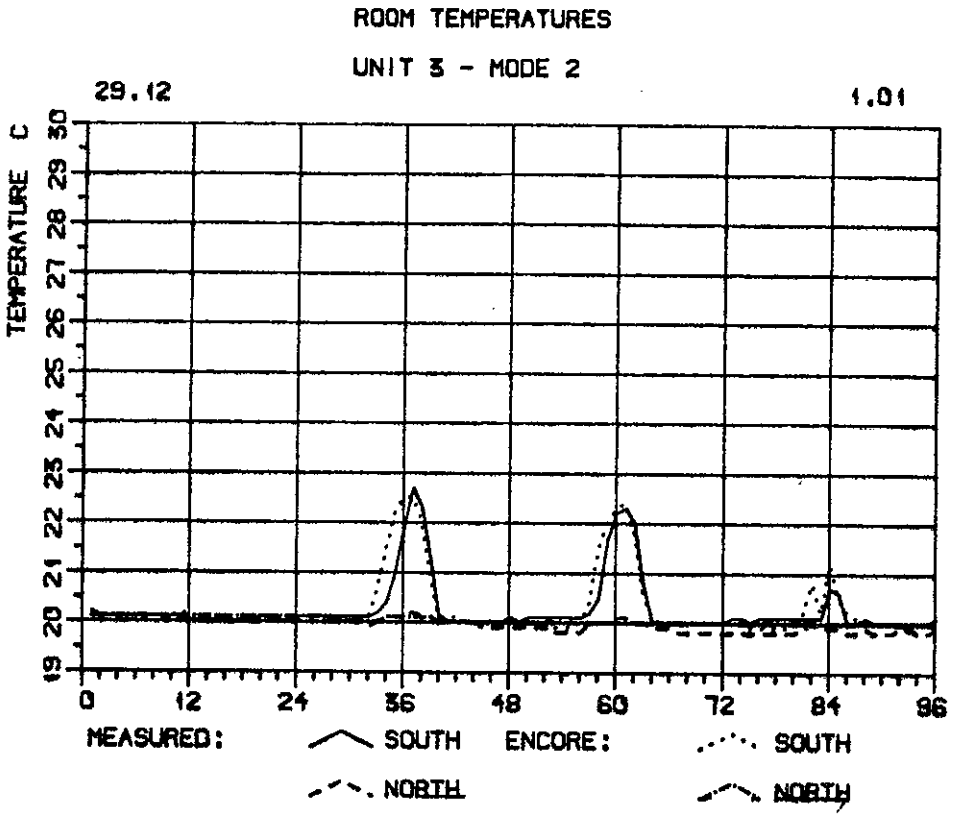

Fig. 5.20 ENCORE results. Room temperatures, 2-zone run.

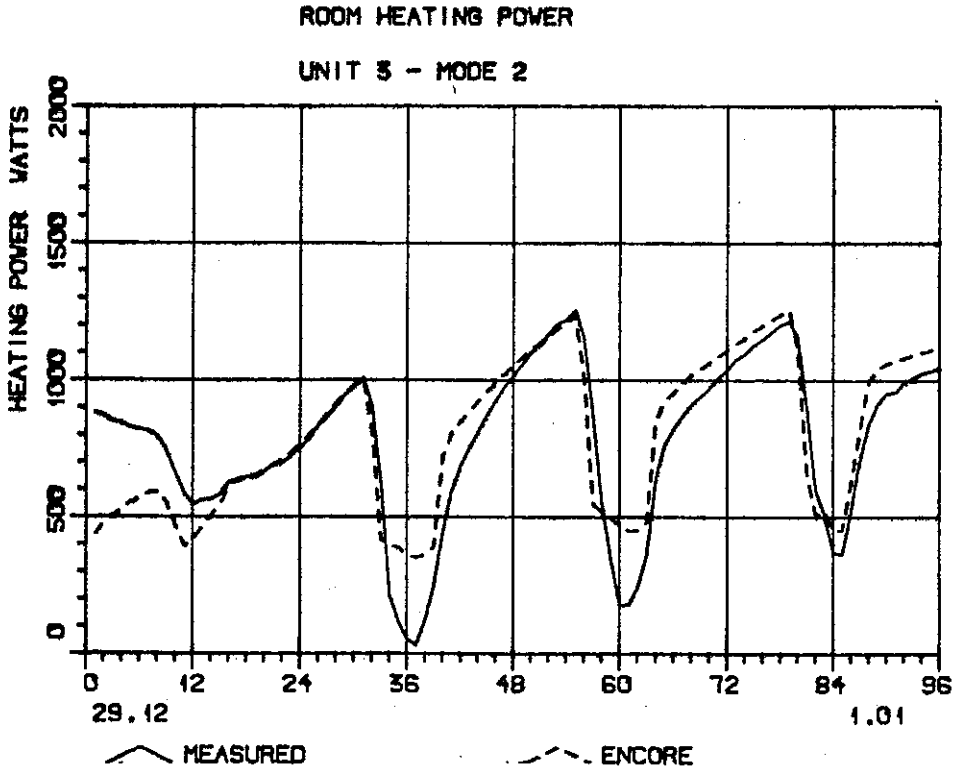

Fig. 5.21 ENCORE results. Heating power, 2-zone run.

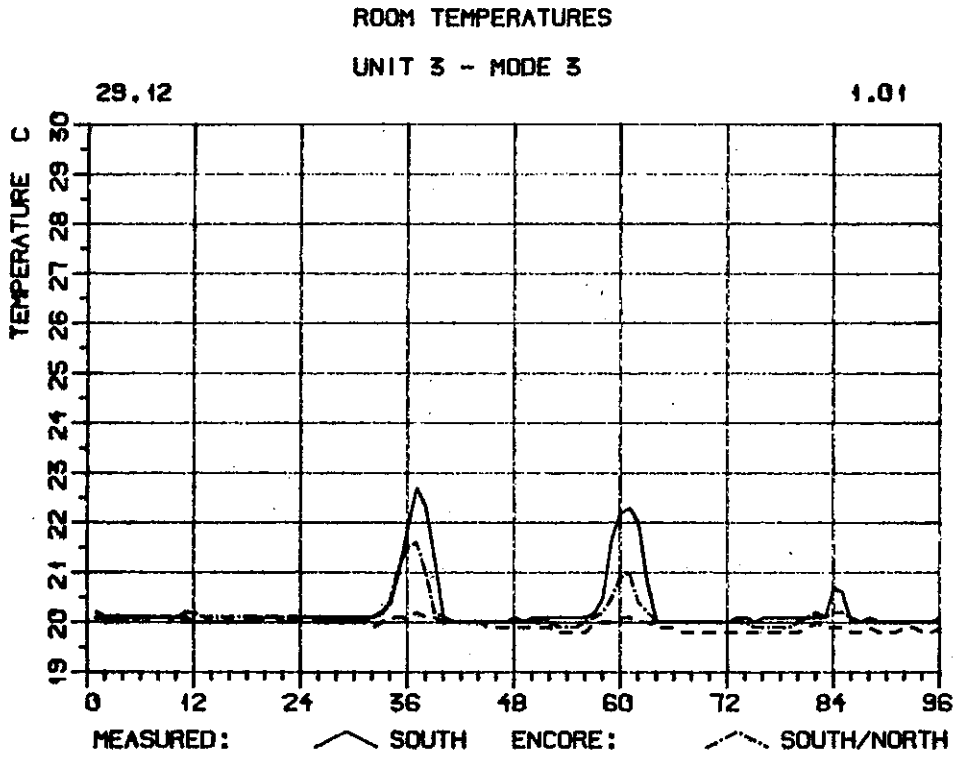

Fig. 5.22 ENCORE results. Room temperatures, single-zone run.

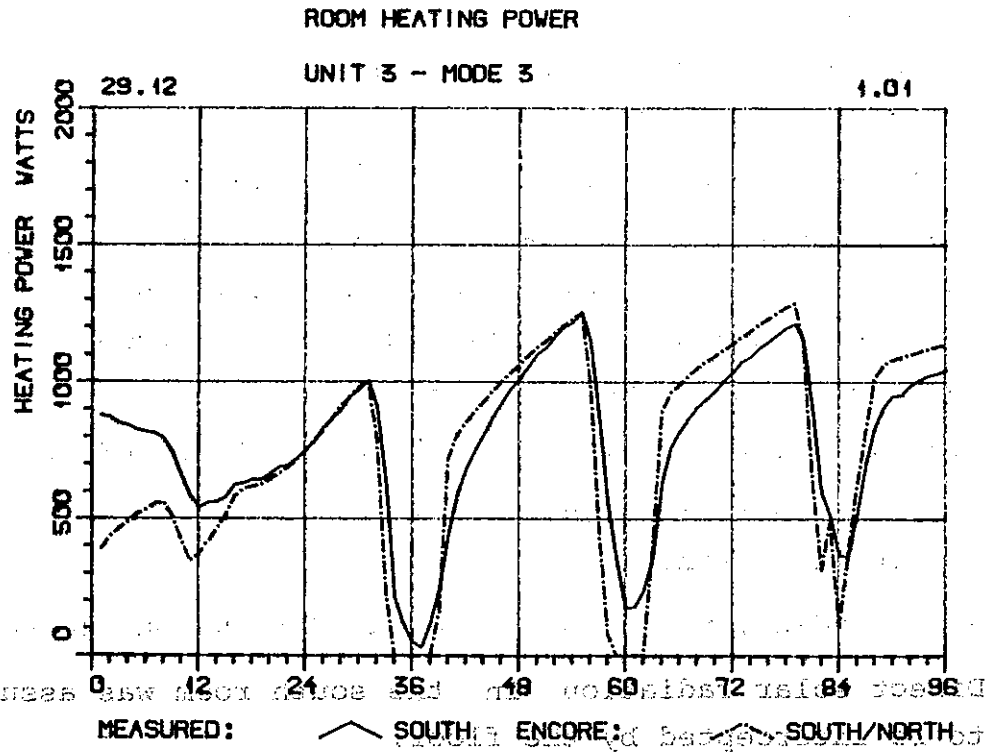

Fig. 5.23 ENCORE results. Heating power, single-zone run.

Mode 3

With the unit modelled as one room, (i.e. with the wall between the north and south room completely removed) there is complete energy exchange between the two rooms. As expected, Fig. 5.22 shows that the room temperature now falls somewhere between the measured temperatures of the two rooms. Fig. 5.23 shows that the calculated combined heating power at noon is less than the measured due to the totally free energy exchange between the two rooms. It can be concluded that a single room model is not as good an assumption to the real situation as that of using a high U-value for the door.

6. Country: UNITED KINGDOM

Simulation Model: ESP

ESP is an energy analysis program that utilizes the finite difference approach (9).

Simulation assumptions

- Dimensions of each room were based on means of internal and external dimensions.
- Wall studs were modelled as separate surfaces.
- The door between the north and south rooms was modelled as a window (to allow for short-wave radiation transfer between the rooms) with an air movement through it equivalent to 4.84 ach.
- Windows and frame given same U-value of 2.7 W/m^2K.
- The attic was simulated as a separate zone with 10 ach for infiltration.
- Solar radiation values were assumed to be on the hour.
- Direct solar radiation in the south room was assumed to be intercepted by the floor.

Results

Graphs of simulated and measured south room air temperature are shown in Fig. 5.24. Agreement is generally fairly good, with local overheating maxima predicted to within 1°C in most cases.

Fig. 5.25 shows simulated and measured north room temperature. Both remain very near 20.0°C.

Fig. 5.26 shows simulated and measured auxiliary heating power (north and south zones combined). Agreement is reasonably good. Certain discrepancies are, however, apparent:

1) There is tendency towards under-prediction of peak loads. Predicted load maxima are typically 100-200 W below observed.

2) There is also a tendency towards over-prediction of minimum loads, by a similar margin. Both these observations suggest the possibility that the available thermal mass may be too high in the simulation. Alternatively, the effects may be due to inaccurate assumptions about the heating system or its control.

3) Predicted load minima often lag behind observed minima by 1-2 hours. This is another possible indication of an overprovision of thermal mass added to the possible lag due to the timing assumption of solar radiation values (values assumed to be on the hour).

7. Country: USA

Three simulation models were used for the validation case, BLAST-3.0, DOE-2.1A and SERIRES-1.0. A number of simulation assumptions were common to all codes and cases; these are:

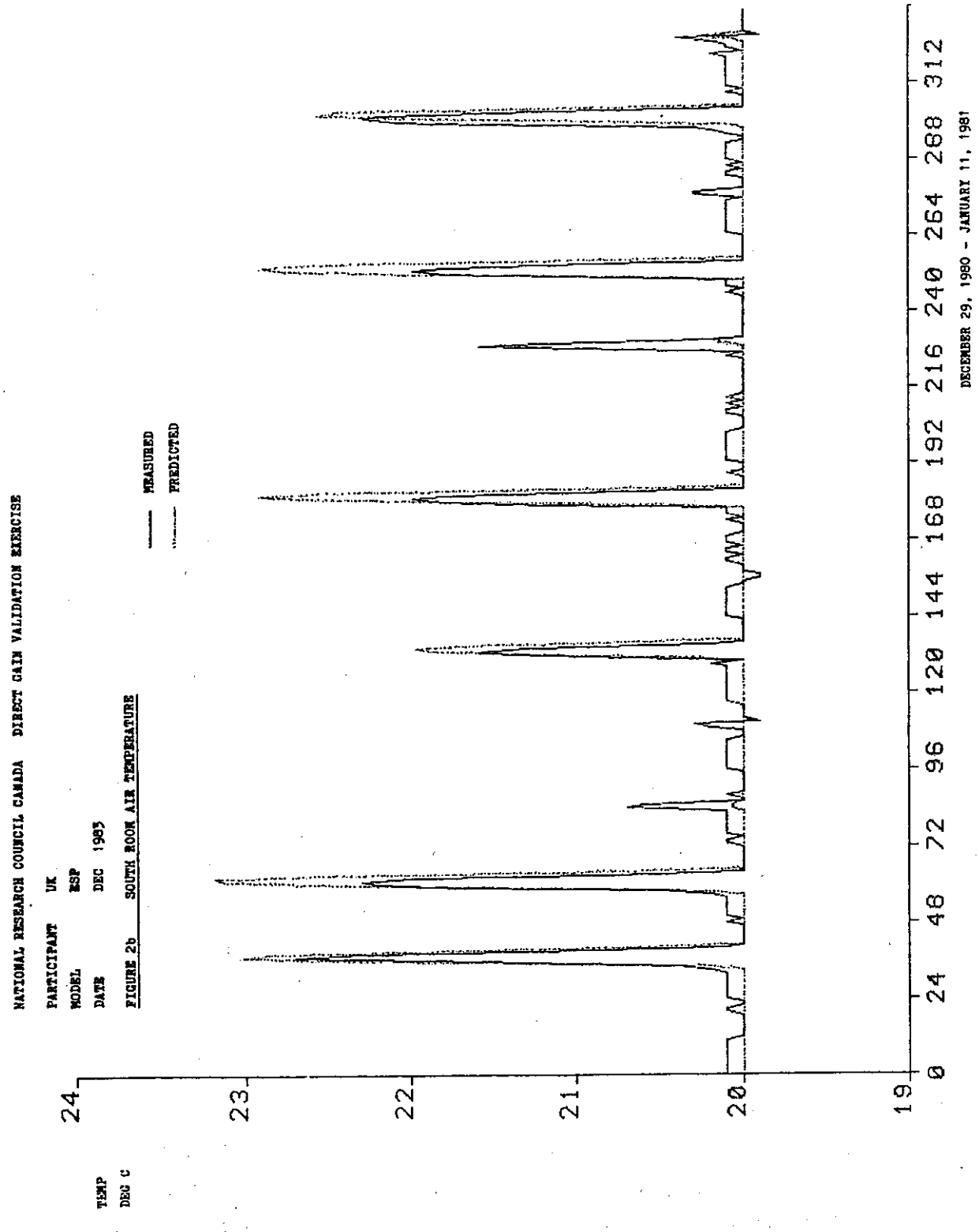

Fig. 5.24 ESP results. South room temperature.

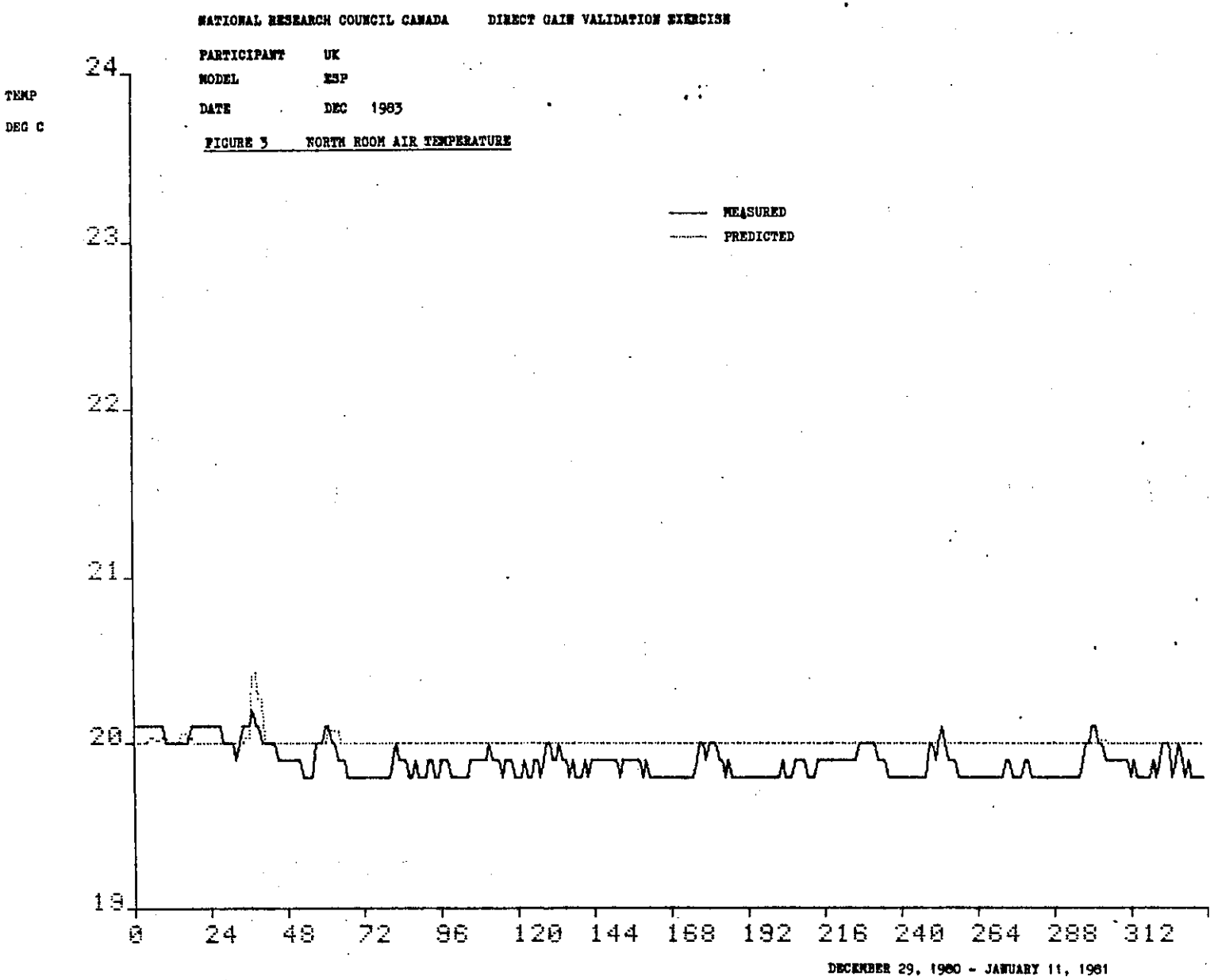

Fig. 5.25 ESP results. North room temperature.

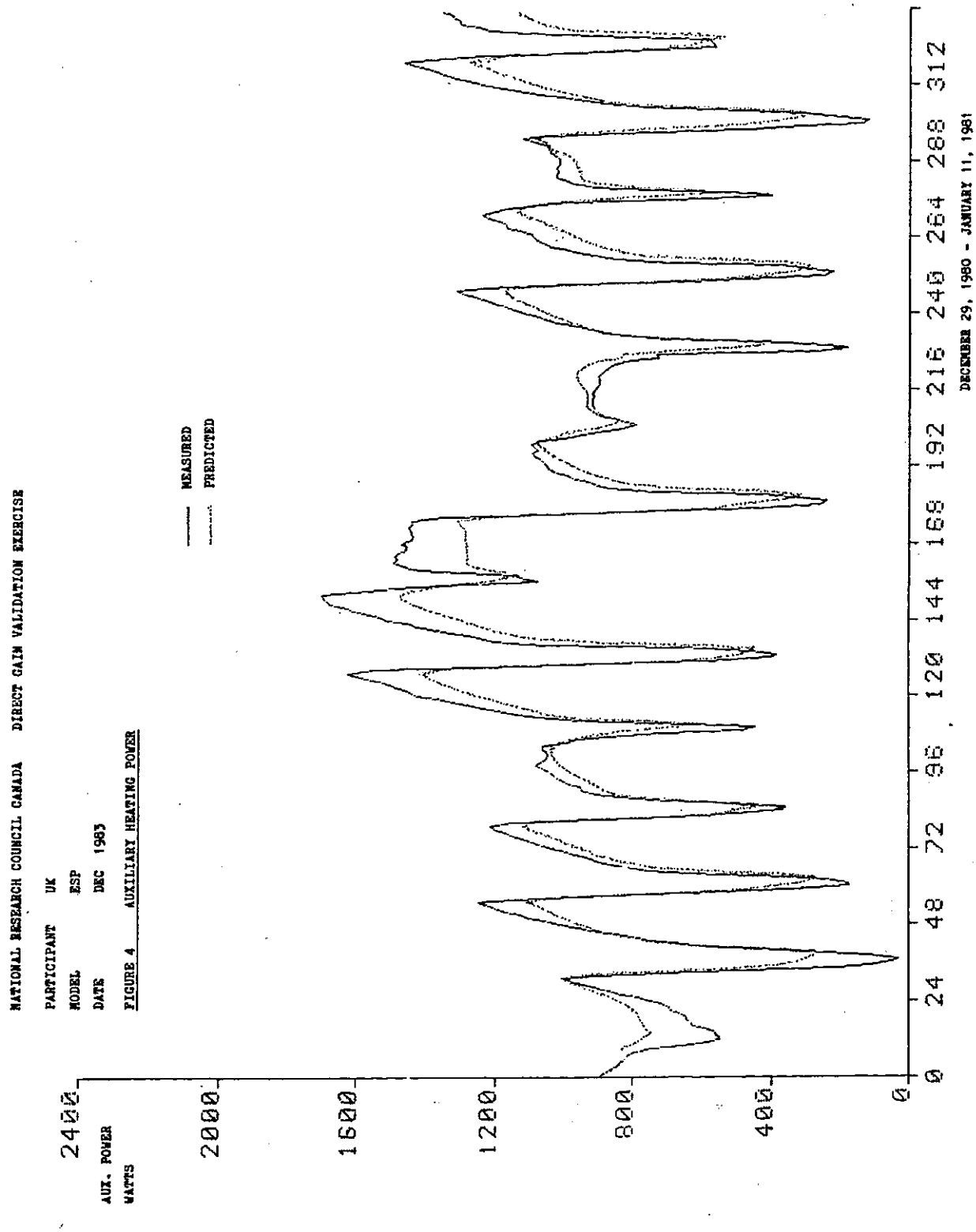

Fig. 5.26 ESP results. Heating power.

- Wall, ceiling, and floor resistances include conductances of studs, joists, and trusses.
- Basement not modelled as a separate zone. Ground temperature defined to equal 20°C and floor between basement and ground floor assumed adiabatic.
- Corridor not modelled as a separate zone. Corridor wall assumed adiabatic.
- Attic not modelled as a separate zone because attic infiltration not specified.
- Building infiltration = 0.
- No exhaust fan was modelled. Instead an ideal cooler was specified which did not allow building temperature to exceed 27°C.
- Heating and cooling equipment assumed large enough to always meet the load.
- No latent loads were modelled.
- Exterior surface solar absorptance = 0.4.

Some differences between the three models are discussed in the following.

a. Simulation Model: BLAST-3.0

BLAST is a computer program which predicts energy consumption and energy system performance in buildings (9). It utilizes the response factor method to calculate conduction through envelope elements and simultaneous solution of heat balance equations for zonal effects.

Simulation assumption

- Ground reflectivity = 0.2. (This is not equivalent to the .7 value used in SERIRES and DOE because ground reflectivity in BLAST depends on a field in the weather file which was not available on the Ottawa data tape. BLAST defaults to .2, which is not alterable by the user).

- Interzone fan modelled with the "Cross-Mixing" algorithm in BLAST set at 0.47 m^3/s.
- Waste heat from interzone fan assumed as .009 kW in south zone and .012 kW in north zone. This was disregarded for the Copenhagen runs.
- Window conductivity (interior glass surface - exterior glass surface) = 5 W/m^2K.
- Exterior and interior film coefficients are calculated hourly.
- Glass index of refraction assumed = 1.526.
- Normal transmissivity of a single pane of glass specified as .8615.

  These glazing specifications define a window in BLAST which is optically equivalent to that in SERIRES.

b. Simulation Model: DOE.2.1A

DOE.2 is a computer program which can be used to examine the energy behaviour of buildings and their associated heating, ventilation and air conditioning systems. It utilizes the response factor approach (12).

Simulation assumption

- Interzone fan modelled as a parallel conductance path based on the volumetric air movement rating of the fan and the volumetric heat capacity of air at sea level.
- Waste heat from interzone fan assumed as .009 kW in south zone and .012 kW in north zone.
- Window conductivity (interior air to exterior glass surface) = 3.12 W/m^2K.
- Exterior film coefficient calculated hourly based on hourly wind speed.

- Window assembly normal transmittance = .75, normal reflectance = .16. (This window is not optically equivalent to those in SERIRES or BLAST, however, it is not possible for the user to adjust the library optical properties in DOE-2.1A).

c. Simulation Model: SERIRES-1.0

SERIRES is a general purpose thermal analysis computer program for residential buildings. It uses the finite difference approach (12).

Simulation assumptions

- Interzone fan modelled as a parallel conductance path = 58.18 W/K (this is based on the volumetric air movement capacity of the fan and the volumetric heat capacity of air at the altitude of Ottawa).
- Waste heat from interzone fan assumed as .009 kW in south zone and .012 kW in north zone.
- Window conductance air-air = 2.86 W/m^2K which includes a constant combined radiative and convective exterior film coefficient of 33.33 W/m^2K.
- Glass extinction coefficient = .0196, index of refraction = 1.526, pane thickness = 3.175 mm.
- For the Copenhagen run, the window conductance (air-air) = 2.764 W/m^2K which includes a constant combined radiative and convective exterior surface coefficient of 26.805 W/m^2K. This was calculated based on an average annual wind speed in Copenhagen of 5m/s.

Results

Results of the three models are shown in Figs. 5.27 to 5.32. The agreement between measured temperature and power values is generally good. The maximum difference between measured and calculated south room temperature is in the order of 1.0^{o}C for the SERIRES run. SERIRES,

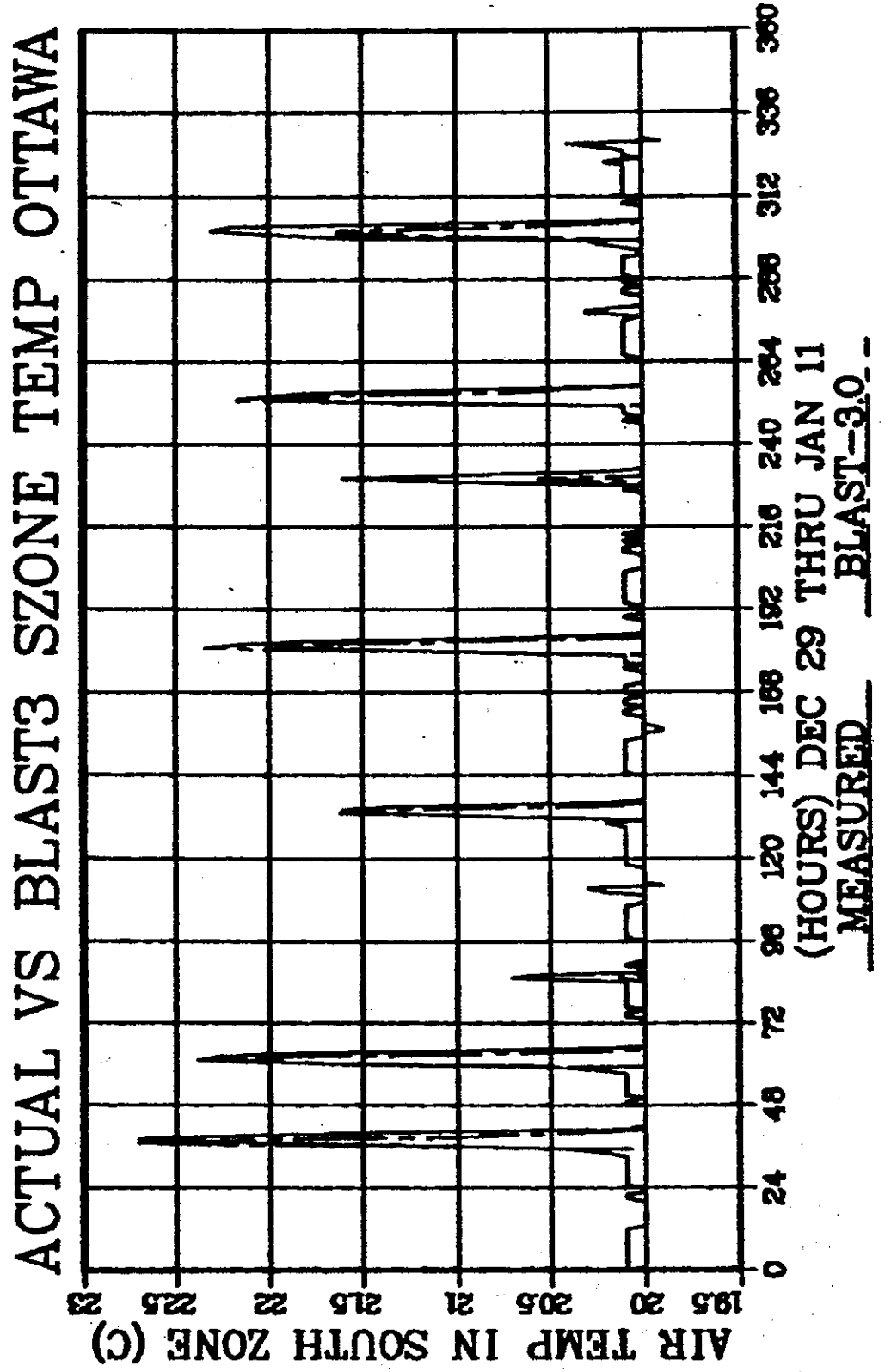

Fig. 5.27 BLAST-3.0 results. South room temperature.

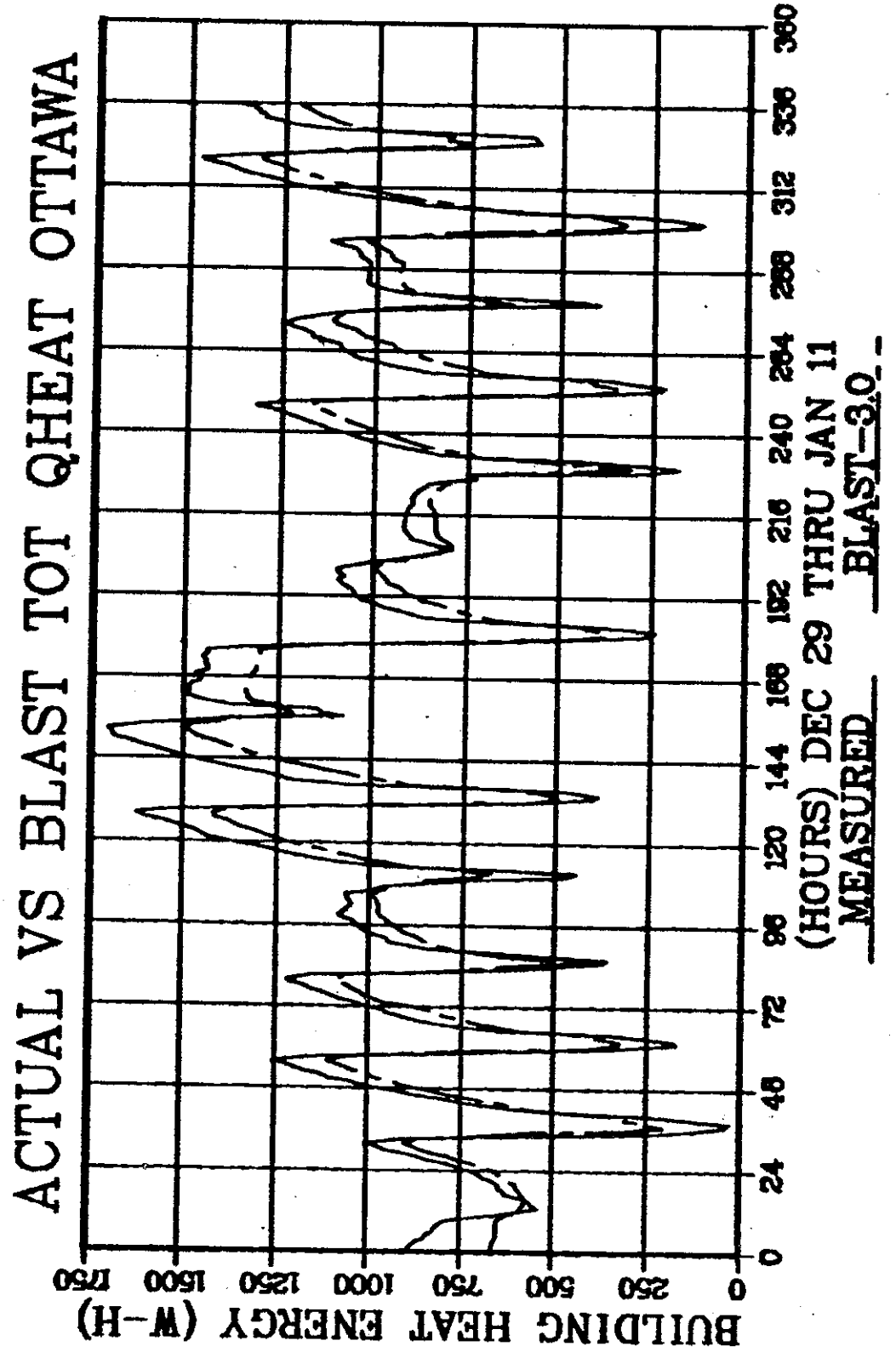

Fig. 5.28 BLAST-3.0 results. Total heating power.

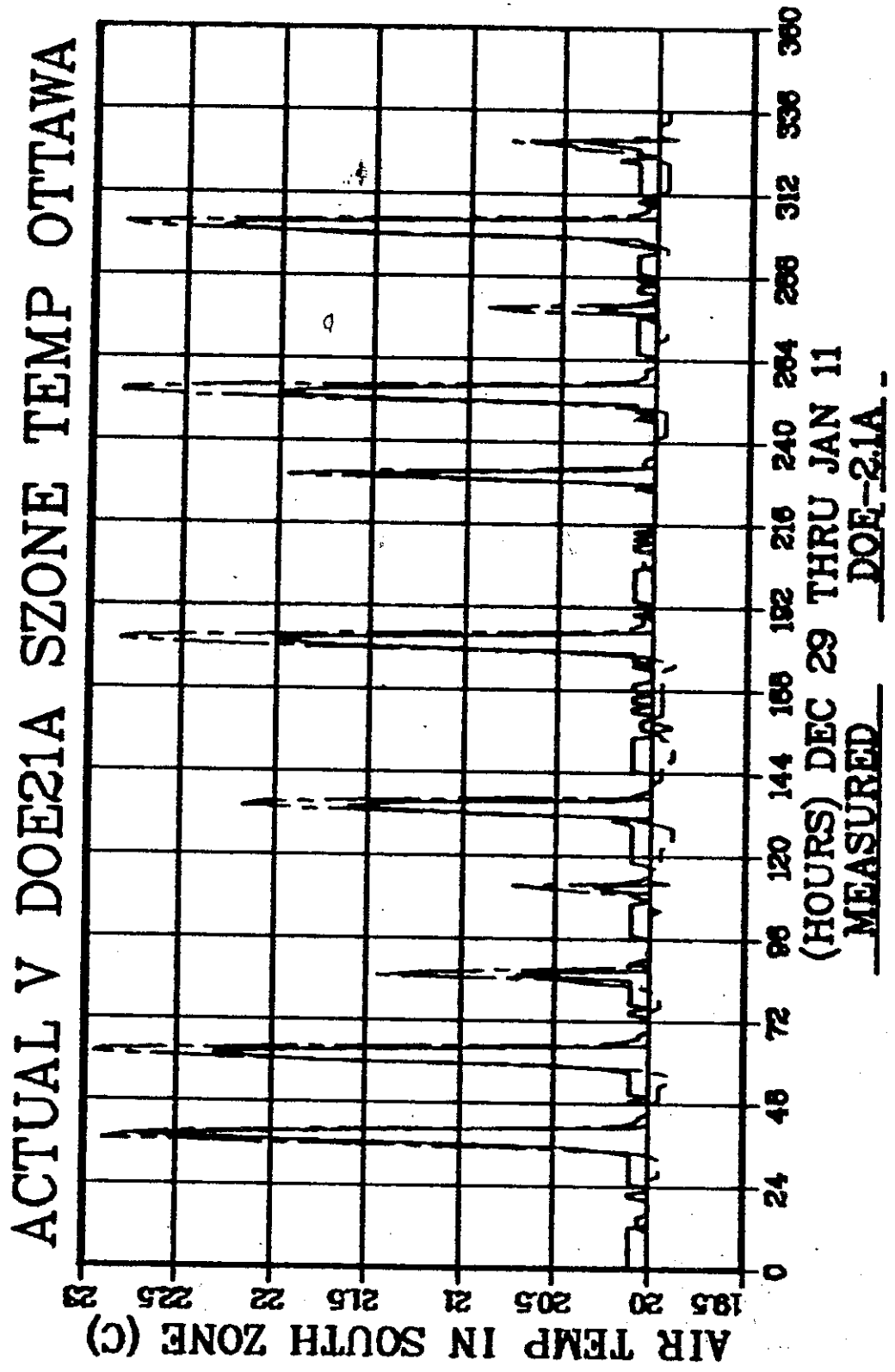

Fig. 5.29 DOE-2.1A results. South room temperature.

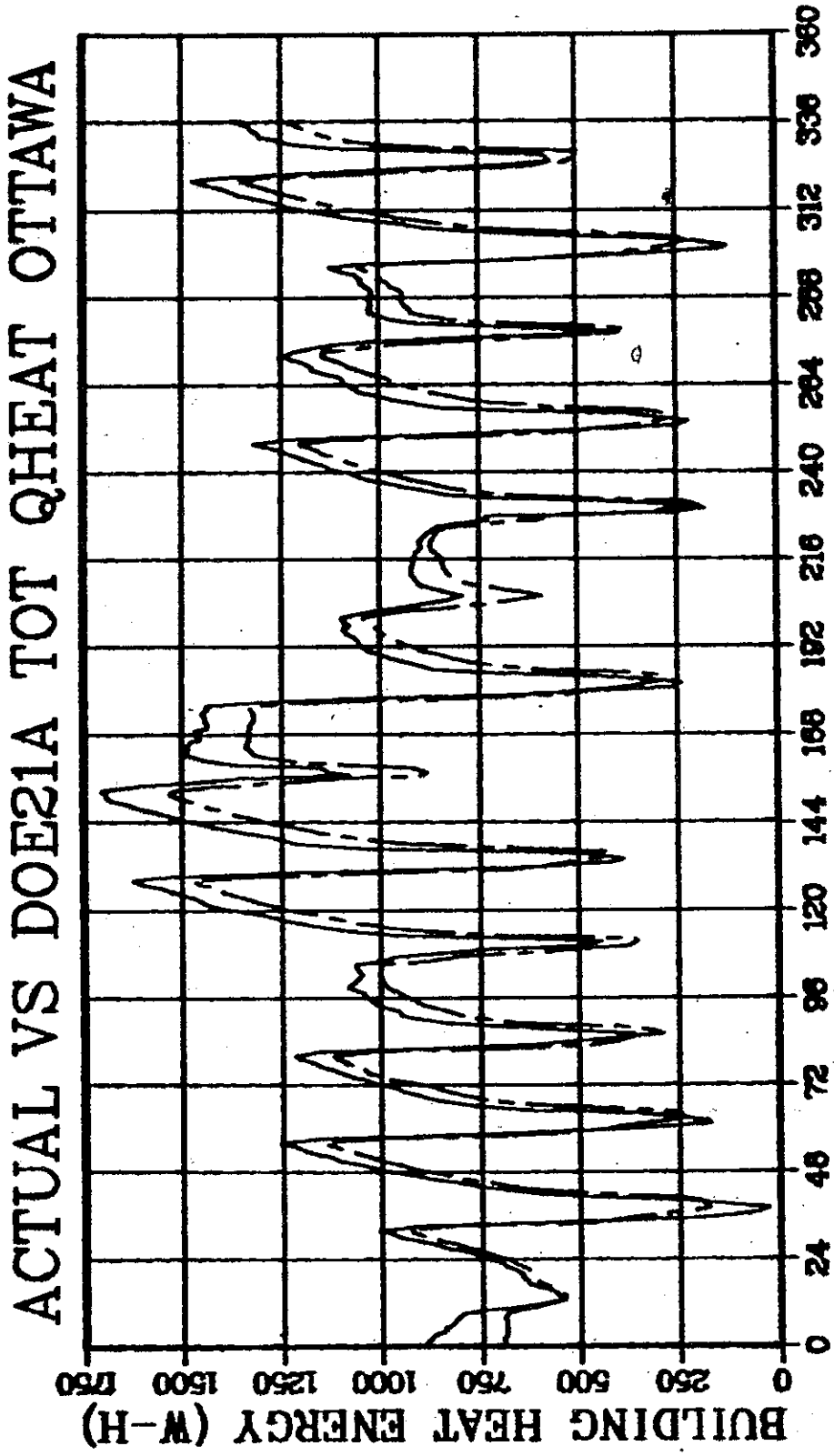

Fig. 5.30 DOE-2.1A results. Total heating power.

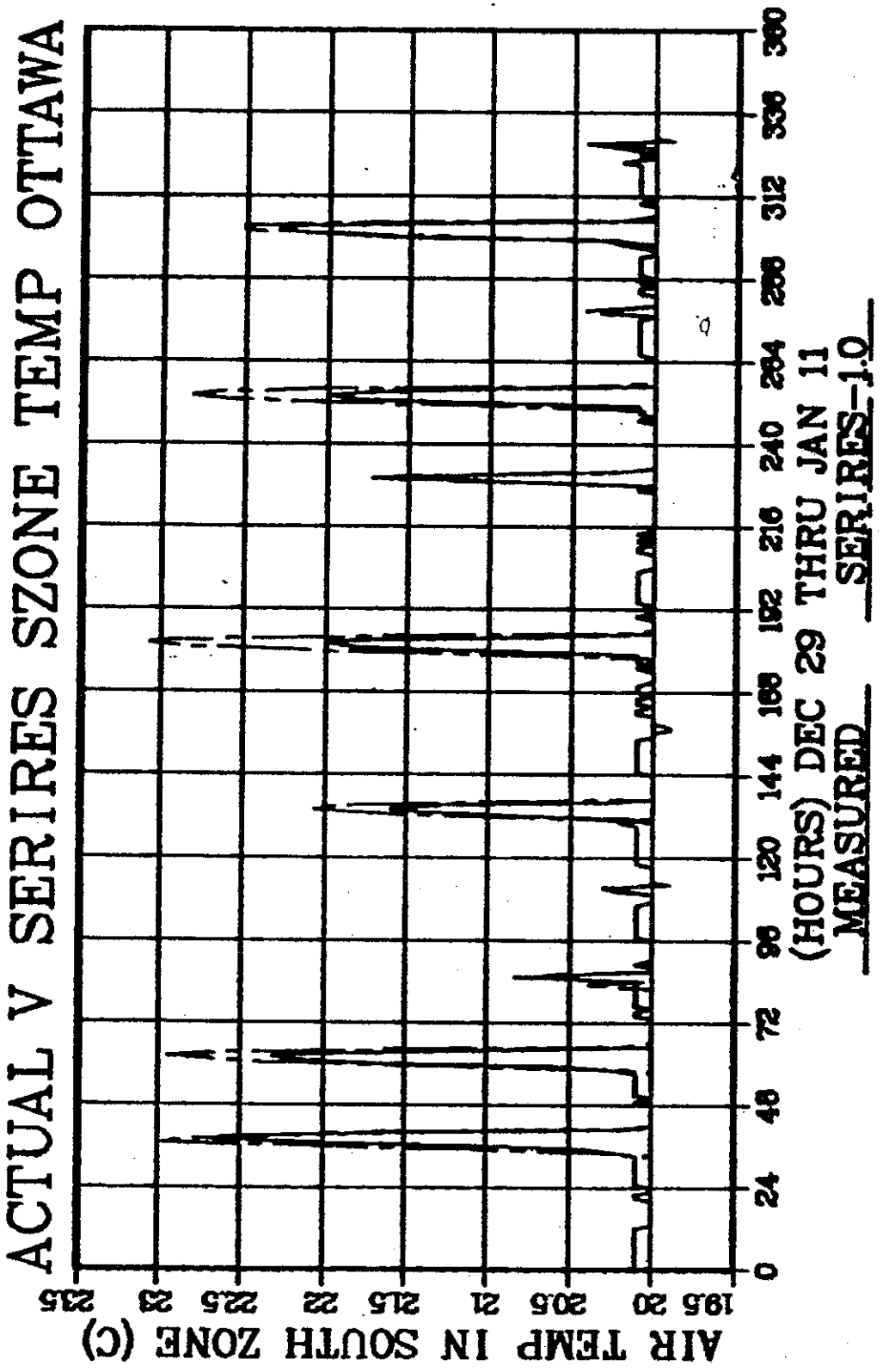

Fig. 5.31 SERIRES-1.0 results. South room temperature.

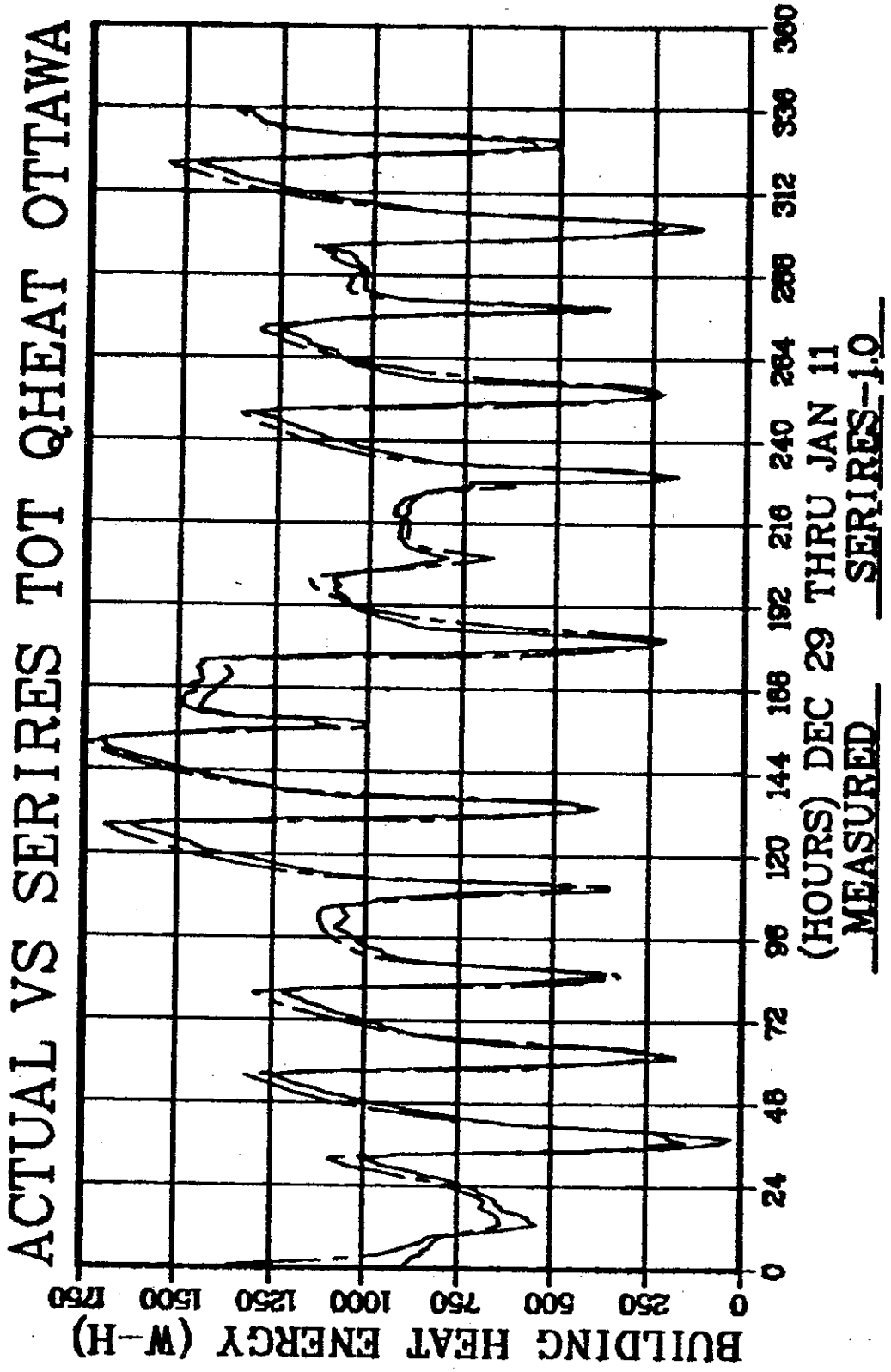

Fig. 5.32 SERIRES-1.0 results. Total heating power.

however, produced the best agreement with measured power data, both BLAST and DOE 2 underestimated the peaks.

Original (first time) results of these programs showed large differences in the heating and cooling loads and zone temperatures predicted by the three programs. A following study (13,15) identified the algorithms responsible for these differences and corrected them to eliminate the problem. The results shown here are the final results.

5.4 Yearly Simulation Results

The simulation models described above were used to model the same building, the Canadian direct gain test Unit 3, using a full year of Copenhagen weather data. The weather data supplied included direct normal radiation, global horizontal radiation, dry bulb and dew point temperatures and wind speed. The ground reflectance was assumed to be 0.2 all year.

Monthly auxiliary heating and cooling values calculated by each program are given in Tables 5.6 and 5.7 respectively. The results show good agreement between programs for heating requirements. The mean value for the yearly heating consumption is 2147.1 kWh with a standard deviation of 160.6 kWh. The presentation method of room temperatures was inconsistent between participants and did not allow a common comparison. Some of the programs, however, listed maximum room temperature each month. For comparison these are given in Table 5.8.

5.5 Summary

A two stage validation effort of direct-gain simulation models was undertaken by seven of the participating countries using twelve computer models. For some of these models, this was a first time validation effort.

TABLE 5.6 YEARLY SIMULATION OF CANADIAN TEST BUILDING, USING COPENHAGEN WEATHER.

	Heating Energy, kWh												
Month	ENCORE CANADA	BA-4	PASOLE	SMP	BFEP	KLI/PAS	ENCORE NORWAY	ESP	BLAST	DOE-2	SERIRES	MEAN	ST. DEV.
1	470	472			464	458	528	496	440	434	465	469.7	28.4
2	362	382			360	357	425	386	349	336	366	369.2	25.9
3	311	324			305	296	312	327	303	280	311	307.7	14.2
4	122	153			135	114	115	146	132	107	138	129.1	15.6
5	14	53			32	13	22	37	30	16	40	28.6	13.5
6	0	1			0	0	0	1	0	0	0	0.2	0.4
7	0	0			0	0	0	2	0	0	0	0.2	0.7
8	0	0			0	0	0	3	0	0	0	0.3	1.0
9	1	13			2	1	10	33	3	1	8	8.0	10.4
10	144	154			142	127	169	186	132	119	148	146.8	20.9
11	300	290			279	273	340	323	268	261	285	291.0	26.1
12	399	395			381	282	477	425	365	363	385	385.8	52.3
TOTAL	2123	2235			2100	2021	2398	2365	2022	1915	2145	2147.1	160.6

TABLE 5.7 YEARLY SIMULATION OF CANADIAN TEST BUILDING, USING COPENHAGEN WEATHER.

	Cooling Energy, kWh												
Month	ENCORE CANADA	BA-4	PASOLE	SMP	BFEP	KLI/PAS	ENCORE NORWAY	ESP	BLAST	DOE-2	SERIRES	MEAN	ST. DEV.
1	-				-	-		-	-	-	-	-	-
2	-				-	-		-	-	-	-	-	-
3	-				-	-		-	-	-	-	-	-
4	-				-	-		4	-	-	-	0.6	1.5
5	-				-	-		3	-	-	-	0.6	1.1
6	26.7				8.6	37.0		39	28.1	50.2	23.6	30.5	13.2
7	12.6				4.0	34.0		29	21.6	46.6	16.7	23.5	14.3
8	23.0				9.4	37.0		36	27.9	45.3	26.7	29.3	11.6
9	-				-	1.0		7	0.9	1.7	0.6	1.5	2.5
10	-				-	-		2	-	-	-	0.3	0.8
11	-				-	-		-	-	-	-	-	-
12	-				-	-		-	-	-	-	-	-
TOTAL	62.3				22.0	109.9		120	78.5	143.9	67.6	86.2	41.0

TABLE 5.8 YEARLY SIMULATION OF CANADIAN TEST BUILDING, USING COPENHAGEN WEATHER.

Month	Maximum Temperature South Room					Maximum Temperature North Room				
	ENCORE CANADA	BFEP	KLI/PAS	ESP	SERIRES	ENCORE CANADA	BFEP	KLI/PAS	ESP	SERIRES
1	22.3	21.7	23	24.8	24.0	20.6	20.0	20	20.0	20.0
2	22.6	23.7	24	27.0	24.9	20.3	20.2	20	20.1	20.3
3	22.5	23.8	24	27.0	24.6	20.6	20.5	20	20.3	20.7
4	23.8	25.8	25	27.0	25.1	22.1	22.6	22	21.1	21.8
5	23.6	24.5	25	27.0	25.1	22.4	22.4	23	22.5	22.2
6	27.0	27.0	27	27.0	27.0	26.8	26.5	27	27.0	26.8
7	27.0	27.0	27	27.0	27.0	26.6	26.4	27	27.0	26.7
8	27.0	27.0	27	27.0	27.0	26.6	26.7	27	25.9	26.8
9	25.6	26.4	27	27.0	27.0	23.9	23.5	25	21.1	24.2
10	24.2	25.3	26	27.0	25.6	22.7	22.7	23	20.4	22.3
11	22.1	22.6	23	25.9	24.0	20.2	20.5	20	20.0	20.4
12	21.4	21.2	22	23.7	22.9	20.0	20.1	20	20.0	20.0

First, the models were used to simulate performance of a test unit of the Canadian Passive Solar Test Facility during a two-week period. The results of the models were compared to the measured data. A summary of the results is given in Fig. 5.33 which presents the total heating energy calculated by each model as compared to the measured. All models except one have predicted total heating load well within 10% of the measured value by a range of 22%. Also, the dynamic behaviour of the building was tracked very well by most of the models. However, the low gain/loss ratio (average ambient temperature approx. $-15^{o}C$) and a low ratio of internal-to-external surface area lead to a low level of interaction between solar gains and internal thermal mass.

Secondly, the models were run on one year Copenhagen weather data files using the same building input file. A summary of the results is given in Figs. 5.34 and 5.35. The agreement on calculated heating energy is good (mean = 2147.1, st.deviation = 160.6, max.deviation = 26%). During the cooling season with a high gain/loss ratio, the program code deviations obtained when predicting cooling energy are much higher (mean = 86.2, st.deviation = 41.0, max.deviation = 650%).

The difference between model results can partly be due to the lack of complete building information required by models since each requires a different level of input specificity. Examples are the details of the window glazing (thickness, transmission, extinction coefficient..etc) and some of the layers comprising the different walls. Other factors affecting the results were the inability of some models to handle multi-zone configuration or to explicitly model the convection between the two zones.

Considering the different approaches utilized by the simulation models, their different level of details and the uncertainties of some of the input data, the agreement between these models and between the models and the measured data was very satisfactory.

A parallel validation effort within the IEA Buildings and Community Systems agreement carried out at different boundary conditions (central unit, weather data Geneva) led to greater differences between the program codes.

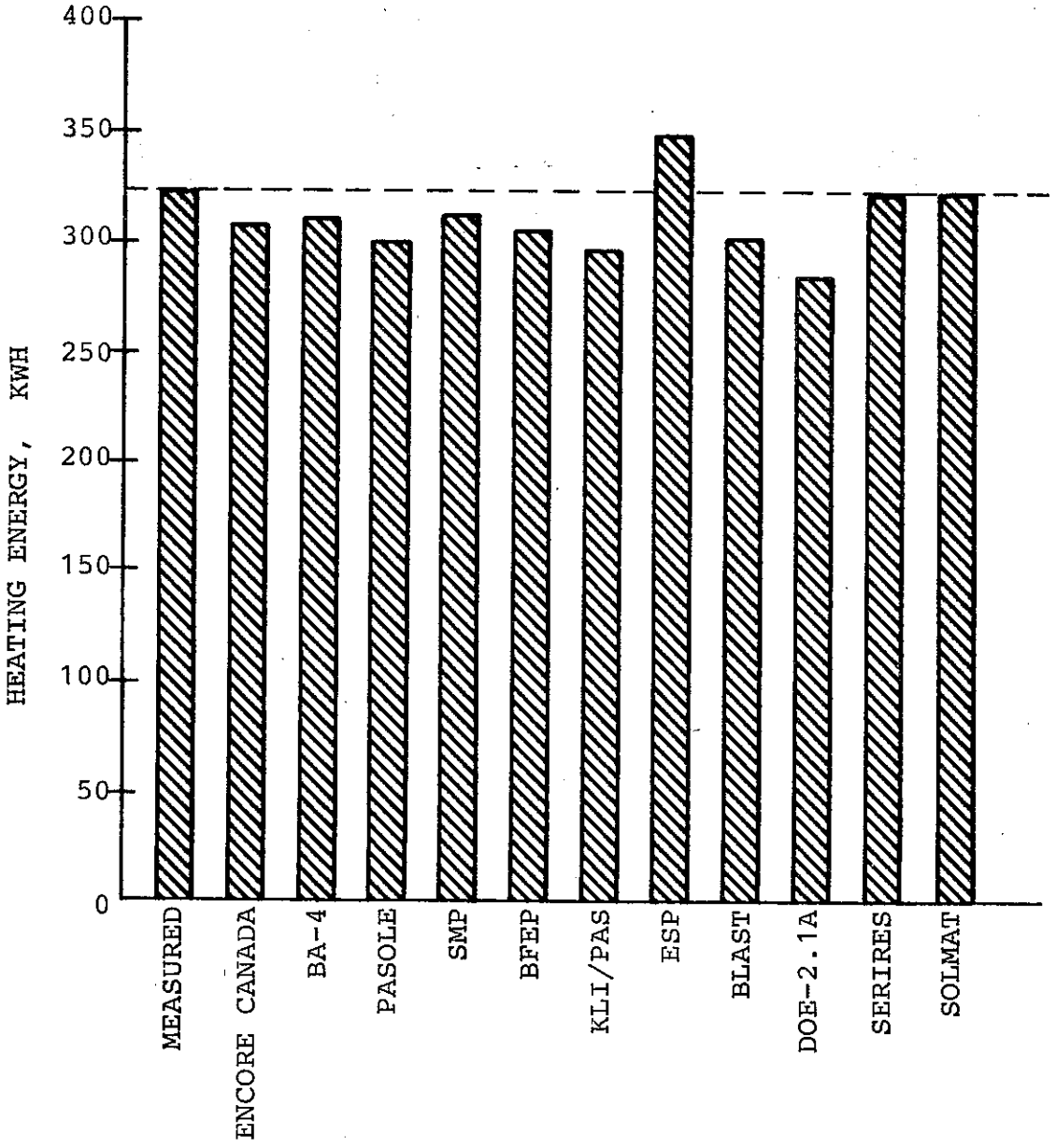

Fig. 5.33 Comparison of auxiliary heating requirements for two weeks in Ottawa.

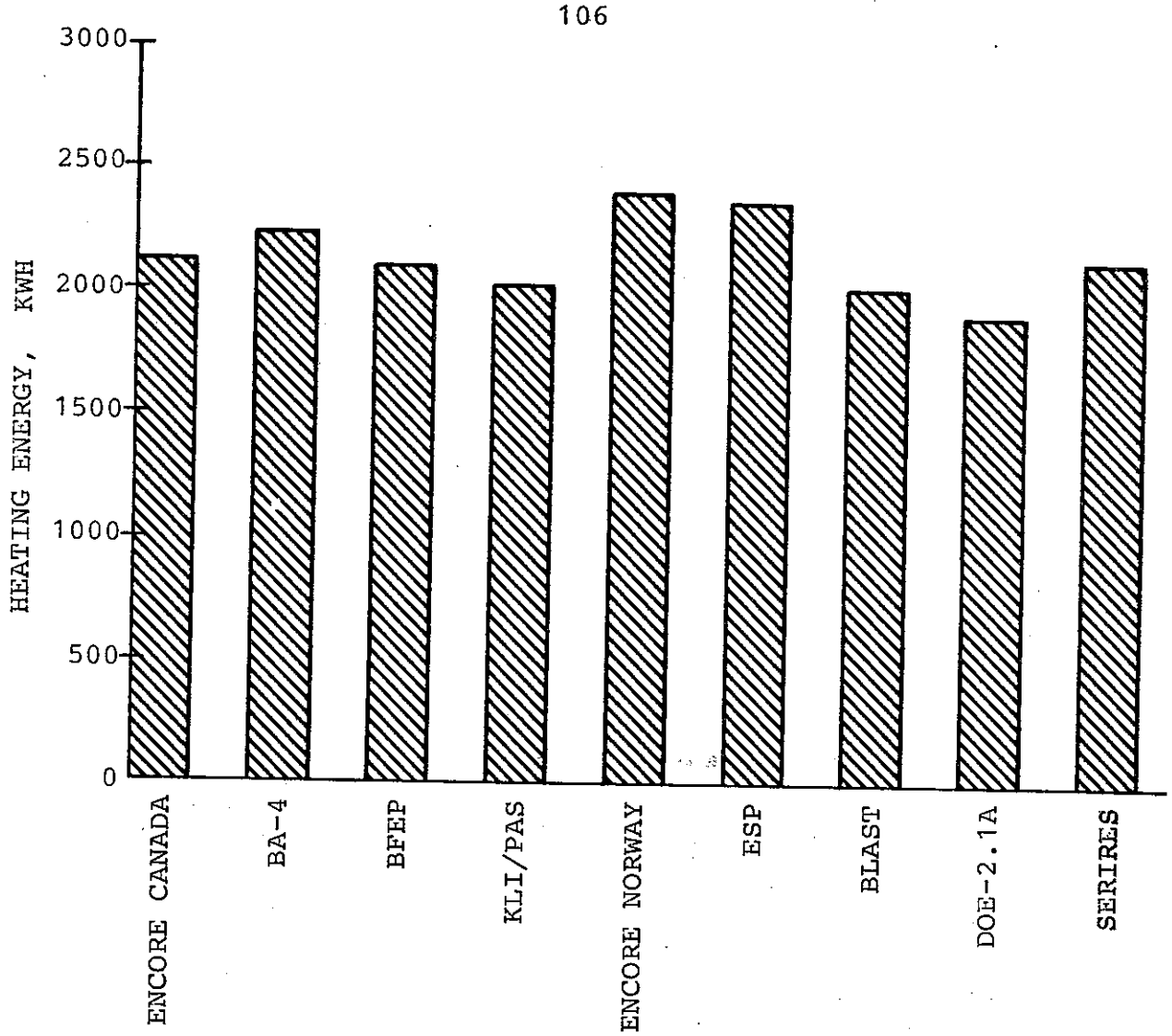

Fig. 5.34 Comparison of seasonal heating requirement for Copenhagen.

Fig. 5.35 Comparison of cooling requirements for Copenhagen.

REFERENCES

1. Barakat, S.A.. Passive Solar Heating Studies of the Divison of Building Research. Building Research Note 188. The Division of Building Research, National Research Council Canada, Ottawa. 1982.

2. Konrad, A. and Larsen, B.T. ENCORE-CANADA. Computer Program for the Study of Energy Consumption of Residential Buildings in Canada. DBR Paper No. 859, NRC 17663, Division of Building Research, National Research Council of Canada, Ottawa. 1978.

3. Lund, H. Program BA4 Users Guide. Thermal Insulation Laboratory, Technical University of Denmark. Report No. 44. Lyngby. 1979.

4. McFarland, R.D. PASOLE: A General Simulation Program for Passive Solar Energy. Los Alamos Scientific Laboratory, LA-7433.MS. 1979.

5. Butera, F., Farrngyia, S., Rizzo, G. and Silvestini, G. Il codice di calcolo SMP per la simulazione del comportamento termico di moduli edilizi solari passivi e convenzionali algoritmi usati e logica funzionale. Quaderni dello I.E.R.EN.-C.N.R., No. 1. 1984.

6. Augenboroe, G.L.M. BFEP: A Computer Program for Temperature Calculations in Buildings allowing Flexible User-Modelling. Proceeding 4th Int. Symposium on the Use of Computers for Environmental Engineering related to Buildings. Toky, 1983.

7. Van der Bruggen, R.J.A. Energy Consumption for Heating and Cooling in Relation to Building Design. 1978.

8. Larsen, B.T. Energy Consumption of Residential Buildings. The Computer Program ENCORE. Part 1, USERS's Manual. EDB program bibliotek No. 12, Norweigan Building Research Institute, Oslo, 1977.

9. Clarke, J.A. Abacus, Environmental Systems Performance (ESP) Users Manual. Dept. of Architecture. University of Strathclyde, Glasgow, UK, 1984.

10. Herron, D., Walton, G., Lawrie, L. Building Loads Analysis and System Thermodynamics (BLAST 3.0). User's Manual-Supplement to Volume 1, CERL-TR-E-171, 3/81. US Army Construction Engineering Research Laboratory, POB 4005, Champaign, IL 61820.

11. DOE-2.1 Reference Manual, Part 1. Edited by York, Tucker. Revision 5/81. National Technical Information Service.

12. SERIRES User's Manual. National Energy Software Center, Palmitre, Wheeling.

13. Judkoff, R. A Comparative Validation Study of the BLAST-3.0, SERIRES-1.0 and DOE-2.1A Computer Programs using the Canadian Direct-Gain Test Building. SERI Report. January 1985.

14. Mørck, O. Modelling and Simulation of Solar Heating Systems. Thermal Insulation Laboratory, The Technical University of Denmark. Report No. 170. November 1985.

15. Judkoff, R. International Energy Agency Building Simulation Comparison and Validation Study. SERI/TP-253-2758. Proceedings, Building Energy Simulation Conference. August 1985.

6. TROMBE WALL MODEL VALIDATION

6.1 Introduction

This chapter presents the results of validation efforts by the participating countries for the Swiss Trombe Wall Test Cell Case. The validation exercise involved modelling the monitored Swiss Trombe Wall Test Cell based on input data provided from the Ecole Polytechnique Fedérale in Lausanne (Prof. A. Faist). Calculated results for a ten-day period of actual measured weather data were then compared to the actual measured hourly zone air temperatures, Trombe wall surface temperatures and energy balance (no auxiliary energy was used during the test period.

Italy, the Netherlands, the United States and Switzerland participated in the Trombe wall test case (see table 1).

TABLE 6.1 PARTICIPATING COUNTRIES AND BUILDING ENERGY ANALYSIS SIMULATION PROGRAMS

COUNTRY	SIMULATION MODEL
Italy	SMP
The Netherlands	BFEP
United States	SERIRES, BLAST-3.0
Switzerland	SERIRES-1.0

6.2 Description of the Swiss Trombe Wall Test Cell

The Swiss Trombe Wall Test Cell is located in Ecublens (latitude 46.5°north, elevation 410 m) near Lausanne. It is characterized by a thermo-circulation loop (see Fig. 6.1) with two different operation modes (vents open or closed).

Figs. 6.2 and 6.3 show a sectional view and the position of the sensors. The Test Cell data are summarized in Table 6.2.

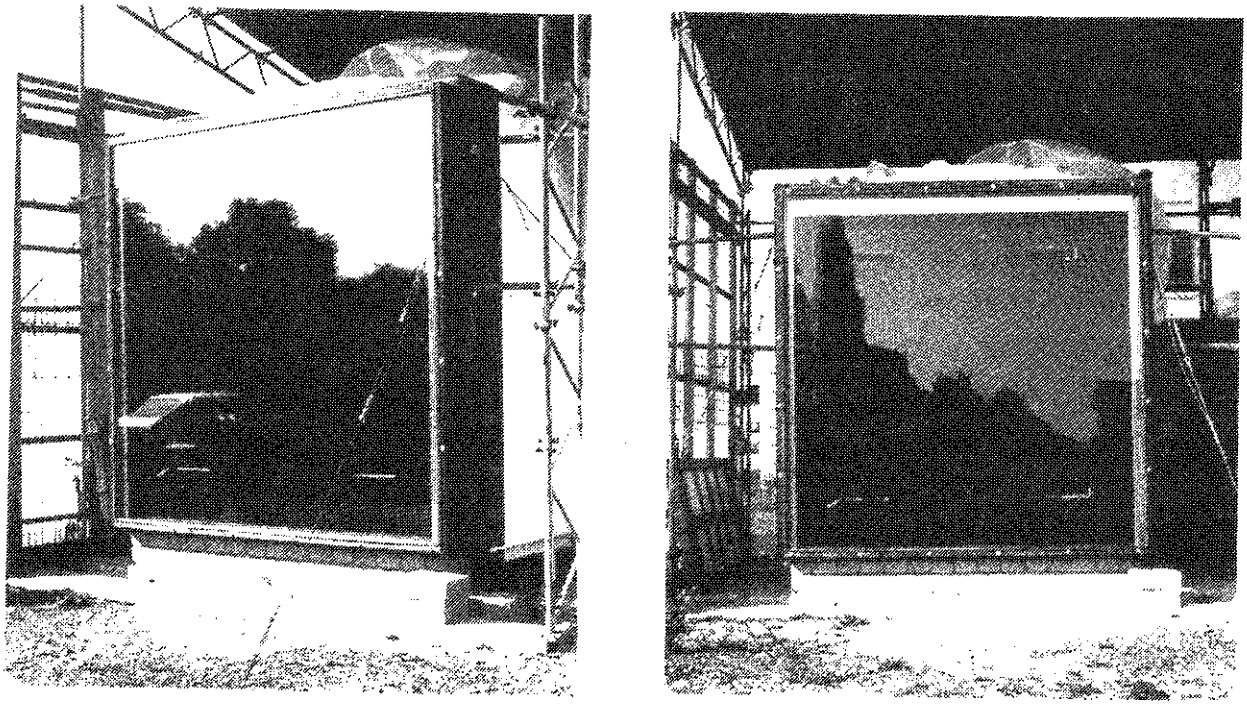

Fig. 6.1 View of Swiss Trombe Wall Test Cell. Thermo-circulation vents can easily be recognized on both pictures

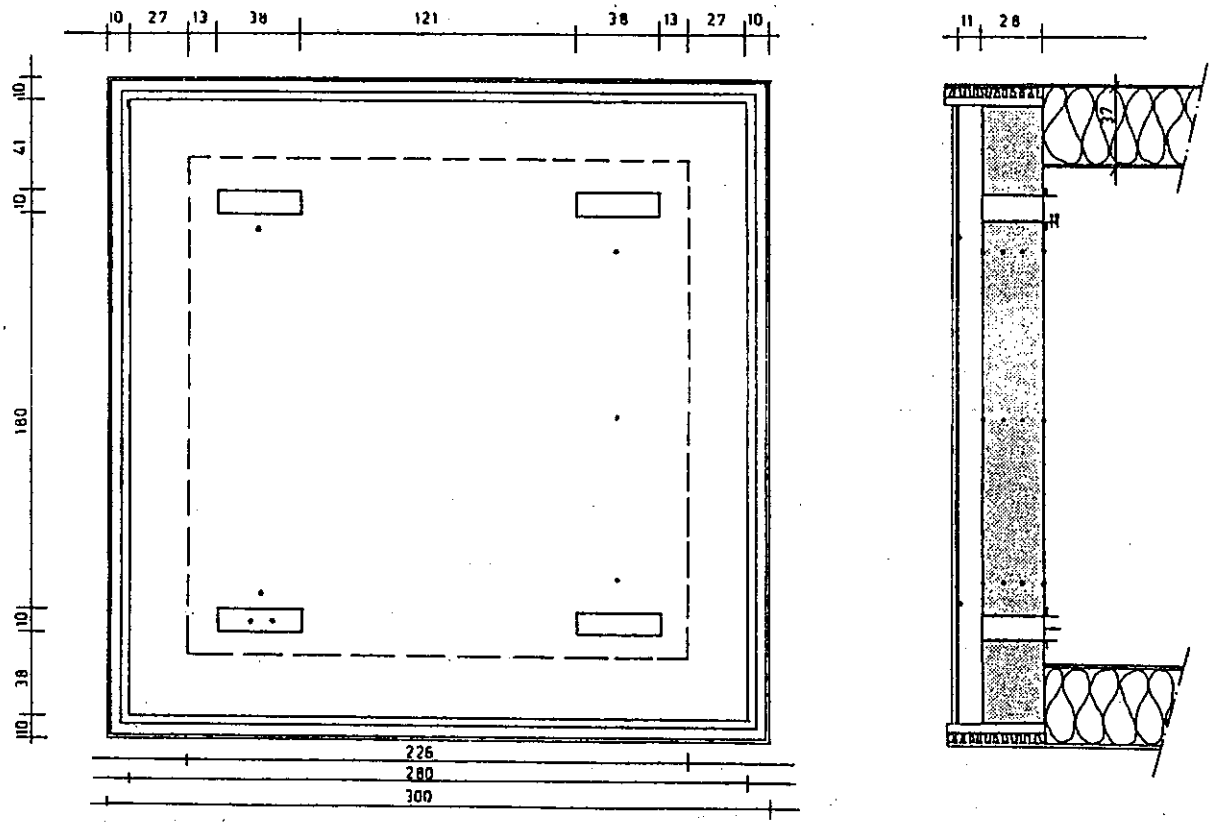

Fig. 6.2 View and elevation of Test Cell.

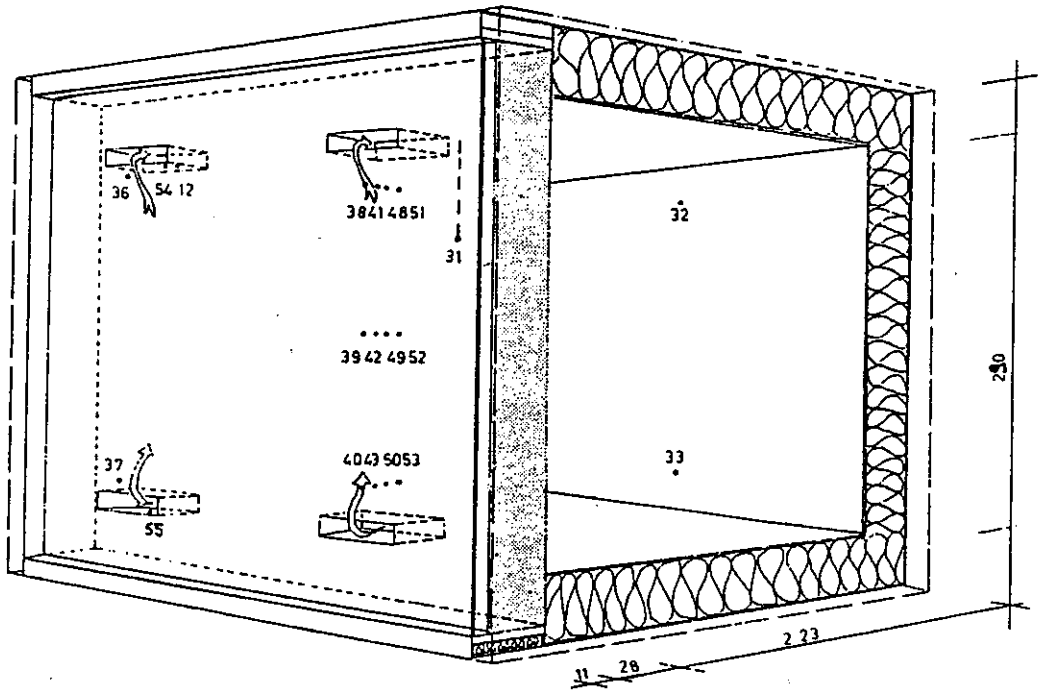

Fig. 6.3 Position of sensors.

TABLE 6.2 TROMBE WALL TEST CELL DATA

TEST CELL	
Indoor volume	12,2 m3
Area of the south aperture	5.06 m2
Insulation of the cell: mineral wool thickness	0,30 m
Thermal heat losses of the cell (without the Trombe wall)	5,2 + 0,2 W/K
Air changes	0,1 hr^{-1}
Auxiliary heating system (electrical with a fan)	600 W no auxiliary
Thermostat setpoint	16°C during test period
Fan, continously operating	12.5 W (Heat source!)
TROMBE WALL	
The wall	
Area 2.76 x 2.76	7,62 m2
Thickness	0,28 m
Material: concrete blocks, Density	1920 kg/m3
Thermocirculation vents:	
Upper vents 2 x 0,38 x 0,1	0,076 m2
Lower vents 2 x 0,38 , 0,1	0,076 m2
Hight between the vents	1,80 m
Colour of the wall	dark blue
Absorption coefficient	0,75
Glazing	
Area 2.76 x 2.76	7,62 m2
Double glazing (8/12/8 mm)	
Normal transmission	0,68
U-Value	2,9 W/m2 K
Space between the wall and the glazing	0,11 m
Night protection (not used)	

6.3 Test Conditions for Validation Exercise

Operating mode

A period with no auxiliary heating (March 25 through April 3, 1980) was selected for the simulation model validation. During this period, the thermo-circulation vents were kept open, even during the night. Also, no night insulation was used. Measured data gave room air temperatures, surface temperatures, upper and lower vent temperatures as well as thermo-circulation air velocities.

Weather data

The weather data file included ambient temperature, total horizontal radiation, total vertical south radiation, diffuse horizontal and albedo. Fig. 6.4 shows global horizontal radiation for the period of March 25 through April 3, 1980.

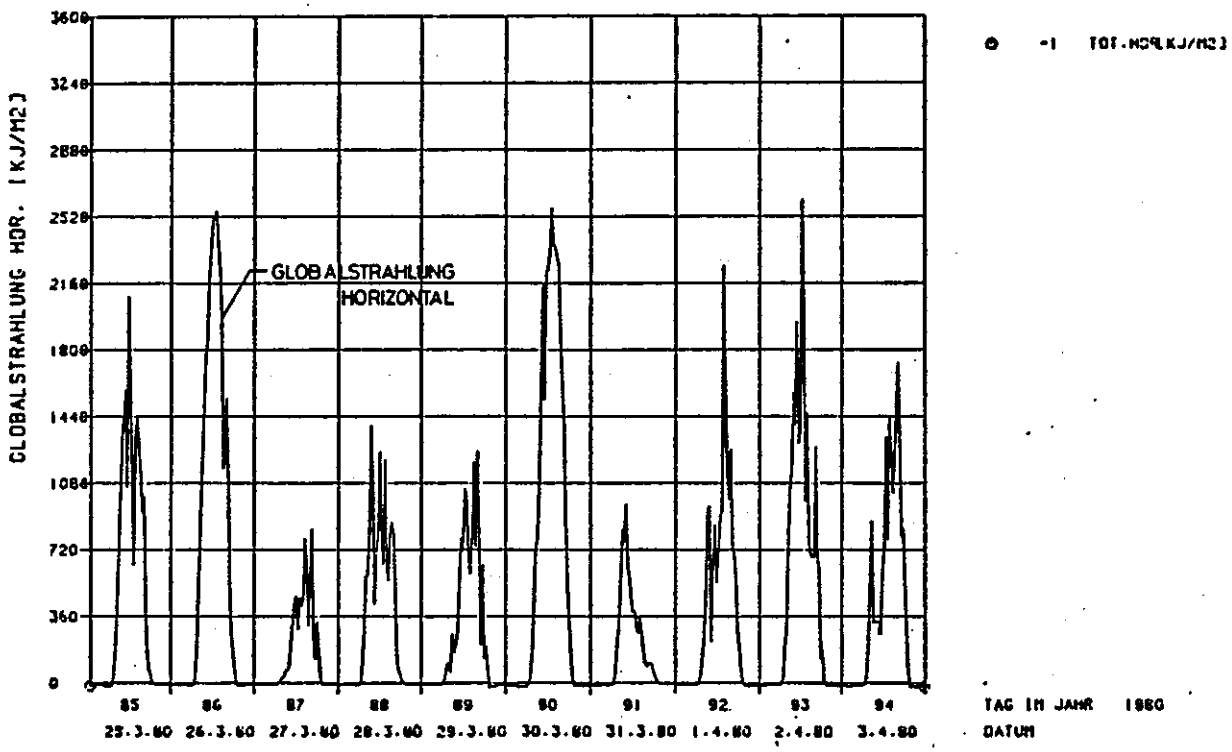

Fig. 6.4 Hourly data for global horizontal radiation.

6.4 Modelling Assumptions and Results

Validation by Switzerland

This work was performed by Charles Filleux from Basler & Hofmann in Zurich, using SERIRES-1.0. The Trombe wall was modelled using six thermal nodes for the mass wall, and a venting coefficient of 0.3. Swiss tests showed that values over 0.5 gave overly large volumetric flow rates and are therefore not recommended.

The results are shown in figs. 6.5 through 6.10. Fig. 6.5 shows measured and computed room air temperature, whereas Figs. 6.6, 6.7 and 6.8 compare Trombe Wall temperatures. Figs. 6.9 and 6.10 show computed mass flow and heat flows respectively. Further relevant data are given in Table 6.3.

TABLE 6.3 SUMMARY OF TROMBE WALL VALIDATION DATA

PARAMETER	SIMULATED VALUE	MEASURED VALUE
Test cell heat loss rate . (without south wall)	5.5 W/K	5.2 W/K
Heat loss rate of south wall	13.1 W/K	-
Mean room air temperature	21.6 ^{o}C	21.4 ^{o}C
Maximum mass flow on March 26	163 m^3/h or 0.045 m^3/s	
Average mass flow on March 26	116 m^3/h	79 m^3/h
Maximum air gap temperature	43.3 ^{o}C	-
Net heat flow through thermo-circulation (entire period)	50.0 MJ	24 MJ
Net heat flow through wall (entire period, no reverse thermo-circulation)	28.0 MJ	36 MJ

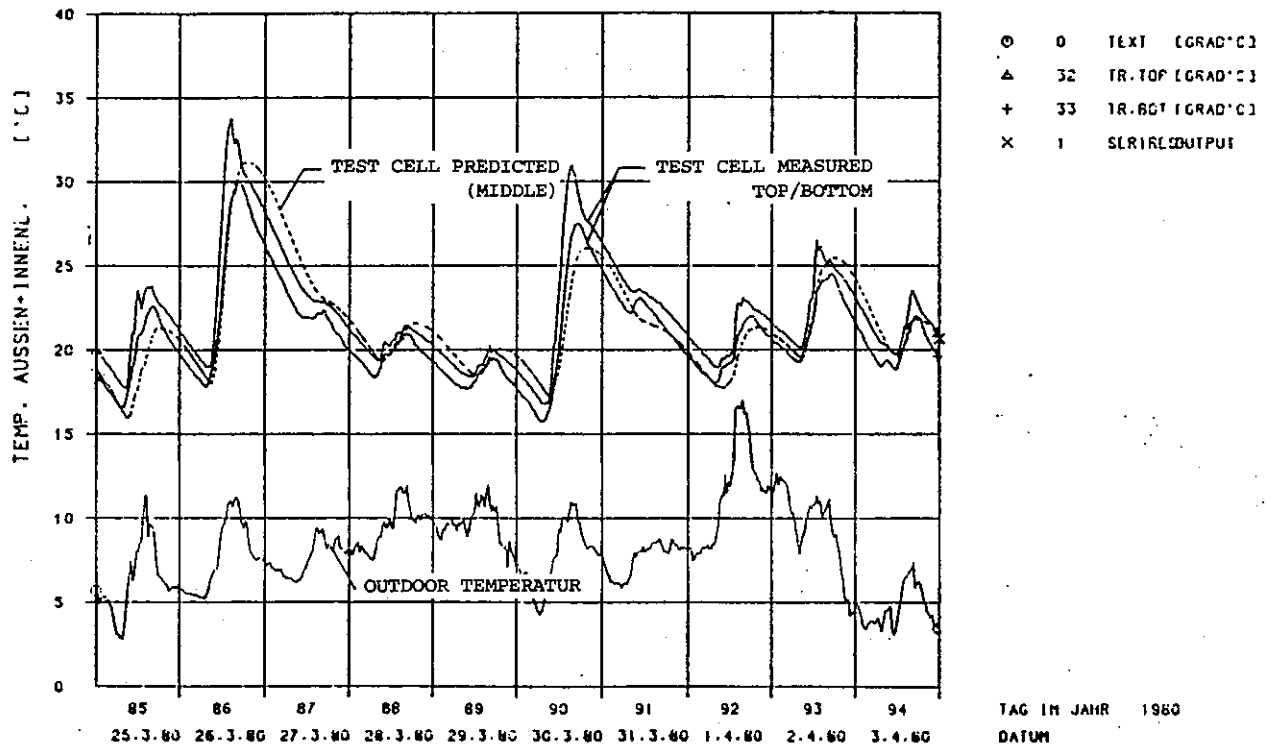

Fig. 6.5 Computed (---) and measured (——) room air temperature.

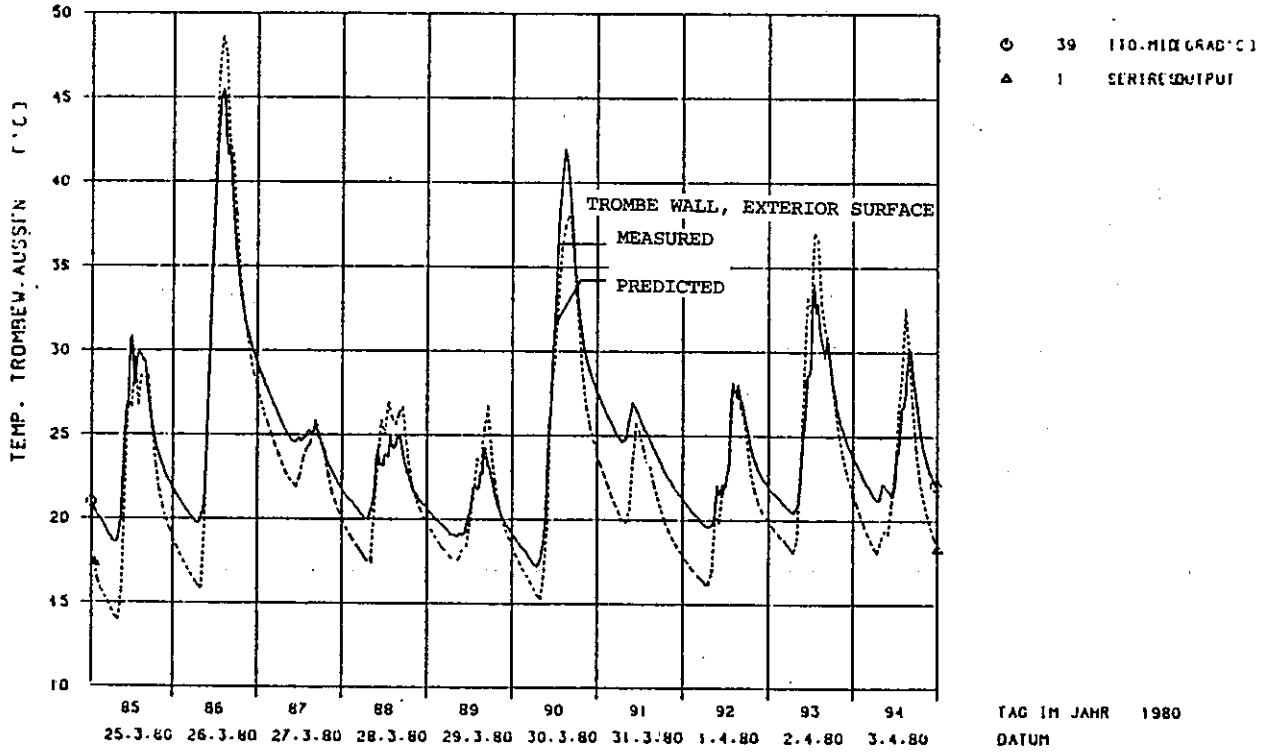

Fig. 6.6. Computed and measured surface temperature for exterior side of Trombe Wall.

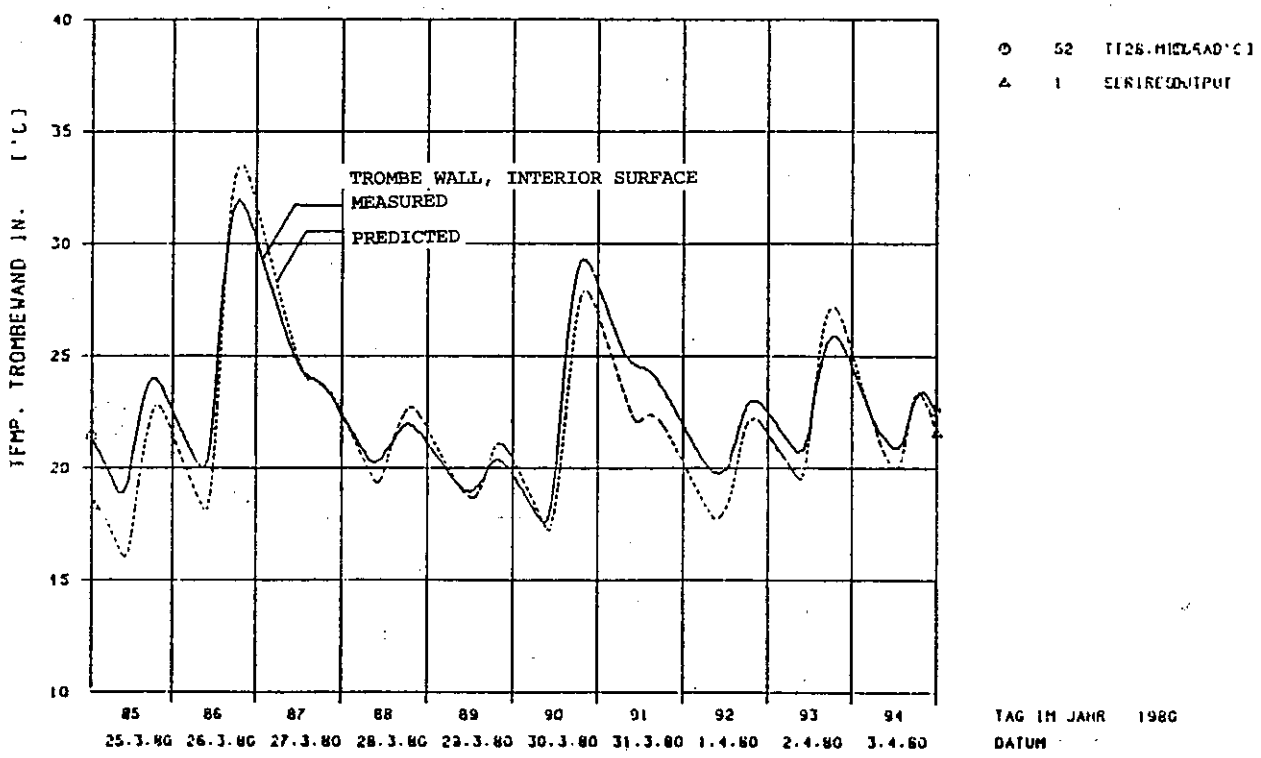

Fig. 6.7 Computed and measured surface temperature for interior side of Trombe Wall.

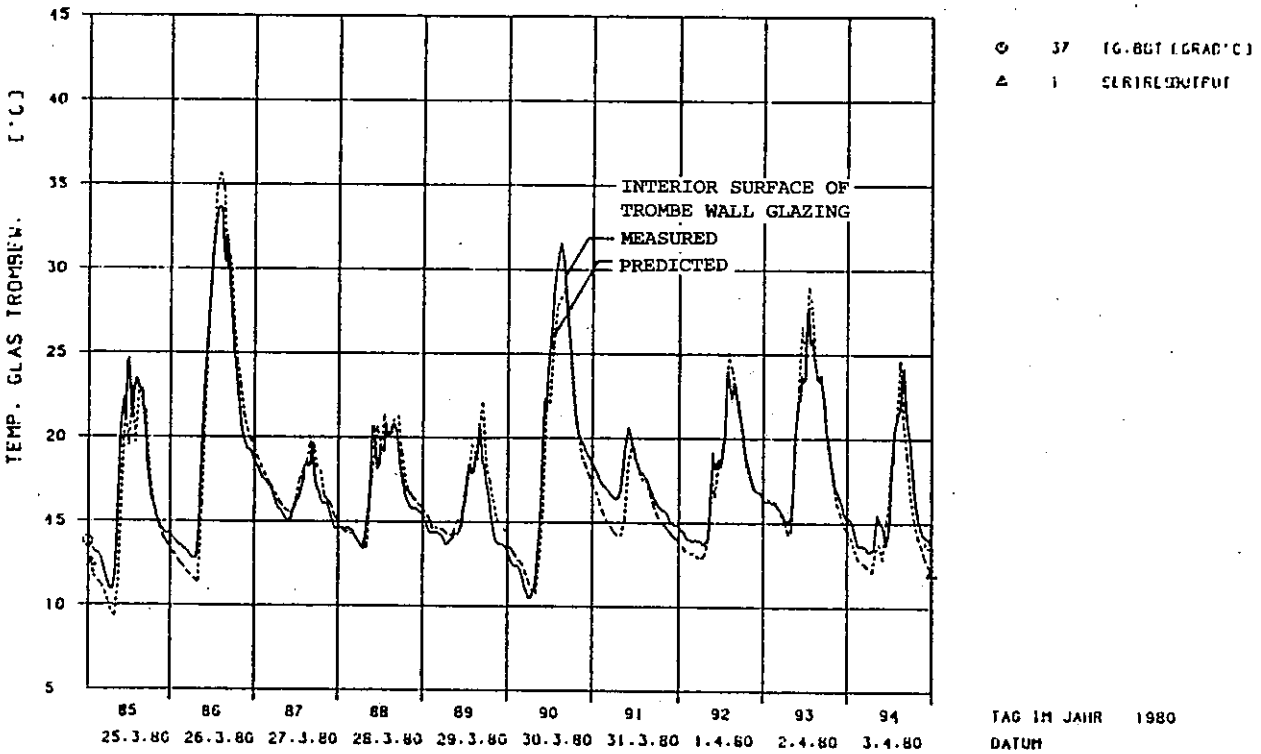

Fig. 6.8 Computed and measured surface temperature for interior side of glazing.

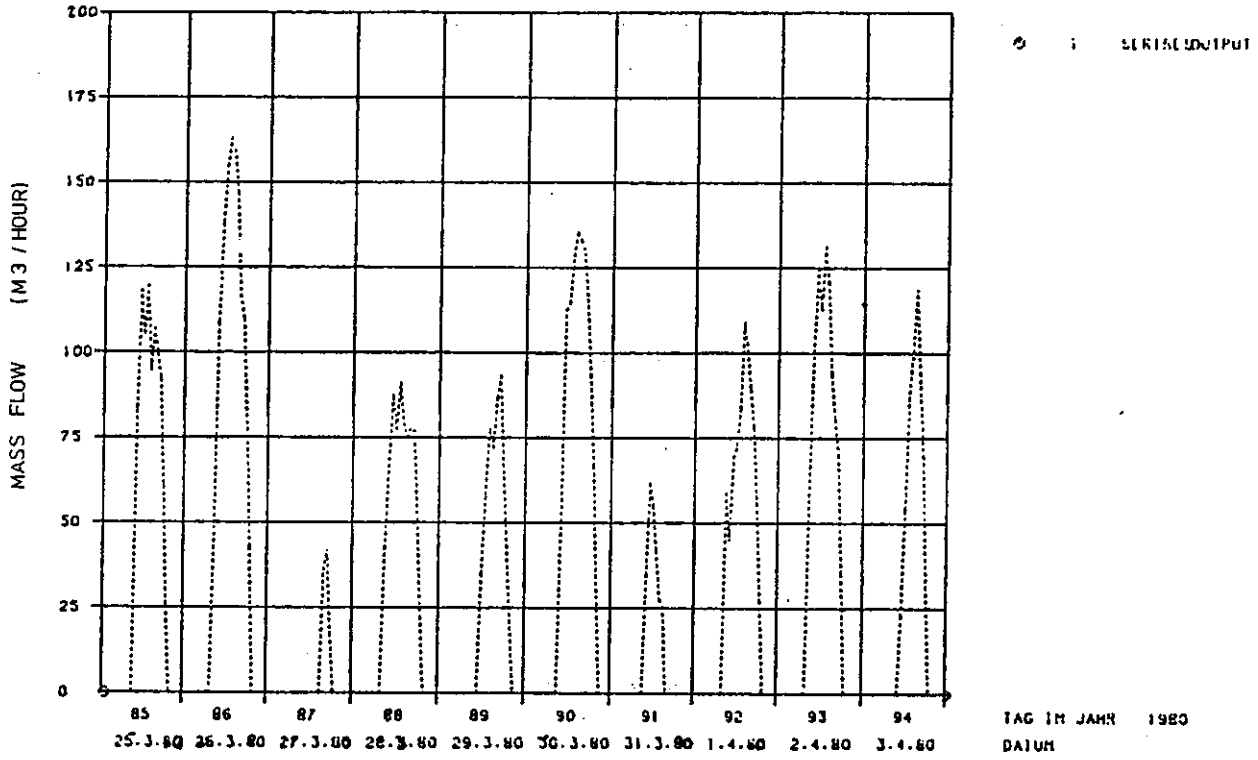

Fig. 6.9 Computed mass flow rates. Note that no reverse thermo-circulation was allowed at night.

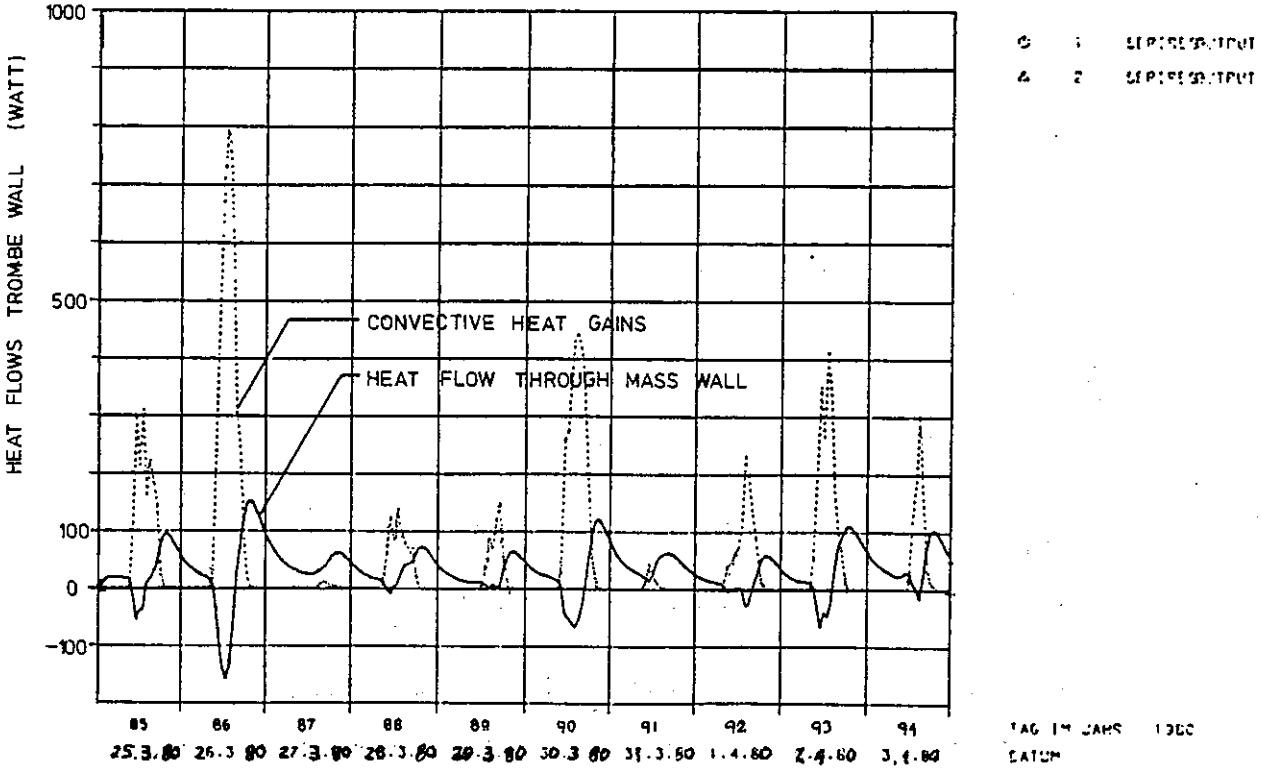

Fig. 6.10 Computed data for convective heat gains and heat flow through mass wall. Note that no reverse thermo-circulation was allowed at night.

Conclusions for Trombe wall validation in Switzerland:

- Simulation of room air temperature as well as surface temperatures of the Trombe wall were in good agreement with measured data.
- The net heat flow through the wall was underestimated by 25%. On the other hand, the thermo-circulation gains were highly overestimated (factor of two). It should be remembered that thermo-circulation gains are highly dependent on the vent coefficient.

Validation by the United States

An attempt to model the Trombe wall with BLAST-3.0 revealed a number of bugs in the BLAST-3.0 Trombe wall subroutine. After multiple attempts to simulate the Trombe wall using the up-dated capabilities of BLAST-3.0, it was found that a bug exists in the code that is extremely sensitive to the required input parameter values and which normally causes the simulation to fail with one of three different error messages:

1. "Exceeded maximum temperature range (CHACS)" -- applies to the special Trombe wall zone.
2. "Exceeded maximum temperature range (HBAIRI)" -- applies to the room behind the Trombe wall.
3. Overflow - infinite value -. This is a system generated error message. (The previous two were generated by the BLAST program). The error occurs in subroutine CHTURB.

The messages occur through slight variations in the input values for:

- Trombe wall ventilation restrictions
- glazing transmissivity
- Trombe wall solar absorptivity
- Trombe wall size
- weather data.

The Trombe wall was also modelled with the SERIRES program. In this case, identical inputs to the Swiss modelling team were used in order to assist in bench-marking their version of this program. The predicted results are essentially identical to those obtained by the Swiss version of SERIRES. Since the Swiss input file was used with the original US version of SERIRES, it can be concluded that installation of the code in Switzerland has been successful.

Validation by Italy

This work was performed by Federico Butera from the University of Palerma using the SMP program. His results are as follows:

Fig. 6.11 shows measured hourly versus calculated temperature for the Swiss Trombe wall in the period March 29 to April 2. (During the first days of the period, wind velocity was not available).

Calculated temperatures for sunny days are lower than measured but they agree very closely for cloudy days and night temperatures. The agreement between measured and calculated outlet air temperaure is also very close (see fig. 6.12); therefore it is difficult to explain the difference during sunny hours.

On one hand, it could derive from the large difference between the glazed and the internal area of the Trombe wall (due to the thickness of the test cell enclosure) or, on the other hand, from a strong temperaure gradient in the room. In fact, in the simulations, outer and inner Trombe wall surfaces are considered equal, and no temperature gradient is allowed for in the cell.

Also solar radiation data were found contradictory at times, and the split between direct and diffuse radiation has been calculated.

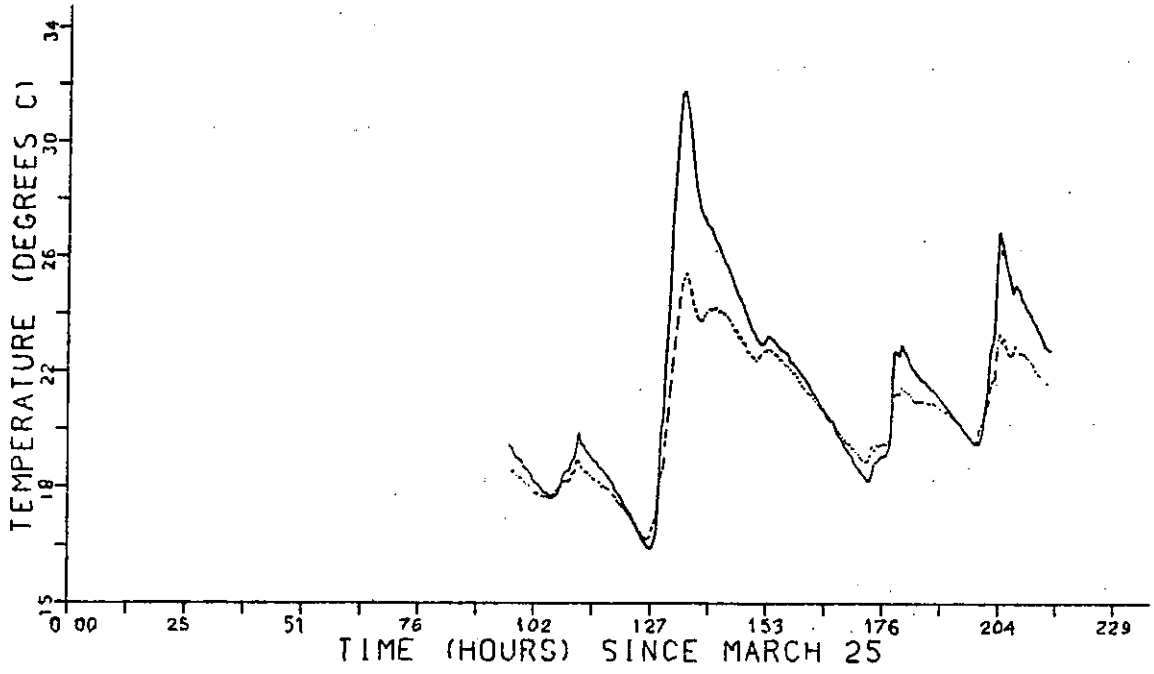

Fig. 6.11 Hourly computed versus measured test cell air temperature.

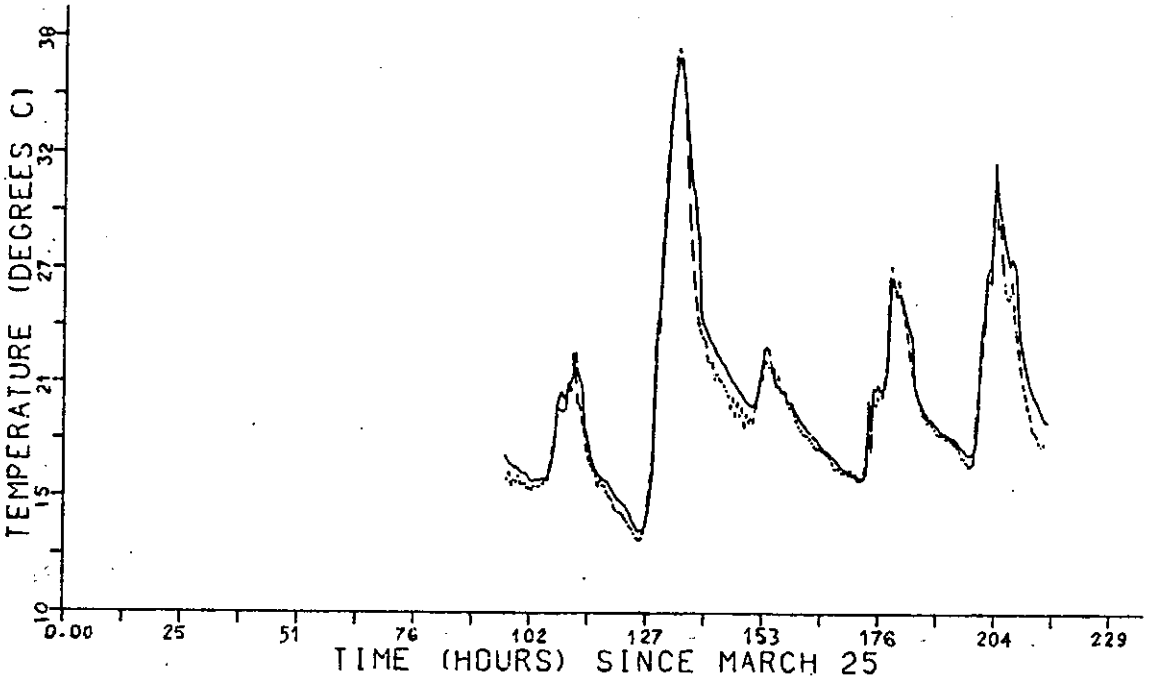

Fig. 6.12 Hourly computed versus measured outlet air temperature.

Validation by the Netherlands

The validation by the Netherlands using BFEP was performed by G.L.M. Augenbroe from the University of Delft and supervised by A. Poel from the Bouwcentrum. The following results were reported:

Inside air temperature

Fig. 6.13 shows the computed (mean) inside air temperature T_{air} compared to the measured data of channel 32 and 33.

Wall surface temperature

Fig. 6.14 shows the computed external surface temperature $T_{s,ext}$ compared to the measured data of channel 39.

Fig. 6.15 shows the computed internal surface temperature $T_{s,int}$ compared to the measured data of channel 52.

Convective heat flow from the channel

Fig. 6.16 shows the computed convective heat supplied through the Trombe wall channel $Q_{TM,ch}$.

Conductive heat flow from the Trombe wall

Fig. 6.16 also shows the computed conductive heat flow $Q_{TM,w}$ at the internal surface of the Trombe wall.

Mass flow from the TM-channel

Fig. 6.17 shows the mass flow V_{TM} entering or leaving the room through the thermo-circulation vents.

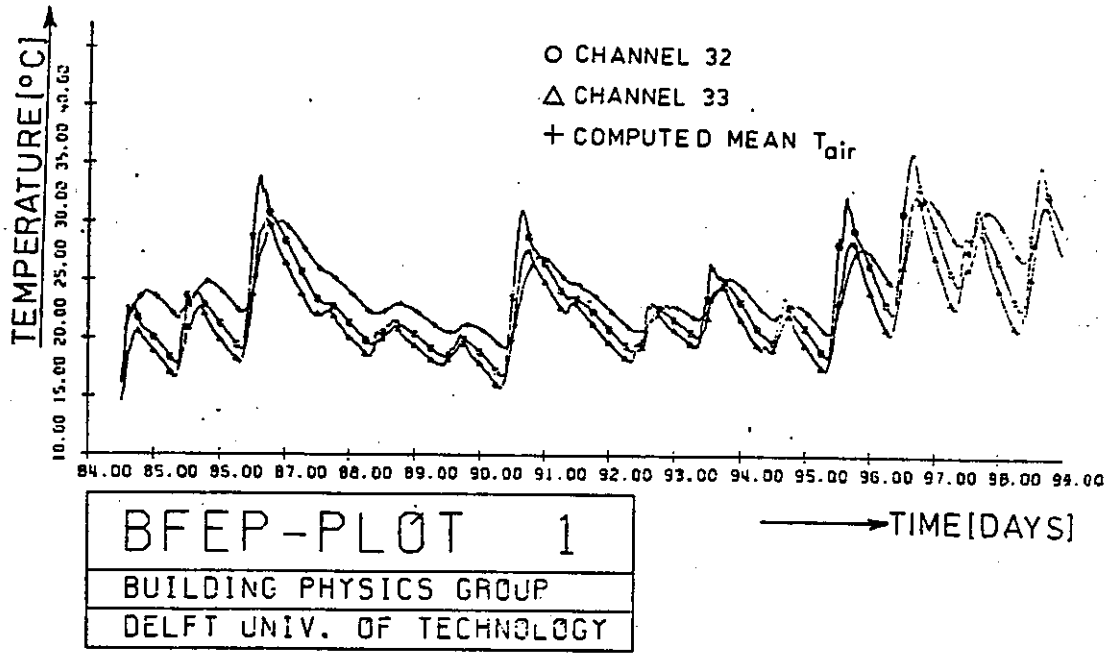

Fig. 6.13 Computed and measured inside air temperature.

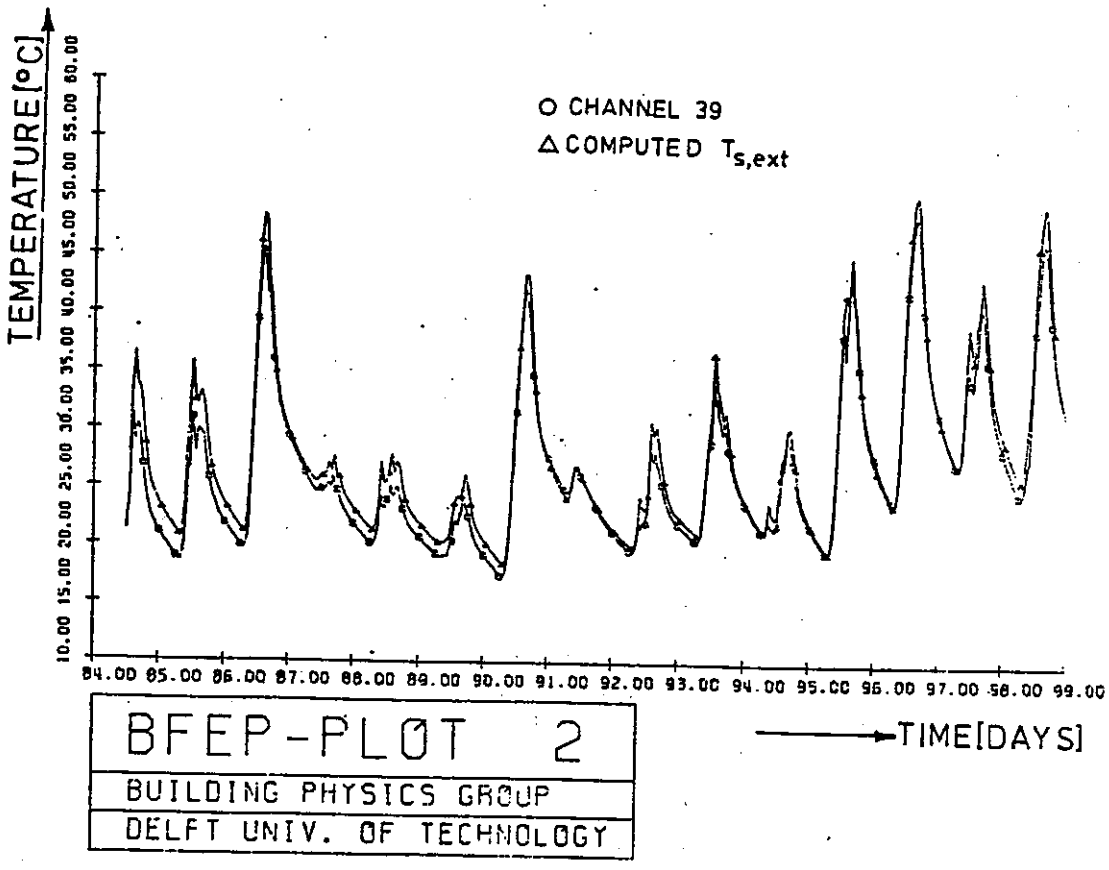

Fig. 6.14 Computed and measured external surface temperature.

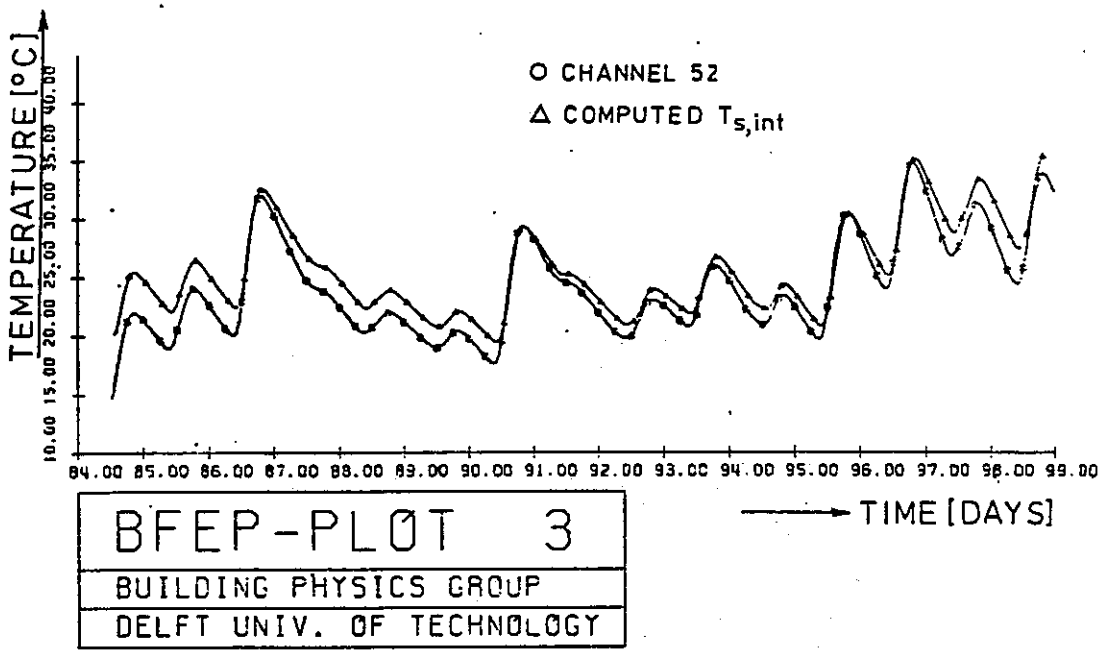

Fig. 6.15 Computed and measured internal surface temperature.

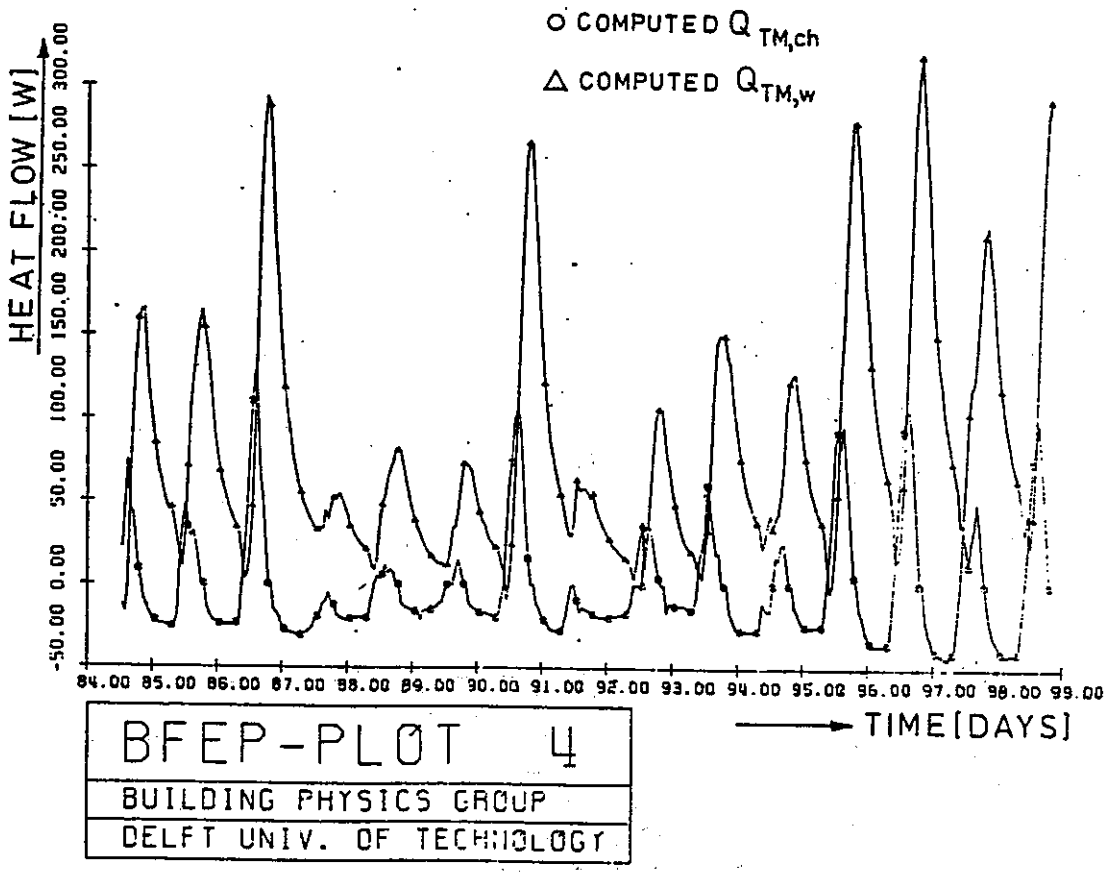

Fig. 6.16 Computed convected heat flow.

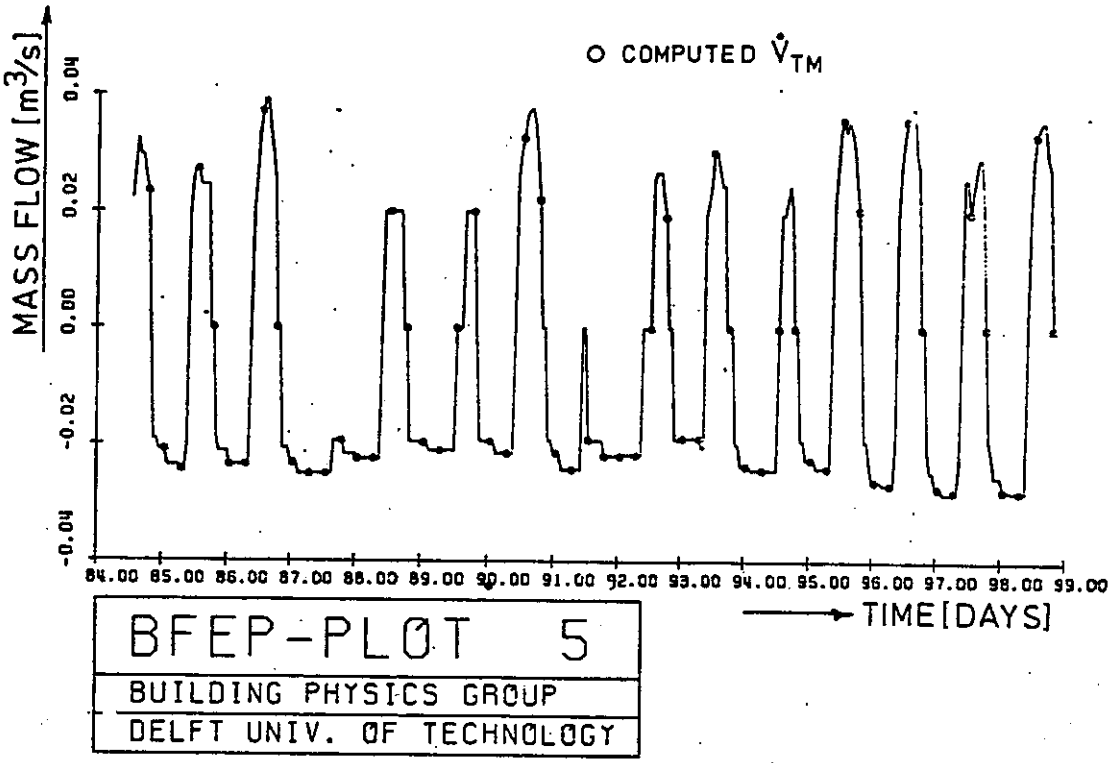

Fig. 6.17 Computed mass flow rate.

The period-totals (14.5 days) for $Q_{TM,ch}$ and $Q_{TM,w}$ were found to be:

$$\int_p^{Q_{TM,ch}} = -1.0 \text{ kWh (because of reverse thermo-circulation)}$$

$$\int_p^{Q_{TM,w}} = 29.1 \text{ kWh}$$

Total: 28.1 kWh

Trombe Wall collector efficiency

Computed mean inside air temperature $\bar{T}_{air} = 24.6^{o}C$

Mean outside air temperature $\bar{T}_{ext} = 7\ ^{o}C$

U-value of Trombe Wall: $U \approx 1.52\ W/m^2K$

Total transmission losses through the wall if solar radiation is not taken into account:

$$Q_{trans} = 63.3 \text{ kWh}$$

Collected solar heat: $63.3 + 28.1 = 91.4$ kWh

Total south insolation: $I_{south} = 282.7$ kWh

$$\eta_{TM} = \frac{91.4}{282.8} = 0.32$$

In spite of the apparent deviations between the measured and computed inside air temperatures (fig. 6.13), no attempts were made to incorporate the effects of temperature stratification inside the room into the computations. Although this would have been a straigtforward matter within the BFEP-computations, it was not attempted due to the lack of an appropriate physical room model, which would be applicable in this case.

Needles to say, stratification effects strongly influence the instantaneous convective heat supply from the room-facing Trombe wall surface as well as the channel inlet temperature.

Furthermore, as detailed information with regard to the initial state at computation start was lacking, not much attention should be paid to the results during the first two or three days.

Negative values for $Q_{TM,ch}$ indicate reverse flow in the channel, i.e. inside air is cooled on its way down the channel.

6.5 Conclusions

Computed results of four simulation models with Trombe Wall routines (SERIRES, SMP, BFEP, BLAST) were compared against measured data from the Swiss Trombe Wall Test Cell. For SERIRES, SMP and BFEP, computed and measured room and surface

temperatures are in reasonable agreement. Apparent differences between computed and measured room air temperatures (see figs. 6.5 and 6.13 resp.) for SERIRES AND BFEP occur mainly because no attempts were made to take into account the effects of temperature stratification. This may also be why computed convective heat flows do not reproduce measured data and differ by a large factor between SERIRES (fig. 6.10) and BFEP (fig. 6.16). This last result is somewhat surprising since mass flow rates (figs. 6.9 and 6.17 resp.) agree quite well for SERIRES AND BFEP.

7. ATTACHED SUNSPACE MODEL VALIDATION

7.1 Introduction

This chapter presents the validation efforts by the participating countries for the attached sunspace case. This effort involved three countries and five simulation programs. These are listed in Table 7.1.

TABLE 7.1 LIST OF SIMULATION PROGRAMS

Country	Simulation Program
The Netherlands	BFEP
The Netherlands	KLI/PAS
Switzerland	DEROB
USA	BLAST-3.0*
USA	SERIRES-1.0*

* only used for yearly simulations

The test cell chosen for this validation study is one of the test cells of the U.S. Los Alamos National Laboratory. A description of the test cell along with the supplied monitored data follows below. The simulation program predictions are compared to the monitored data. Finally, the results of yearly simulations using Copenhagen and Denver climate data are presented and compared.

7.2 Description of the Test Cell

During the winter of 1980-81, 11 different test cell configurations were monitored at the US Los Alamos National Laboratory (LANL) in New Mexico. The LANL Solar Laboratory is located at 106.3^{o}west longitude and 35.8^{o}north latitude and at an altitude of 2158 m. A description of the test cells and the measured data is given in ref. 1 from which the following information is taken.

The test cell chosen for this study has an attached sunspace with a 60^{o} sloping double glazed window in front of two small rooms. A floor plan of the test cell is shown in Fig. 7.1.

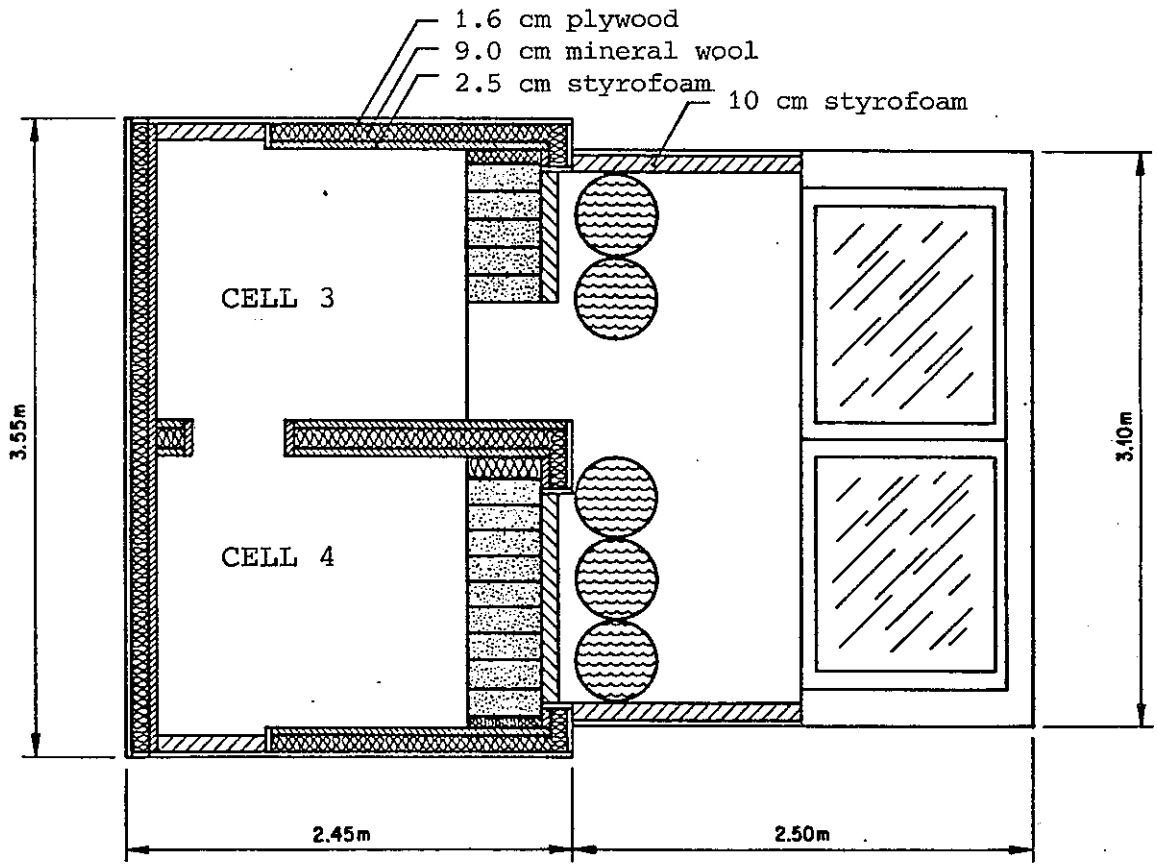

Fig. 7.1 Floor plan of test cell in Los Alamos.

A sunspace doorway provides thermo-circulation heat transfer from the sunspace to the eastern room which is thermally connected to the western room by another door. The door between the two rooms was always open whereas the sunspace doorway was closed at night until February 22; after that, the door was open at all times. Nighttime insulation was employed on the outside of the sunspace glazing from 4.30 p.m. to 8.00 a.m.

In the configuration used for the validation simulations, the mass wall between the sunspace and the two rooms was insulated with extruded styrofoam and five water-filled drums were

placed on the sunspace floor along its north wall. For the yearly simulations, the mass wall was not insulated and the water drums not present. Besides the water drums, sunspace mass was located in the floor consisting of 14 cm high concrete blocks.

The characteristics of the test cell are summarized in Table 7.2. The cells have insulated wood frame construction walls, floor and ceiling, the components of which are briefly given in Table 7.3.

TABLE 7.2 CHARACTERISTICS OF TEST CELL

Inside measures:	
Room depth, m	2.18
Room width, m	1.57
Room height, m	3.05
Floor area per room, m^2	3.44
Heating set point, ^oC	18.3
Ventilation rate, ach	3.0
Sunspace width, m	2.87
Sunspace depth at the floor, m	2.26
Sunspace depth at the ceiling, m	1.22
Sunspace height at common wall, m	2.19
Sunspace floor area, m^2	6.49
Net sunspace glazing area, m^2	5.04
Thermal resistance of sunspace glazing, m^2K/W	
Sunspace doorway area, m^2	1.06
Sunspace floor thermal capacity, MJ/K	1.7
Water drums thermal capacity, MJ/K	2.1
Common wall thermal capacity, MJ/K	3.1

TABLE 7.3 DETAILS OF BUILDING ELEMENTS

ELEMENT TYPE	CONSTRUCTION	THERMAL RESISTANCE m^2K/W
Cell wall*	Extruded styrofoam, wood frame with fiber glass, insulated and plywood	2.2
Cell floor	Plywood, fiberglass between joists (5x15 cm)	2.4
Cell ceiling	Corrugated metal, fiberglass between joists (5x15 cm)	2.4
Sunspace wall and roof	Extruded styrofoam, plywood	2.8
Sunspace glazing	Thermo pane/with insulation	0.2/1.43
Sunspace glazing	Overall solar transmission at normal incidence	0.69

* All walls are of wood frame construction, 5x10 cm studs at 0.4 in centres

The sunspace floor and the water drums were painted flat black (α = 0.95, ε = 0.90). The extruded styrofoam insulation on the sunspace ceiling and end walls was left unpainted and had an absorptivity of 0.3. The mass wall insulation was painted dark brown (α = 0.87).

Auxiliary heating of each test cell room was provided with six 100 Watt light bulbs. The light bulbs were controlled by the on-line computer maintaining a set point of 18.3^{o}C using measured globe temperatures.

Monitored data

Data were supplied for the heating season 1980-81 during which period the test cell was operated in different modes and configurations. The period chosen for this study covered 14 days from February 14 to February 27, a cold period with considerable

sunshine. Except for the change in sunspace doorway operation, the test cell configuration was left unchanged during this period. Reference 1 includes a graphical presentation of two of the monitored data for this period. This graph is shown in Fig. 7.2.

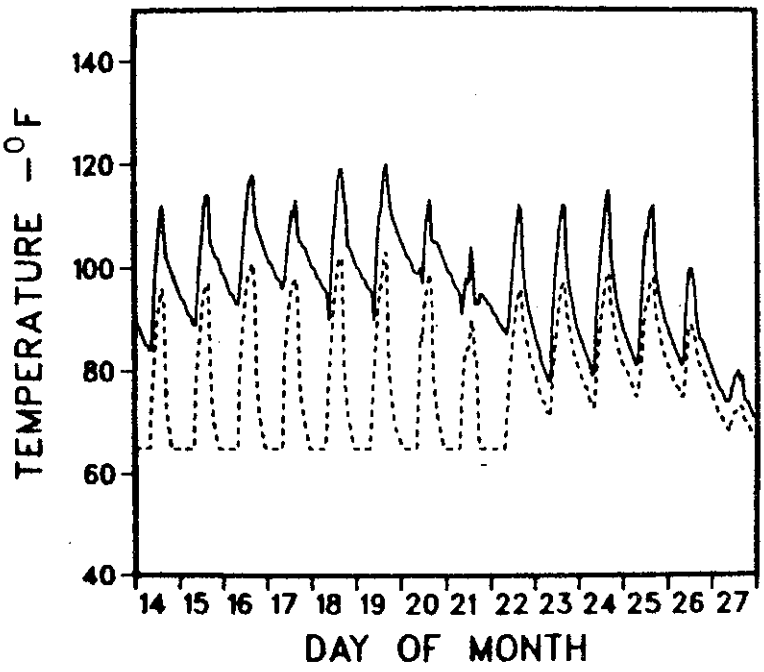

Fig. 7.2 Measured temperatures in sunspace (solid line) and east cell (dashed line).

The supplied data tape contained 20 channels including wall, floor, air and globe temperatures at different locations, as well as auxiliary power requirements for each hour. All temperatures in ^{o}F and power in watts, averaged over the previous hour.

The hourly weather conditions were given by 18 channels including both instantaneous and averaged values of the following weather data:

- Vertical surface insolation, Btu/ft^{2}h
- 60^o surface insolation, Btu/ft^{2}h
- 36^o surface insolation, Btu/ft^{2}h
- Horizontal surface insolation, Btu/ft^{2}h
- 45^o surface insolation, Btu/ft^{2}h
- Dry bulb temperature, ^{o}F
- Wind speed, mph
- Wind direction, degrees from north
- Dew-point temperature, ^{o}F

7.3 Summary of Simulations and Results

Three models were used to simulate the test cell for the comparison of predictions to measured performance. The results for each of these models are presented along with a brief list of assumptions specifically used for the model. A brief general description of each model is given in chapter 5.

1. Country: SWITZERLAND

   Simulation Model: DEROB

   The test cell was simulated as two zones, the cell and the sunspace. In order to keep the model simple, the water in the drums was considered as an additional layer of the south wall. The larger solar exposure of this wall was compensated by reducing the absorption factor of the surface. Problems arose with the modelling of the door between the two zones. Modelling an open door during daytime and closed during nighttime was not possible with DEROB. It was therefore decided only to consider the last 5 days of the period during which the door was open all the time.

Simulation results

DEROB predictions of sunspace air temperatures and cell air temperatures are compared in Fig. 7.3. From this figure it is seen that the DEROB predictions are in good agreement with the measured data for this period.

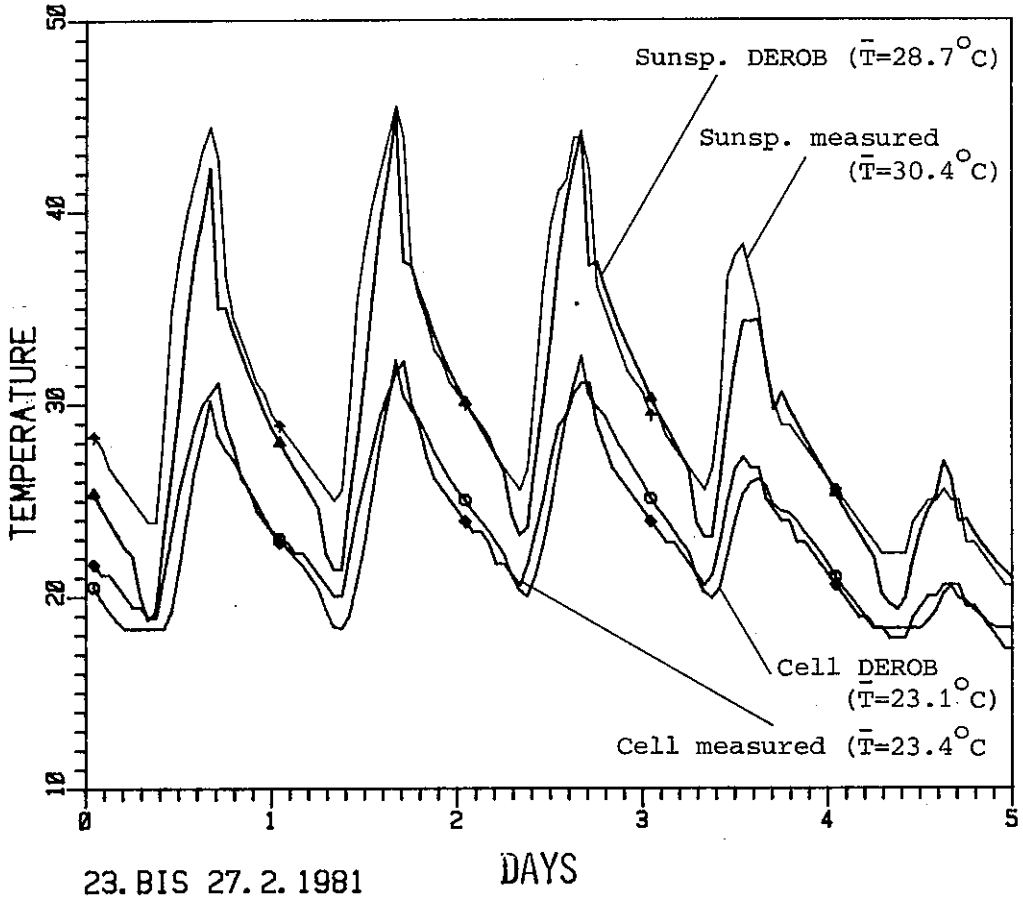

Fig. 7.3 Result of simulation of the test cell with attached sunspace in Los Alamos, DEROB.

2. Country: THE NETHERLANDS

Simulation Model: BFEP

Except for the natural convection air flow between doors, all components and phenomena were modelled by previously established model components. The test cell was modelled as a three zone building with natural convection air flows through the two doors. A simple one-node mean temperature model was used for each zone.

- Natural convection through doorways: Several modes were tested and the one which proved most accurate was chosen. The testings showed, however, that both temperature profiles and auxiliary loads were rather insensitive to the choice of model. The model chosen is represented by the following function of ΔT - the temperature difference between the two rooms:

$$f(\Delta T) = 20 \text{ W/K}, \quad \text{for} \quad \Delta T \leq 2K$$

$$= 20 + 46.2\ (\Delta T-2)^{\frac{1}{2}}, \quad \text{for } 2K < \Delta T < 5K$$

$$= 100 \text{ W/K}, \text{ for} \quad \Delta T > 5K$$

- Short wave radiation exchange: Part of direct radiation on door area is computed and absorbed in east-cell if the door is open.
- Water drums: modelled as separate components within the sunspace; longwave radiation exchanges with the surrounding wall and glass surfaces are accounted for. Each drum was modelled with 3 nodes, 2 for the surface and one for the water.

Simulation results

The BFEP hourly temperature and auxiliary heating power predictions are compared to the measured performance data in Figs. 7.4 to 7.8.

Whereas the measured temperatures are represented rather well by the computed results, the measured and computed auxiliary loads show some significant deviations.

It is apparent that the west room requires a larger amount of auxiliary heat, contrary to the measurements which show a remarkably overall balanced load in both rooms.

One would expect the energy stored daily in the mass walls in both rooms to contribute significantly to the nightly energy supply. As the mass wall in the east room acquires a higher temperature during daytime, this could

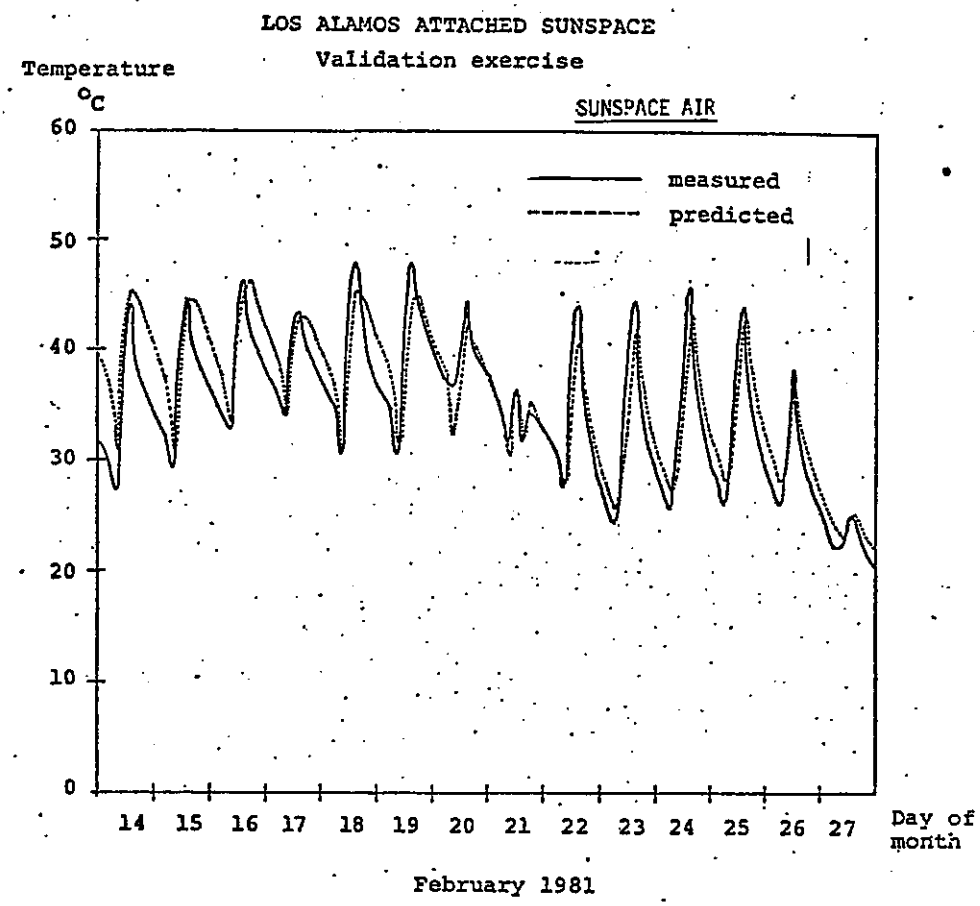

Fig. 7.4 BFEP results, sunspace air temperature, ^{o}C.

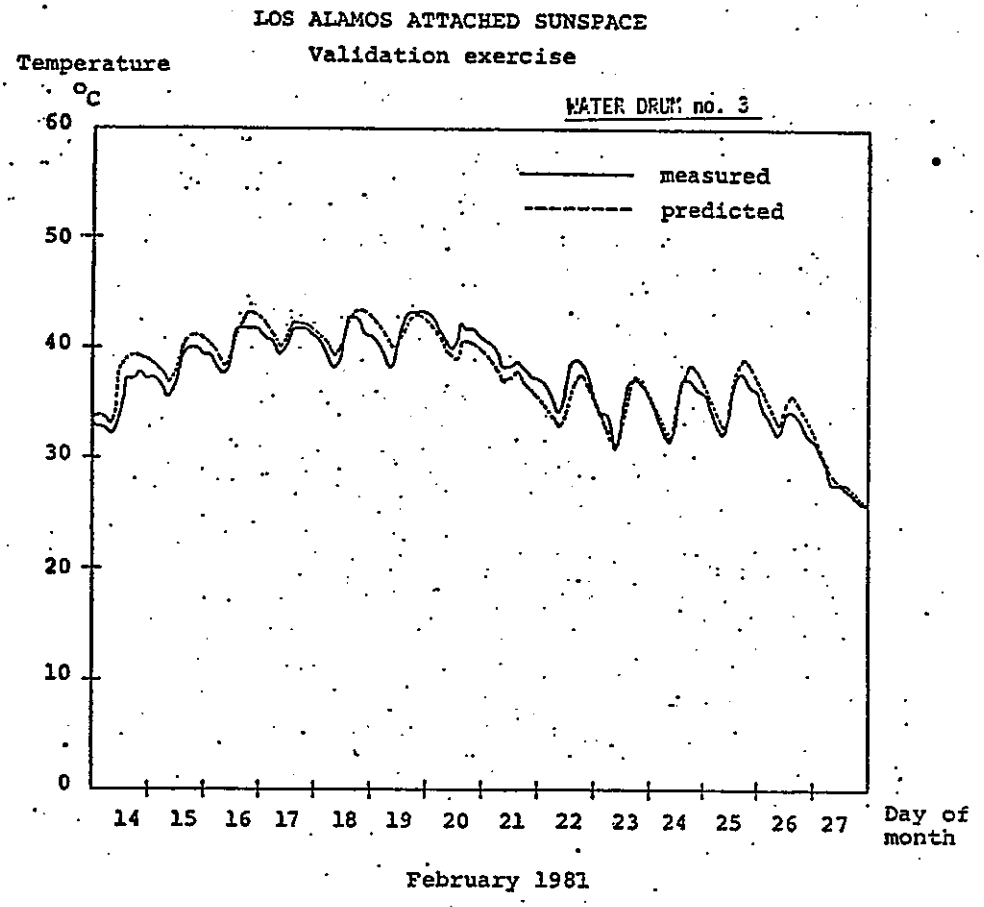

Fig. 7.5 BFEP results, water drum temperature, ^{o}C.

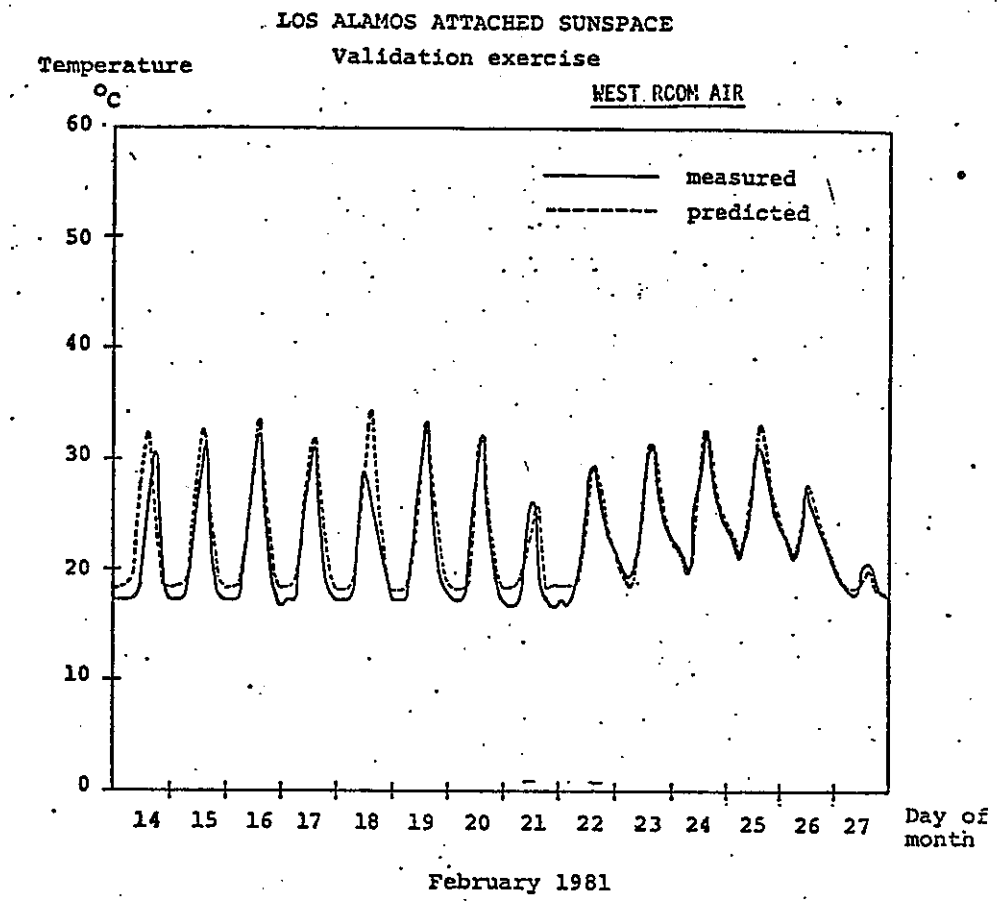

Fig. 7.6 BFEP results, west room air temperature, °C.

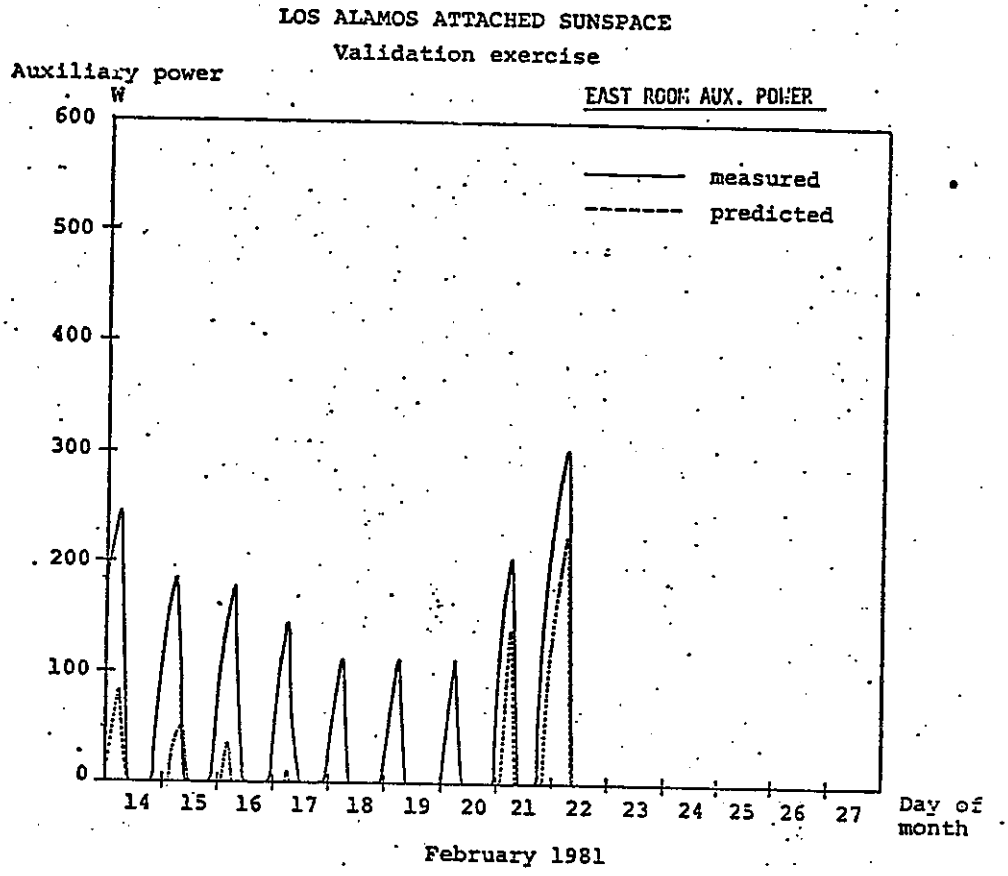

Fig. 7.7 BFEP results, east room auxiliary power, W.

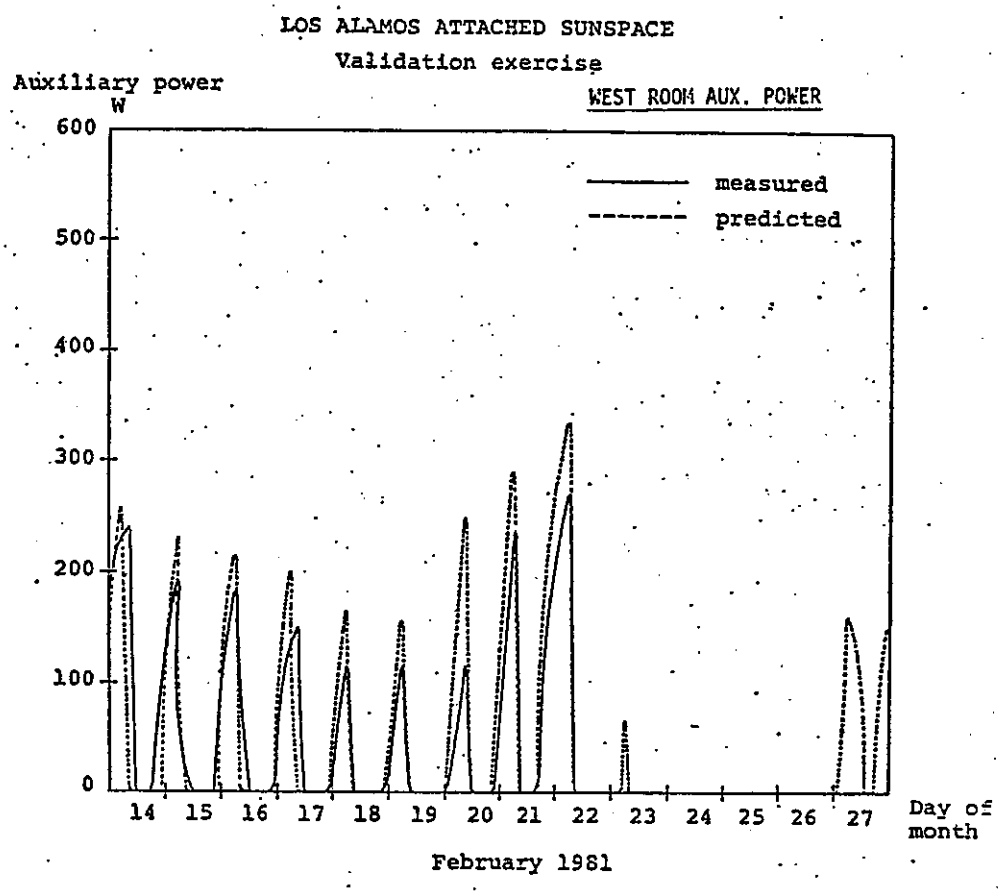

Fig. 7.8 BFEP results, west room auxiliary power, W.

obviously lead to a larger contribution during the night.

The failure of this expectation to be substantiated by the measurements can be attributed to the following:

- The cell-to-cell open door heat flow model is inadequate (especially in case of small temperature differences between the rooms);
- The convective heat exchanges, i.e. heat exchanges with the mass walls, are modelled incorrectly. (Air velocities in the small rooms are very hard to predict).

Moreover, the fact that the combined total predicted auxiliary loads were found to be well below the ones measured, (20.9 compared to 25.9 kWh), leaves one in doubt as to whether the predicted Building Loss Coefficient (BLC) is not too small.

Several trial runs showed that in order to find a total of 25.9 kWh, a BLC-value of approximately 16 W/K had to be used (instead of 13.8).

3. Country: THE NETHERLANDS

Simulation Model: KLI/PAS

- Test cell modelled with a two-zone model.
- Natural convection inter-zone air movement modelled by:

$$V = 95 \cdot \sqrt{T_{sunspace} - T_{cells}}, \quad m^3/h.$$

- No short wave radiation exchange between zones modelled.
- Sunspace assumed to be rectangular. Glass area equal to description. Incident solar radiation is the incident solar radiation used for a tilted plane.
- Water drums modelled as a layer in the wall between the sunspace and the cells (as in DEROB).

- Radiation distribution: 50% of the incoming direct radiation is submitted to the "water-drum-wall" and 40% to the sunspace floor. The rest of the direct radiation and all diffuse radiation are equally distributed to all the internal surfaces of the sunspace zone.

Simulation results

The KLI/PAS hourly temperature and auxiliary heating power predictions are compared to the measured performance data in Figs. 7.9 to 7.13.

From Figs. 7.9 to 7.11, it appears that KLI/PAS dynamically tracks the performance of the test cell rather well, but generally predicts considerably lower temperatures than measured. Also, the predicted auxiliary power requirement shown for both rooms (total divided by 2 for each room) in Figs. 7.10 and 7.11 are lower than the measured. The total predicted heating load for the period was 21 kWh which is the same as predicted by BFEP.

7.4 Yearly Simulations

As many of the computer simulation programs used by Task VIII participants could not be used to model the natural convection through the sunspace doorway, it was decided to construct a slightly modified theoretical test case for the yearly simulations. Ron Judkoff, the Subtask participant from the U.S. prepared an input specification for this case (2). The major modifications to the original test case were as follows:

1. The building is configured as described for the time period December 20 through January 3.
2. The door between the sunspace and cell 3 is always shut.
3. The door between cells 3 and 4 is always open.
4. No water drums have been placed in the sunspace.
5. The sunspace doorway is 28 cm wide.

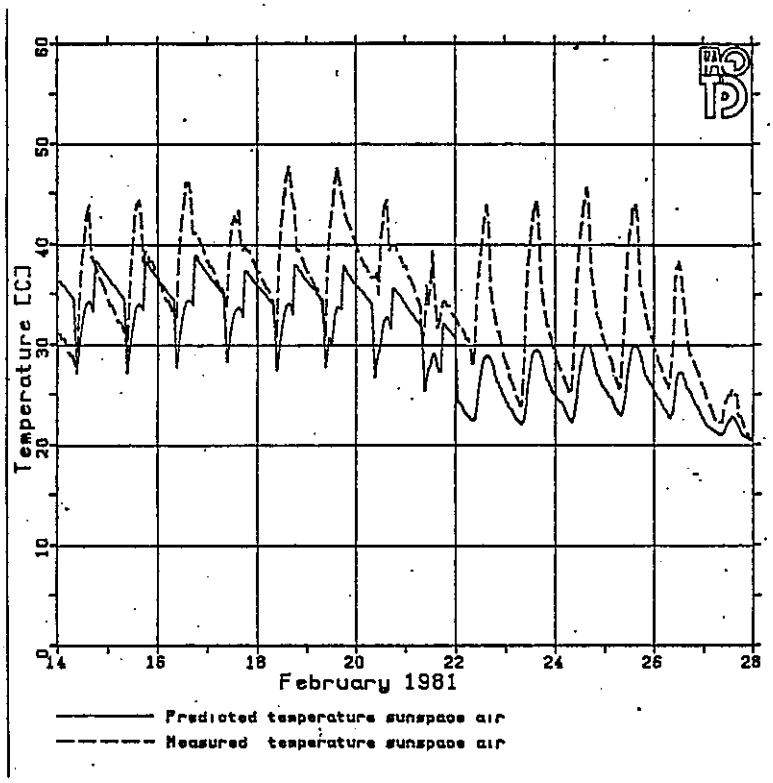

Fig. 7.9 KLI/PAS results, sunspace air temperature, °C.

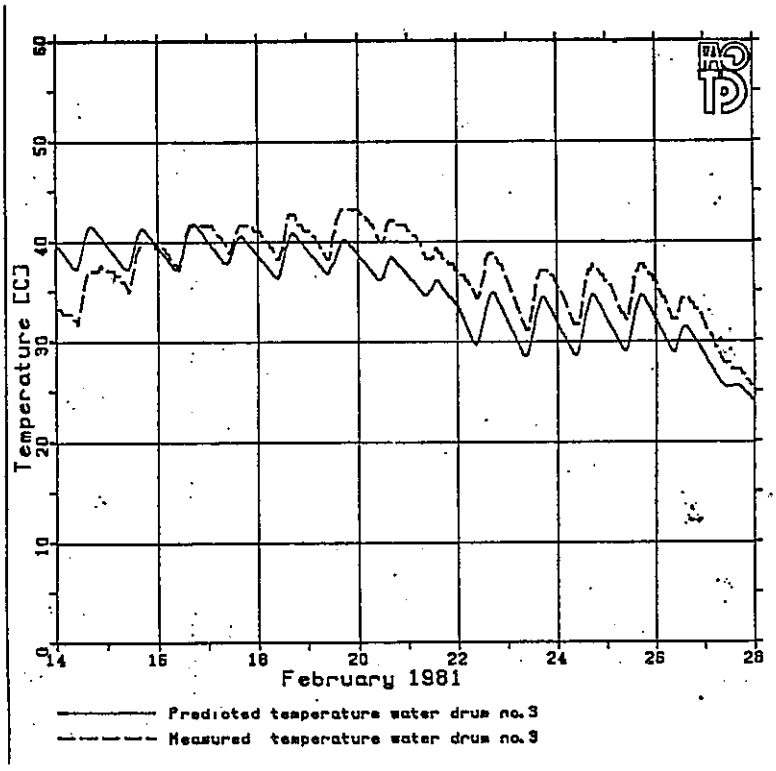

Fig. 7.10 KLI/PAS results, water drum temperature, °C.

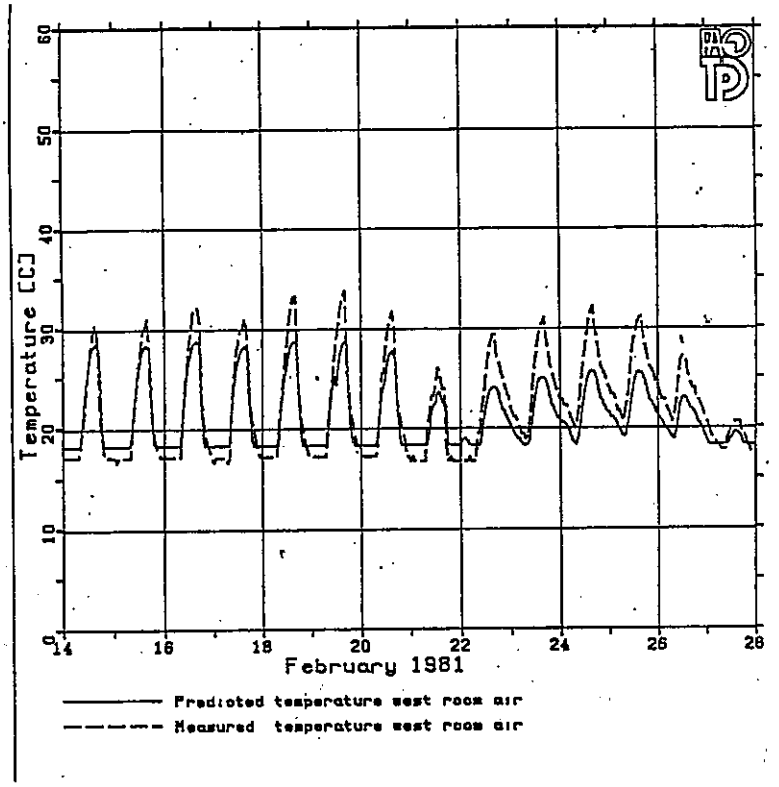

Fig. 7.11 KLI/PAS results, west room air temperature, ^{o}C.

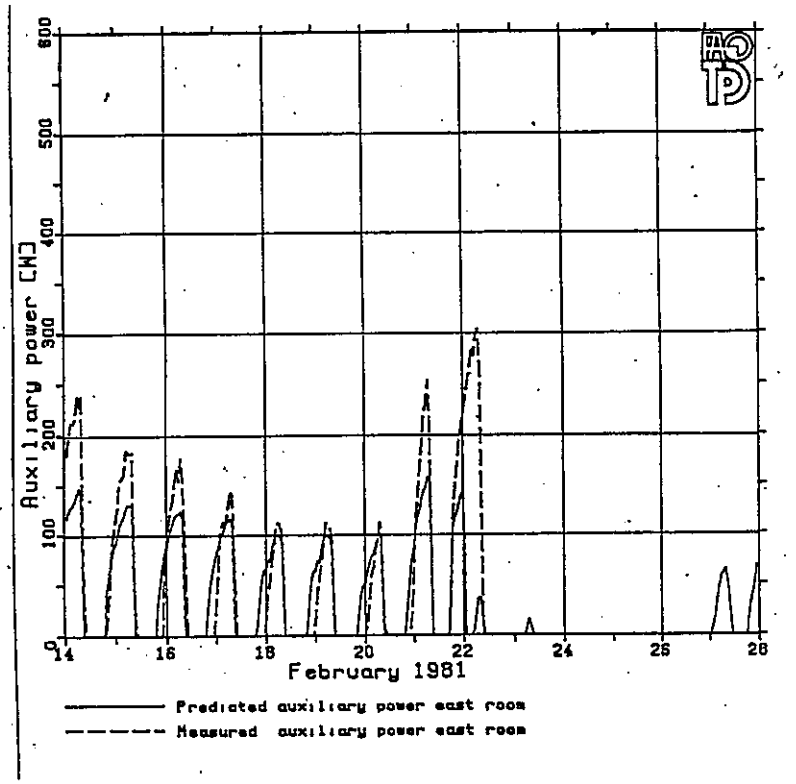

Fig. 7.12 KLI/PAS results, east room auxiliary power, W.

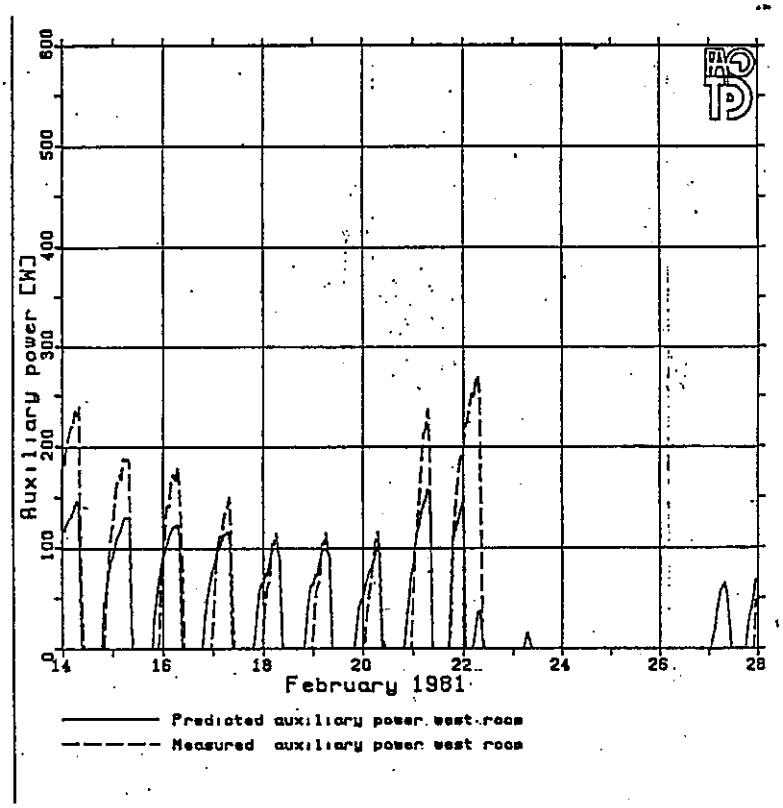

Fig. 7.13 KLI/PAS results, west room auxiliary power, W.

6. No insulation layer has been placed over the mass wall.
7. The mass floor and wall have not been painted black, but remain their natural unpainted colour (solar absorptivity = .7, infrared absorptivity = .9).
8. Cells 3 and 4 were modelled as a single zone.
9. The heating setpoint temperature was 18.33°C.
10. For purposes of the intercode comparison, a cooling setpoint of 27°C, even though the real building had no cooling or venting.
11. There is no convection between the sunspace and the backzone.

Four programs were used to simulate the US test cell using Copenhagen and Denver yearly weather data. Tables 7.4, 7.5 and 7.6 summarize the results.

TABLE 7.4 SUNSPACE TEST CELL YEARLY SIMULATIONS, COPENHAGEN DATA. HEATING AND COOLING AUXILIARY ENERGY CONSUMPTION AND PEAK LOADS.

Program	Aux. Energy, kWh		Peak Load, kWh	
	Heating	Cooling	Heating	Cooling
SERIRES	2324	25	1.0	0.2
BLAST	2298	12	1.0	0.2
DEROB	2235	117	1.0	0.5
DOE-2.1C	2099	19	0.9	0.2

TABLE 7.5 SUNSPACE MAXIMUM AND MINIMUM TEMPERATURES, COPENHAGEN CLIMATE.

Program	Maximum, °C	Minimum, °C
SERIRES	65.9	3.5
BLAST	57.9	3.8
DEROB	82.7	5.6
DOE-2.1C	65.6	6.2

TABLE 7.6 BACK ROOM MAXIMUM AND MINIMUM TEMPERATURES, DENVER CLIMATE.

Program	Maximum, ^{o}C	Minimum, ^{o}C
SERIRES	38.7	-13.9
BLAST	36.8	-13.9
DEROB	40.2	-3.2
DOE-2.1C	36.6	-10.3

From the tables it appears that the DEROB program seems to overpredict the cooling load compared to BLAST-3.0 and SERIRES. Furthermore, it does not predict nearly so low a minimum temperature for the back room as the two other programs.

Some additional information concerning the effect on heat demand of interzone solar radiation transfer and the influence of internal walls can be obtained from another code comparison (3). In this, DEROB and SERIRES/SUNCODE results were compared for a mid-terraced apartment with a sunspace. This has a window in the living room facing into the sunspace. That comparison leads to an even higher heat demand deviation of about 50%.

7.5 CONCLUSIONS

Predictions by the three simulation programs of the thermal behaviour of the test cell were compared to the measured data.

Two of these programs showed acceptable agreement to the measured temperatures within the sunspace and the test cell, whereas rather large differences were observed for the prediction of auxiliary heating requirement. The third program underpredicted the temperatures considerably, and to a lesser extent, the auxiliary heating power.

Yearly simulations of a modified test cell were compared for four programs showing acceptable agreement on auxiliary heating power and peak heating loads. However, substantial differences were observed for maximum and minimum temperatures as well as for the cooling load.

REFERENCES

1. McFarland, R.D. (1982). Passive Test Cell Data for the Solar Laboratory, Winter 1980-81. Los Alamos National Laboratory. LA-9300-Ms.

2. Judkoff, R. International Energy Agency Sunspace Intermodel Comparison. SERI/TR-254-3/BLG 661, April 1986.

3. Erhorn, H., Stricker, R., Szerman, M. Sunspace Calculation Comparison SUNCODE-DEROB. Working document IEA Task VIII, Fraunhofer Institut für Bauphysik, Stuttgart, May 1986.

8. CONCLUSIONS AND RECOMMENDATIONS

8.1 Conclusions

Simulation programs play an important role in the design of passive and hybrid solar low energy buildings. Because of the complexity of these models and the continuing development of new routines and entirely new programs, a need for validation is evident. At the outset of the work in Task VIII, validation experience was limited. Very few studies using adequate performance data had been conducted and documented. The test cell validation study, documented in this report, has significantly helped to fill this gap.

Validation of building thermal analysis simulation programs is a very difficult process. It can never be achieved in any absolute sense, i.e. we can never be sure that a simulation program showing close agreement to measured data in one case can be assumed to possess the same accuracy for any other building type, climate, occupancy profile, etc. The generally accepted understanding of "validation" is therefore more accurately described by the phrase "increase the confidence in". It should also be stressed that the user can influence the results through the assumptions he/she makes, or through input errors. The study conducted by the U.S. participant on the yearly simulations of the Canadian Test Cell (1) clearly illustrates the importance of the use of correct assumptions, assumptions which are often inherent in the programs and therefore difficult or impractical to alter.

From the results of the validation effort on the individual test buildings, it appears that simple, modestly sized passive solar heating systems can be handled adequately by all the programs evaluated. Such a case was exemplified by the direct gain building in which the ratio of the solar aperture-to-floor area was about 10%. This system was simple in the sense that such complex heat transfer mechanisms as natural interzone convection, ground conduction and natural

infiltration were suppressed. Also, because of a low gain/loss ratio (average ambient temperature = -15°C), the dynamic interaction of solar gains and internal thermal mass was working on a minimum level (no change of heat flow direction).

The Trombe wall and sunspace cases both represented larger and more complex passive solar heating systems. In the Trombe wall case, the solar aperture-to-floor area ratio was approximately 1. Ground and infiltration heat transfer was minimal, and natural convection through the Trombe wall vents was a major mode of heat transfer. For this case, the disagreement between predicted and measured zone temperature was, in general, much larger than for the direct gain case. Disagreement between the various codes used in the study was also generally greater for the Trombe wall than for the direct gain case.

The sunspace case was also quite complex. The solar aperture-to-floor area ratio was about 30% for the entire building, and 70% for the sunspace zone. Interzone natural convection through an open doorway was an important mode of heat transfer. Infiltration was suppressed in the back room, but was present in the sunspace. Solar radiation transfer from sunspace to back zone was not considered as the test cell did not contain a glazed area within the separation wall. Ground heat transfer was relatively small. Here again, temperature and energy predictions showed markedly greater disagreement with the measured values than in the direct gain case. The range of disagreement among code predictions was also much larger than in the direct gain case.

In general, it appears that prediction inaccuracy increases as 1) the solar forcing functions become stronger, and 2) the solid conduction heat transfer mode becomes dominated by other more complex heat transfer mechanisms. A third reason for increased inaccuracy occurs when a code simply does not contain an algorithm or subroutine to reasonably model some aspect of the building, its equipment or controls. These sources of inaccuracy can work independently or together.

(Note: there are many other reasons for inaccuracy. However, we are concerned here only with those sources of error which are internal to the code themselves, and which pertain to the prediction of "building fabric" thermal performance. For a more complete discussion of potential sources of inaccuracy, see section 4.2.1).

The results of this study and other validation efforts support the following general conclusions:

- Diffusion of heat in solid media is adequately modelled by the current generation of building energy analysis simulation programs (assuming one dimensional heat transfer and constant thermal properties).
- The major sources of error and disagreement among codes used to model passive and hybrid low energy buildings are due to the algorithms which handle:
  - . calculation of interior and exterior radiative and convective surface coefficients
  - . calculation of exterior and interior incident solar radiation and interzone radiation transfer
  - . interzone natural convection heat transfer and stratification
  - . ground heat transfer
  - . latent loads
- Except for latent loads, the presence of strong solar forcing functions in the building exacerbates the inaccuracies caused by the above algorithms and subroutines.

8.2 Recommendations

In the previous paragraph, a number of sources for inaccurate modelling of passive and hybrid solar systems were listed. The extent of the effect on the accuracy of the simulation results varies greatly among these sources from case to case. In cases where absolute accuracy of the simulation results is not crucial, e.g. for most design purposes, it is question-

able whether the extra effort necessary to accurately model phenomena which are not directly part of the design is worthwhile. In other cases, where a high degree of accuracy is required, e.g. when a simulation program is used for research purposes or some detailed design analyses, serious attention to these phenomena is required. A list of specific recommendations for the phenomena in question is as follows:

Exterior convective film coefficients

Constant exterior convective film coefficients may not be adequate, especially for short periods and high glazing areas. Time varying coefficients are preferable. One simple commonly used time varying algorithm is a second order polynomial in wind speed. Programs using constant coefficients should adopt some time varying approach.

Interior convective film coefficients: Constant interior convective film coefficients are not adequate in strongly passive solar buildings. The heat flows into and out of glazing and high conductivity mass elements are improperly modelled in such situations. These coefficients should be modelled as a function of the temperature difference between the interior surface and zone air, and the direction of heat flow. Also, the coefficients should change when mechanical ventilation equipment is in use.

Interior radiative surface coefficients: A number of simplified approaches to calculating interior infra-red radiation exchange have been suggested. Among these, the Walton "MRT/Balance" method (2) and the Carroll "MRT Network" method (3) exemplify algorithms which are both computationally efficient, and reasonably accurate for common room geometries. Authors of programs using constant interior radiative coefficients should consider adopting one of the simplified time varying approaches.

Exterior radiative surface coefficients: Exterior radiative surface coefficients can be quite difficult to model because

of the uncertainties in the surface temperatures and effective emittances of the external surroundings. For codes currently using constant coefficients, algorithms should be added, which at least account for the radiation exchange on skyward facing surfaces. Simplified approaches exist which correlate wet bulb temperature and effective sky temperature or effective sky emittance. Other approaches correlate the radiation exchange to cloud cover. Any of these approaches is preferable to the constant assumption.

Exterior incident solar radiation: More research is needed to develop appropriate sky modelling algorithms. Some programs use isotropic models, some use anisotropic models. There is little evidence to support the use of one over the other.

Interior incident solar radiation: The distribution of absorbed solar radiation in the building effects the accuracy of predictions in passive solar buildings to some extent. Algorithms which automatically calculate this distribution would be preferable to user-defined constant distributions in strongly passive solar buildings.

Interzone natural convection heat transfer and stratification: More research is needed to develop acceptable accurate algorithms for these phenomena.

Ground heat transfer: More research is needed to adequately account for this phenomenon.

Latent loads: More research is needed to adequately account for this effect.

Closing remarks

There is a shortage of high quality measured data suitable for validating dynamic thermal models (4), in particular multizoned structures subject to climate regimes typical of Western Europe.

There is uncertainty in both the experimental and modelling phases of the empirical validation process, and there may be compensating errors within models themselves. Therefore, comparisons between model predictions and data measured at the building system level, cannot be the sole determinant of the fundamental validity of dynamic thermal models.

Future monitoring experiments need to be very carefully planned if the data is to be of value for validating dynamic thermal models.

REFERENCES

1. Judkoff, R.D. (1986). International Energy Agency Simulation Comparison and Validation Study. International Climatic Architecture Congress, Louvain-La-Neuve.

2. Walton, G.N. A new Algorithm for Radiant Interchange in Room Loads Calculations. ASHRAE Trans. No. 2590.

3. Carroll, J.A. An MRT Method of Computing Radiant Energy Exchange in Rooms. Proceedings of the 2nd Systems Simulation and Economic Analysis Conference, San Diego 1980. 343-348.

4. Lomas, K.J. and Bowman, N.T. The Evaluation and Use of existing Data Sets for Validating Dynamic Thermal Models of Buildings. The 5th Cib/Cibse international symposium on the use of computers for environmental engineering related to buildings. Bath, UK, 1986.

BIBLIOGRAPHY

Merriam, Richard L., and Scott J. Feldmand, A. D. Little Inc., Solar Heating and Cooling System Simulation Programs, Palo Alto, Ca: Electric Power Research Institute.

Smith, Hinchman, and Grylls Associates Incs., Value Engineering Analysis of Computer Simulation Energy Profile Systems for Institutional and Administrative Buildings, NASA.

Verstegen, P. L., Survey of Currently Used Simulation Methods, McLean, VA: Science Apllications, Inc. 1978.

Solar/Passive Building Design Computer Programs: A Brief Survey with Comments, New England Solar Energy Association, 1979.

Cuba, J. F., and G. Crall, Bibliography on Avaliable Computer Programs in the General Area of Heating, Refrigerating, Air Conditioning, and Ventilating, ASHRAE Research Project GRP-153, Columbus, OH: Battelle Laboratories, Rann Document Center National Science Foundation, 1975.

Science Applications, Inc., Survey of Component Modeling Activities, McLean, VA: SAI, Dec. 1978.

North Carolina Research Group, AIA Computer Research Survey 1967-1968, 18 May 1968.

Boston Architectural Center, Architecture and the Computer: Proceedings BAC Conference, December 5, 1964. Boston, MA: Boston Architectural Center 1964.

National Electrical Contractors Assn., Inc., Basics of Building Automation, Washington, DC: National Electrical Contractors Assn., Inc., 1973.

Forwood, Bruce, The Development of a Computer-Aided Building Environment and Services Simulation Model, Sydney, Australia: Department of Architectural Science, University of Sydney, 1971.

Fulbright, Ben E., S. L. Ferden, and R. D. Stalling, ESOP (Energy Systems Optimization Program): Its Description and Comparative Analysis, Houston, TX: NASA Johnson Space Center, 1975.

Wortman, D., Assumptions, Accuracy and Results of Building Energy Simulation Codes, SERI/TP-721-1331, Golden, CO: Solar Energy Research Institute, unpublished work.

McKinstry, M. et al., "System Performance Evaluation at the Class A Level, Performance Evaluation of Passive/Hybrid Solar Heating and Cooling, App.B, PO-NQ-9-4059-1, Golden, CO: Solar Energy Research Institute, unpublished work.

Government Servies Administration, Energy Conservation Computer Software, Washington, DC: GSA, March 1977.

Graven, Robert M., A Comparison of Computer Programs Used for Modeling Solar Heating and Air-Conditioning Systems For Buildings, Berkeley, CA: Lawrence Berkeley Laboratory, University of California, June 1974.

Oak Ridge National Laboratory/NSF, Inventory of Current Energy Research and Development. Vol. I, II, and III. U.S. GPO Stock Numbers 5270-02174 and 4270-02175, January 1974.

Kusuda, Tamami, Use of Computers for Environmental Engineering Related to Buildings, Washington, DC: National Bureau of Standards, October 1971.

Lee, Kaiman, Eric Teicholz, and Clifford Stewart, Computer Architecture Programs, Boston, MA: Center for Environmental Research, 1970.

Lokmanhekim, M., and R. H. Henninger, "Computerized Energy Requirement Analysis and Heating/Cooling Load Calculations of Buildings," ASHRAE Journal, April 1972.

McClure, Charles J.R.,. "Optimizing Building Energy Use", ASHRAE JOURNAL, September 1971.

Negroponte, Nicholas, The Architecture Machines: Toward a More Humane Environment, Cambridge, MA: MIT Press, 1970.

Lokmanhekim, M., ed., Procedure for Determining Heating and Cooling Loads for Computerized Energy Calculations-Algorithms for Building Heat Transfer Subroutines, ASHRAE, June 1971.

Reinschmidt, Kenneth F., "Computer Methods for Building System Design", Presented at the ASCE National Meeting on Structural Engineering, Baltimore, MD. 19-23 April 1974.

Science Applications, Inc., Validation Status of Solar Heating and Cooling Systems Models, McLean, VA: SAI, March 1979.

National Science Foundation, Solar Heating and Cooling for Buildings Workshop: Part I; Technical Sessions, 21-22 March 1973. Washington, DC: NSF, 1973.

Webster et al., User Perspectives of Selected Solar Design Tools, Los Alamos, NM: Los Alamos Scientific Laboratory, 1978.

Bloomfield, D., "Appraisal Techniques for Methods of Calculating the Thermal Performance of Buildings, BSER+T Vol. 6, No. 1, 1985.

Bowman, N. and K. Lomas, "Building Energy Evaluation", CICC Conference Nottingham, April 1985.

Allen, E. et al., "Analytical and Empirical Validation of Dynamic Thermal Building Models", BESC Conference, Seattle, August 1985.

Lomas, K.J., and N.T. Bowman, "The Evaluation and Use of Existing Data Sets for Validating Dynamic Thermal Models of Buildings", Bath Conference, July 1986.

Bloomfield, D., "The Use of Thermal Models for the Production of Design Guidelines", International Climatic Architecture Congress, Louvain, Belgium, June 1986.

Bland, B.H. and D.P. Bloomfield, "Validation of Conduction Algorithms in Dynamic Thermal Models", Bath Conference, July 1986.

APPENDIX A

IEA Solar Heating and Cooling Programme, Task VIII

Subtask B Representatives

Austria	Dr. Manfred Bruck Austrian Solar and Space Agency Garnisongasse 7 A - 1090 Vienna
Belgium	Prof. A. De Herde Unite d'Architecture-Fac. Sciences Appl. Place du Levant 1 B - 1348 Louvain - la - Neuve
Canada	Sherif Barakat Division of Building Research Thermal Performance Section National Research Council of Canada Ottawa, Ontario K1A OR6
Denmark	Dr. Ove Mørck Thermal Insulation Laboratory Technical University of Denmark Building 118 DK - 2800 Lyngby
Germany	Rolf Stricker, Hans Erhorn Fraunhofer Institute of Building Physics (Dir.: Prof. Dr.Ing. habil K.A. Gertis) Nobelstrasse 12 D - 7000 Stuttgart 80
Italy	Federico Butera Instituto di Fisica Tecnica Facolta di Ingegneria Universita di Palermo Vialle delle Science I - 90128 Palermo
the Netherlands	A. Poel Bouwcentrum Weena 700 NL - 3000/ AG Rotterdam
New Zealand	Michael Donn School of Architecture Private Bag Wellington

Norway	Civ.Ing. Terje Wolleng Norwegian Building Research Institute P.O.Box 322 Blindern N - Oslo 3
Spain	Eduardo Mezquida INTA Torrejon de Ardoz Madrid
Sweden	Staffan Salö Dept. of Building Science P.O. Box 118 S - 221 00 Lund
Switzerland	C. Filleux Basler and Hofmann Forchstr. 395 CH - 8029 Zurich
United Kingdom	David Bloomfield Building Research Establishment Department of the Environment Garston, Hertfordshire
United States	Ronald Judkoff SERI 1617 Cole Boulevard Golden, 80401 Colorado